

AN ABSTRACT OF THE THESIS OF

Wen-Shu Hwang for the degree of Doctor of Philosophy

in Chemistry presented on December 14, 1979

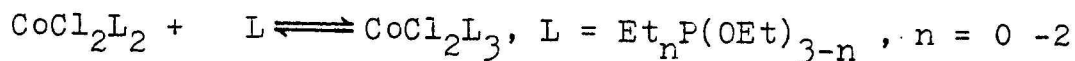
Title: TERTIARY PHOSPHORUS ESTERS: THEIR REACTION WITH
DIOXYGEN, THEIR COMPLEXES WITH COBALT(II) CHLORIDE,
AND THE CATALYSIS OF THEIR AUTOXIDATION BY COBALT(II)

Redacted for Privacy

Abstract approved:

 John T. Yoke III

The equilibrium constants and thermodynamic functions for the reactions



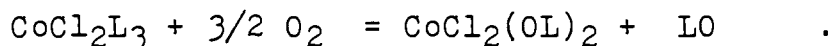
in benzene solution have been determined over the temperature range 10 - 45°C by the Evans nmr method. The CoCl_2L_2 and CoCl_2L_3 complexes differ in paramagnetic spin state. The equilibrium constants decrease irregularly in the order $n = 1, 2, 0$. Each of the three types of species involved in the equilibrium is independently susceptible to oxidation by oxygen.

Improved methods have been developed for the gas chromatographic analysis of the organophosphorus ligands L and their phosphoryl oxidation products LO. The products and

kinetics of the AIBN-initiated autoxidation at 50° of the free ligands L in benzene have been determined. The conversion of triethyl phosphite to triethyl phosphate is zero order in phosphite, first order in oxygen, and first order in AIBN. Diethyl ethylphosphonite and ethyl diethylphosphinite autoxidations at constant oxygen pressure are pseudo-first order in phosphorus ester and give the mixture of oxidation products predicted by Buckler's radical chain mechanism for the autoxidation of phosphines.

The complexes CoCl_2L_2 , $\text{L} = \text{Et}_n\text{P}(\text{OEt})_{3-n}$, $n = 0 - 3$ in benzene at 25° undergo facile autoxidation to give $\text{CoCl}_2(\text{OL})_2$ in which there is no change in the value of n going to the phosphoryl product. Initial rate measurements show pseudo-first order dependence on cobalt complex concentration.

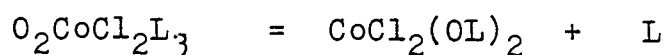
At a $\text{L}:\text{CoCl}_2$ mole ratio of 3 in benzene, all components of the equilibrium are present, with CoCl_2L_3 as the major solute species. Such solutions at 25° undergo autoxidation with the stoichiometry



The kinetics are first order in cobalt and first order in oxygen. At $\text{P}(\text{OEt})_3:\text{CoCl}_2$ mole ratios in the range 53 to 153, all the phosphite is readily oxidized, with initial rates proportional to the concentration of cobalt catalyst.

The previously postulated formation of cobalt dioxygen adducts $\text{O}_2\text{CoCl}_2\text{L}_2$ or $\text{O}_2\text{CoCl}_2\text{L}_3$ as autoxidation reaction intermediates is confirmed by low temperature studies. One

mole of O_2 at 1 atm is taken up per mole of $CoCl_2 \cdot 3EtP(OEt)_2$ at -46° in t-butylbenzene and is not lost at -23° after vacuum line freeze - pump - thaw cycles. The kinetics of unimolecular decomposition of the adduct, according to the demonstrated stoichiometry



were studied in the -9 to $+11^\circ$ temperature range. Extrapolation of the rate constant to 25° for comparison with the rate constant for autoxidation shows that rate determining step is formation of the dioxygen adduct.

Tertiary Phosphorus Esters: Their Reaction with Dioxygen,
Their Complexes with Cobalt(II) Chloride, and the
Catalysis of Their Autoxidation by Cobalt(II)

by

Wen-Shu Hwang

A THESIS

submitted to

Oregon State University

in partial fulfillment of
the requirements for the
degree of

Doctor of Philosophy

June 1980

APPROVED:

Redacted for Privacy

Professor of Chemistry
in charge of major

Redacted for Privacy

Chairman of Department of Chemistry

Redacted for Privacy

Dean of Graduate School

Date thesis is presented _____ December 14, 1979

Typed by May-Ying Hwang for Wen-Shu Hwang

ACKNOWLEDGEMENTS

I wish to express my sincere thanks to my research adviser, Dr. John T. Yoke, not only for his expert direction of my academic work including this research but also for his fatherly concern and support.

Thanks are also expressed to the National Science Foundation for a Research Assistantship held during the year 1976-1977, and to the Department of Chemistry for a Teaching Assistantship held during the rest of my graduate studies at Oregon State University. The receipt of gifts of chemicals from the Ethyl Corporation is acknowledged with thanks. I am grateful for the assistance of Dr. Terry Miller of the Department of Agricultural Chemistry for his assistance with the electron paramagnetic resonance experiment. All the nmr measurements were made by Susan Randall of the Department of Chemistry, and I thank her for her essential contribution to the research.

I am deeply grateful to my parents, my sister, my brother-in-law, my parents-in-law, and other persons who have encouraged me and given me inspiration in this effort.

Most of all, I thank my loving wife May for her patience and understanding during the course of this endeavor. I am also grateful for her assistance in preparing this dissertation.

TABLE OF CONTENTS

<u>Chapter</u>	<u>Page</u>
I. INTRODUCTION	1
II. HISTORICAL	6
A. Gas Chromatographic Methods of Analysis of $\text{Et}_n\text{P}(\text{OEt})_{3-n}$ and $\text{Et}_n\text{P}(\text{O})(\text{OEt})_{3-n}$ Compounds	6
B. Autoxidation of Free $\text{Et}_n\text{P}(\text{OEt})_{3-n}$ Ligands	10
C. Cobalt(II) Halide Complexes of $\text{Et}_n\text{P}(\text{OEt})_{3-n}$ and $\text{Et}_n\text{P}(\text{O})(\text{OEt})_{3-n}$ Ligands	19
D. Cobalt(II) Dioxygen Adducts	23
E. Autoxidation of Coordinated Phosphorus Ligands	31
III. EXPERIMENTAL	42
A. Materials	42
1. Solvents	42
a. Benzene	42
b. t-Butylbenzene	42
c. Other Solvents	42
2. Reagents	42
a. Ethanol	42
b. N,N-Diethylaniline	43
c. Cobalt(II) Chloride	43
d. Tetraethyl Lead	43
e. Phosphorus Trichloride	43
f. Ethyldichlorophosphine	43
g. Diethylchlorophosphine	45
h. Azobisisobutyronitrile(AIBN)	46
i. Oxygen	46
j. Air	46

<u>Chapter</u>	<u>Page</u>
III. A. 3. Organophosphorus Esters and Their Phosphoryl Derivatives	46
a. Triethyl Phosphite	46
b. Diethyl Ethylphosphonite	46
c. Ethyl Diethylphosphinite	47
d. Triethylphosphine	47
e. Ethyl Diethylphosphinate	47
f. Diethyl Ethylphosphonate	47
g. Triethyl Phosphate	47
4. Complexes	47
a. Dichlorobis(triethylphosphine)cobalt(II)	47
B. Techniques	48
C. Instrumentation	50
1. Melting Point Determinations	50
2. Gas Chromatography	50
3. Infrared Spectra	51
4. Visible Spectra	51
5. Nuclear Magnetic Resonance	52
6. Electron Paramagnetic Resonance	52
D. Development of Gas Chromatographic Analytical Methods	54
1. Introduction	54
2. Preparation of Columns	55
3. Qualitative Analysis	56
4. Quantitative Analysis	58
IV. DETERMINATION OF THE THERMODYNAMIC FUNCTIONS FOR THE $\text{CoCl}_2\text{L}_2 \rightleftharpoons \text{CoCl}_2\text{L}_3$ EQUILIBRIA IN BENZENE	66
A. Introduction	66
B. Theory	67
C. Methodology	71

<u>Chapter</u>	<u>Page</u>
IV. D. Results and Discussion	73
V. AUTOXIDZTION OF FREE $\text{Et}_n\text{P}(\text{OEt})_{3-n}$ LIGANDS IN BENZENE	79
A. Methodology	79
B. Results	80
C. Discussion	90
VI. STUDIES OF A COBALT DIOXYGEN ADDUCT INTERMEDIATE	94
A. Introduction	94
B. Chemical Evidence for the Dioxygen Adduct	95
C. Low Temperature EPR Studies	97
D. Kinetics of Decomposition of the Dioxygen Adduct	98
E. Discussion	102
VII. AUTOXIDATION OF CoCl_2 COMPLEXES WITH $\text{Et}_n\text{P}(\text{OEt})_{3-n}$ LIGANDS IN BENZENE	106
A. Methodology	106
B. Autoxidation Using a Ligand:Cobalt Chloride Mole Ratio of 2	107
C. Autoxidation Using a Ligand:Cobalt Chloride Mole Ratio of 3	112
D. Catalysis of Autoxidation at High Ligand: Cobalt Chloride Mole Ratios	113
E. Discussion	119
VIII. GENERAL DISCUSSION AND SUMMARY	127
BIBLIOGRAPHY	138
APPENDEX I: NMR Shift Data and Equilibrium Constant Calculations	144
APPENDEX II: Spectrophotometric Data on Dioxygen Adduct Decomposition	181

LIST OF FIGURES

<u>Figure</u>	<u>Page</u>
1. Mechanism of Autoxidation of Free Trialkylphosphines	13
2. Reaction Apparatus for Study of O_2 Adduct Decomposition	53
3. Qualitative G.C. Analysis on a UC-W 98 Column	59
4. Qualitative Analysis on a Reoplex 400 Column	60
5. Quantitative G.C. Working Curves for $P(OEt)_3$ and $P(O)(OEt)_3$	62
6. Quantitative G.C. Working Curves for $EtP(OEt)_2$ and $EtP(O)(OEt)_2$	63
7. Quantitative G.C. Working Curves for Et_2POEt and $Et_2P(O)(OEt)$	64
8. Autoxidation of 0.2M Triethyl Phosphite in Benzene with 0.02913M AIBN under 1.00 Atm. of Oxygen	81
9. Autoxidation of 0.2M Triethyl Phosphite in Benzene with 0.0105M AIBN under 1.00 Atm. of Oxygen	82
10. Autoxidation of 0.2M Triethyl Phosphite in Benzene with 0.6414M AIBN under 1.00 Atm. of Dry Air	83
11. Autoxidation of 0.2M Diethyl Ethylphosphonite in Benzene	86
12. Autoxidation of 0.2M Ethyl Diethylphosphinite in Benzene	87
13. Pseudo-First Order Kinetic Plot for the Autoxidation of $EtP(OEt)_2$ and Et_2POEt	89
14. Electron Paramagnetic Resonance Spectrum of the Dioxygen Adduct in Frozen t -Butylbenzene	99

<u>Figure</u>	<u>Page</u>
15. Pseudo-First Order Kinetic Plot for Autoxidation at L:CoCl ₂ Mole Ratio 2.00	110
16. Pseudo-First Order Kinetic Plot for Autoxidation at L:CoCl ₂ Mole Ratio 3.00	114
17. Autoxidation of Triethyl Phosphite at High L:CoCl ₂ Mole Ratios	117
18. Formation of Triethyl Phosphate at High L:CoCl ₂ Mole Ratios	118

LIST OF TABLES

<u>Table</u>	<u>Page</u>
I. Properties of the Tertiary Phosphorus Esters	3
II. Product Distribution in the Uninitiated Autoxidation of the Free Ligands	16
III. Gas Chromatographic Separations	57
IV. Densities as a Function of Temperature	74
V. Thermodynamic Functions and Equilibrium Constants	76
VI. Kinetic Data For Triethyl Phosphite Autoxidation in Benzene at 50°	85
VII. Comparison of Rates of Initiation and Autoxidation in Benzene at 50°, 1.00 Atm Oxygen	91
VIII. First Order Rate Constants for Decomposition of the O ₂ Adduct	102
IX. Pseudo-First Order Rate Constants for Autoxidation at Mole Ratio L:CoCl ₂ 2.00 in Benzene at 25°	111
X. Initial Distribution of Oxidizable Species and Pseudo-First Order Rate Constants for Autoxidation at Mole Ratio L:CoCl ₂ 3.00 in Benzene at 25°	111
XI. Apparent Initial Second Order Rate Constants, M ⁻¹ sec ⁻¹ , in Benzene	134
XII. Data for Equilibrium Constant Calculation from NMR Shifts:Cobalt(II) Chloride Triethyl Phosphite System	145
XIII. Data for Equilibrium Constant Calculation from	

<u>Table</u>	<u>Page</u>
XIII. NMR Shifts:Cobalt(II) Chloride Diethyl Ethylphosphonite System	156
XIV. Data for Equilibrium Constant Calculation from NMR Shifts:Cobalt(II) Chloride Ethyl Diethylphosphinite System	168
XV. Calculation of Thermodynamic Parameters from Equilibrium Constants: Cobalt(II) Chloride-Triethyl Phosphite System	178
XVI. Calculation of Thermodynamic Parameters from Equilibrium Constants: Cobalt(II) Chloride-Diethyl Ethylphosphonite System	179
XVII. Calculation of Thermodynamic Parameters from Equilibrium Constants: Cobalt(II) Chloride-Ethyl Diethylphosphinite System	180
XVIII. Calculation of First Order Rate Constant for Thermal Decomposition of $O_2CoCl_2(EtP(OEt)_2)_3$ from Spectrophotometric Data at -9°	182
XIX. Calculation of First Order Rate Constant for Thermal Decomposition of $O_2CoCl_2(EtP(OEt)_2)_3$ from Spectrophotometric Data at $-2^\circ C$	184
XX. Calculation of First Order Rate Constant for Thermal Decomposition of $O_2CoCl_2(EtP(OEt)_2)_3$ from Spectrophotometric Data at $3^\circ C$	186
XXI. Calculation of First Order Rate Constant for Thermal Decomposition of $O_2CoCl_2(EtP(OEt)_2)_3$ from Spectrophotometric Data at $7^\circ C$	188
XXII. Calculation of First Order Rate Constant for Thermal Decomposition of $O_2CoCl_2(EtP(OEt)_2)_3$ from Spectrophotometric Data at $11^\circ C$	190

TERTIARY PHOSPHORUS ESTERS: THEIR REACTION WITH DIOXYGEN,
THEIR COMPLEXES WITH COBALT(II) CHLORIDE, AND THE
CATALYSIS OF THEIR AUTOXIDATION BY COBALT(II)

I. INTRODUCTION

This research is a continuation of a project on transition metal catalysis of the autoxidation of organic compounds. It involves the oxidation of cobalt(II) complexes with organophosphorus ligands $\text{Et}_n\text{P}(\text{OEt})_{3-n}$ (Et = ethyl, n = 0 - 3).

The reactions of dioxygen with organic compounds are very important. There are several known types of such autoxidations. Commonly, the uncatalyzed pathway involves a radical chain mechanism. Another type may involve a non-radical pathway, via a metal complex of the organic substrate. Here, there may be not only a different reaction rate, but also a different distribution of products than arise in the uncatalyzed radical autoxidation. For example, the autoxidation of free trialkylphosphines, PR_3 , in organic solvents is known to give a mixture of four organophosphoryl compounds $\text{R}_3\text{P}(\text{O})$, $\text{R}_2\text{P}(\text{O})(\text{OR})$, $\text{RP}(\text{O})(\text{OR})_2$, and $\text{P}(\text{O})(\text{OR})_3$, by a free radical mechanism (Buckler, 1962; Floyd and Boozer, 1963). Schmidt (1970) found that if the trialkylphosphine is first coordinated to cobalt(II) chloride, the only product of the quantitative autoxidation reaction in organic solvents was the trialkylphosphine oxide (in its cobalt complex). It was demonstrated experimentally that the

cobalt-catalyzed reaction is non-radical in character.

The ligands $\text{Et}_n\text{P}(\text{OEt})_{3-n}$ react with cobalt(II) chloride to form bis-complexes $\text{CoCl}_2 \cdot 2\text{Et}_n\text{P}(\text{OEt})_{3-n}$. These have spectral and magnetic properties typical of pseudo-tetrahedral high-spin cobalt(II) compounds. Low-spin five-coordinate tris-complexes $\text{CoCl}_2 \cdot 3\text{Et}_n\text{P}(\text{OEt})_{3-n}$, formed by addition of a third phosphorus ligand to the bis-complexes, can be isolated for only the two middle members of the series (Studer, 1972). Dichlorobis(triethylphosphine)cobalt(II) does not coordinate additional triethylphosphine (Hatfield and Yoke, 1962). The formation of $\text{CoCl}_2 \cdot 3\text{P}(\text{OEt})_3$ in solution was observed spectroscopically, but the complex itself could not be isolated (Studer, 1972).

These results demonstrate the importance of both electronic and steric effects on complex stability. Some data relevant to these effects are given in Table I. Tolman (1970) assigned a dominant role to the steric effect on the relative stabilities of nickel(0) complexes of similar phosphorus ligands. The steric cone angle for the $\text{Et}_n\text{P}(\text{OEt})_{3-n}$ series decreases from 132° for the phosphine to 109° for the phosphite, with intermediate values for the phosphinite and phosphonite. Bresan and Rigo (1975) also assigned a dominant role to steric effects in the tendency for phosphine ligands to form five-coordinate complexes with cobalt(II). Trivalent phosphorus bases coordinate to transition metal ions by a sigma bond of the regular

Table I. Properties of the Tertiary Phosphorus Esters

Formula	Name	Cone Angle ^o	Electron Binding Energies (eV) ^c		NMR Data	
			P _{2s}	P _{2p}	³¹ P ^d	¹ H(δ)
Et ₃ P	Triethylphosphine	132 ^a	193.50±.11	135.90±.10	+19.5 (m) ^e	1.13 (m) ^e
Et ₂ POEt	Ethyl Diethylphosphinite	124 ^b	194.21±.12	136.84±.08	-182 (m) ^f	1.32 (m), 3.94 (m)
EtP(OEt) ₂	Diethyl Ethylphosphonite	117 ^b	195.13±.14	137.49±.11	-135 (m) ^f	1.28 (m) 3.84 (m)
P(OEt) ₃	Triethyl Phosphite	109 ^a	195.83±.12	138.28±.09	-142 ^g	1.19 _h 3.85

(a) Tolman (1970).

(b) Tolman, Seidel, and Grosser (1974).

(c) Jen and Thomas (1976).

(d) Chemical shift, ppm from H₃PO₄.

(e) Axtell and Yoke (1973).

(f) Joedicke, Studer, and Yoke (1976).

(g) Septet, J_{POCH}=7.4 Hz.

(h) Jones and Coskran (1971).

Lewis acid-base adduct type. Successive replacement of alkyl groups (R) by more electronegative alkoxy groups (OR) in this series $\text{Et}_n\text{P}(\text{OEt})_{3-n}$ would be expected to decrease the sigma donor ability of the ligands. This decrease in electron density on phosphorus is reflected experimentally by the monotonic increase in phosphorus core electron binding energies in this series (Jen and Thomas 1976). In addition, it is commonly supposed that back pi bonding is also important in phosphorus-transition metal coordination, in which electrons of the metal are in d orbitals of appropriate symmetry to interact with low-lying empty d orbitals of phosphorus. A decrease in the electron density on phosphorus would promote back pi bonding. The combination of these factors may be reflected in the irregularity of the ^{31}P nmr data for these ligands.

The primary purpose of this research is the kinetic study of the cobalt catalyzed autoxidation reaction of these ligands. Since both high spin four-coordinate and low spin five coordinate cobalt complexes exist in the equilibrium $\text{CoCl}_2\text{L}_2 + \text{L} \rightleftharpoons \text{CoCl}_2\text{L}_3$, and since the geometry of the reacting complex and its paramagnetism may be important, the knowledge of the equilibrium constants is a prerequisite to the kinetic work. Joedicke (1976) determined the equilibrium constants in nitrobenzene and t-butylbenzene. It was found that these solvents were not

suitable for autoxidation studies, because of solubility and solution stability problems. The complete composition range $\text{CoCl}_2\text{L}_2 + \text{L} \rightleftharpoons \text{CoCl}_2\text{L}_3$ is available in benzene. Therefore, a preliminary goal of this research is determination of the equilibrium constants in benzene so that subsequent autoxidation studies can be conducted in this solvent.

In addition, study of autoxidation kinetics requires the application of appropriate methods for the quantitative analysis of the reaction mixtures. Development of these analytical methods is an additional important preliminary part of this research.

Dioxygen adducts, such as $\text{O}_2\text{CoCl}_2(\text{L})_2$ or 3 , were postulated to be autoxidation reaction intermediates both by Schmidt (1970) and by Joedicke (1976). Such cobalt-dioxygen adducts are the subject of widespread current interest and investigation. An additional goal of this research will be to determine if such adducts are in fact involved as reaction intermediates, and to characterize them if possible.

II. HISTORICAL

A. Gas Chromatographic Methods of Analysis of $\text{Et}_n\text{P}(\text{OEt})_{3-n}$ and $\text{Et}_n\text{P}(\text{O})(\text{OEt})_{3-n}$ Compounds

Gas chromatography has served as a very valuable method for the analysis of organophosphorus compounds. It is a major analytical tool in this research work. Only limited reports are available which concern separation and identification of $\text{R}_n\text{P}(\text{OR})_{3-n}$ and $\text{R}_n\text{P}(\text{O})(\text{OR})_{3-n}$ compounds in mixtures. Walling and Rabinowitz (1958) used gas chromatography to identify and estimate the product of the reaction of thiol or alkoxy radicals with trialkyl phosphites. However, no details as to gas chromatographic conditions were given in their paper.

Gudzinowicz and Campbell (1961) analyzed mixtures of aryl phosphines and their phosphine oxides by gas chromatography. Plumb and Griffin (1963) analyzed oxidation products of some aliphatic tertiary phosphites, using either 20 % Carbowax 20M (for analysis of tri-methyl, isopropyl, and n-butyl phosphites) or 20 % SE-30 (for tri-ethyl and triphenyl phosphites) on 60-80 M Chromosorb P columns. Column temperatures from 175° to 250° were used. The quantitative work based on integrated peak areas used standard mixtures of authentic materials for calibration. In all cases, they found that clean separations of all the compounds of the reaction mixtures were obtained and the

phosphites and phosphates gave symmetrical peaks with no evidence of tailing. The gas chromatographic analysis of mixtures of $R_nP(OR)_{3-n}$ and $R_nP(O)(OR)_{3-n}$ compounds with $R=n$ -butyl and cyclohexyl were studied by Feinland, Sass, and Buckler (1963). They used an F&M Model 500 instrument with a thermal conductivity detector and 6-foot columns containing 60-80M Chromosorb W as the inert support. With the cyclohexyl compounds, they found that 20 % silicone grease as the stationary phase gave adequate separation of the compounds, except that cyclohexyl phosphate failed to be eluted. With the butyl compounds, however, using the silicone column at 200°, several components of the mixture were not adequately resolved, and tailing was a problem with several peaks. For quantitative analysis, they picked three compounds which were adequately resolved for testing, Bu_3P , Bu_3PO , and $BuP(O)(OBu)_2$, and prepared standard solutions in benzene with bibenzyl as the internal standard. The working curves for the two phosphoryl compounds were satisfactorily linear, but the peak area vs. concentration function (relative to the internal standard) was unsatisfactory for Bu_3P due to excessive tailing of its peak. This problem was solved by using a 20 % Reoplex 400 column, which gave good resolution of all peaks in the complete $Bu_nP(OBu)_{3-n}$ and $Bu_nP(O)(OBu)_{3-n}$ series. An interesting result found for the compounds $Bu_nP(O)(OBu)_{3-n}$ was that the order of elution on both columns varied irregularly with n . The elution order was

$n=1,0,2,3$. Davis et al (1963) used a 250 cm glass column packed with SE-30 on Chromosorb W and with helium carrier gas for the separation of crude trimethyl phosphite, triethyl phosphite, and other phosphorus containing compounds. They suggested that direct injection on the column, the use of glass columns, careful drying of the carrier gas, special treatment of the support to reduce tailing and rearrangement on the column, and the use of temperature programming are helpful in the gas chromatographic analysis of phosphorus compounds.

Berlin and his coworkers (1963) used an instrument with a hydrogen flame detector and with 10 % silicone rubber (on Chromosorb W), 10 % Apiezon L (on Chromosorb W), and 10 % Apiezon K (on Fluoropak 90) columns to check the purity of trimethyl phosphite, methyl diphenylphosphinate, and dimethyl methylphosphonate and to analyze the reaction products of organophosphorus esters with Grignard Reagents. In another paper (1956), Berlin and his coworkers present analytical results for some other $R_nP(OR')_{3-n}$ and $R_nP(O)(OR')_{3-n}$ compounds obtained similarly. They found that although the silicone rubber on Chromosorb W gave very satisfactory results with all the $R_nP(OR')_{3-n}$ compounds under study, the chromatograms from the analysis of $R_nP(O)(OR')_{3-n}$ compounds exhibited unsymmetrical peaks due to excessive tailing. This problem was solved by using a column of 5 % silicone rubber on acid-washed and dimethyl-

dichlorosilane (DMCS) pretreated Chromosorb G. This column gave superior separation for not only $R_nP(OR')_{3-n}$ but also for $R_nP(O)(OR')_{3-n}$ compounds, with reasonable retention times and much more symmetrical peaks. For a mixture containing several different types of organophosphorus compounds, temperature programming is usually necessary for the complete analysis.

In this laboratory, Schmidt (1971) used the temperature programmed F&M 700 gas chromatographic instrument with a thermal conductivity detector and $\frac{1}{4}$ -inch o.d. 6-foot stainless steel columns to check the purity of triethylphosphine and its autoxidation products in benzene solution. On a column packed with 10 % SE-30 on Chromosorb W, the components of a benzene, triethylphosphine, *o*-dichlorobenzene (internal standard), and triethylphosphine oxide mixture were easily separated, eluting in the order given. With both Reoplex 400 and silicone on Chromosorb W columns, the order of elution of the components $Et_nP(O)(OEt)_{3-n}$ was $n=1,0,2,3$. This is the same irregular order found by Feinland, Sass, and Buckler in $Bu_nP(O)(OBu)_{3-n}$ compounds. The retention times of the ethyl substituted phosphoryl compounds were quite close; the separation was adequate for identification by comparison with authentic samples, but not for quantitative analysis. Joedicke (1976) studied the $Et_nP(OEt)_{3-n}$ and $Et_nP(O)(OEt)_{3-n}$ compounds, where $n=0,1,2$,

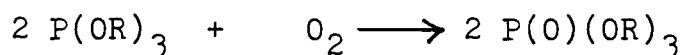
in t-butylbenzene solution. By using a Reoplex 400 column, pairs of compounds $\text{Et}_n\text{P}(\text{OEt})_{3-n}$ and $\text{Et}_n\text{P}(\text{O})(\text{OEt})_{3-n}$ for each n , separately in t-butylbenzene, were well resolved from each other, from the solvent, and from the internal standard o- $\text{C}_6\text{H}_4\text{Cl}_2$. For all six compounds, plots of concentration vs. peak area, relative to the internal standard, showed good linearity.

B. Autoxidation of Free $\text{Et}_n\text{P}(\text{OEt})_{3-n}$ Ligands

Tertiary phosphites ($n=0$) are in general somewhat susceptible to autoxidation to phosphates $\text{P}(\text{O})(\text{OR})_3$ and some have been used as antioxidants and u.v. stabilizers for polymers (Humphris and Scott, 1973). Aliphatic tertiary phosphines ($n=3$) are notoriously sensitive to oxygen and may inflame in air when their vapor pressure is high. There have been a number of studies of products, rates, and so forth bearing on the mechanism of autoxidation of phosphites and phosphines. Much less has been done with phosphonites ($n = 1$) and phosphinites ($n = 2$), although they too undergo autoxidation. For example, it has been reported (Arbuzov and Rizpolozhenskii, 1952) that neat diethyl ethylphosphonite reacts vigorously with air, while the more volatile dimethyl ethylphosphonite is spontaneously inflammable. A general reactivity order $\text{R}_3\text{P} > \text{R}_2\text{P}(\text{OR}) > \text{RP}(\text{OR})_2 > \text{R}(\text{OR})_3$ has been postulated (Razumov, Mukhacheva, and Sim-Do-Khen,

1952; Floyd and Boozer, 1963) for reactions with dioxygen as well as with alkyl halides, though there is no real evidence to support this postulate and such reactions would be expected to have completely different mechanisms.

The autoxidation of low molecular weight aliphatic tertiary phosphites,



generally requires heat and catalysis, or radical or photo-initiation at room temperature. For example, 90 to 95 % yields are obtained using aluminum oxide at 120^o (Hooker Chemical Co., 1964). At room temperature in the absence of initiation, triethyl phosphite gave no reaction with air (Cox and Westheimer, 1958) or with dioxygen (Joedicke, 1976). The following examples show that the autoxidation reaction has a radical mechanism. Dialkyl peroxides, which give alkoxy radicals on thermolysis, oxidize tertiary phosphites to phosphates (Walling and Rabinowitz, 1959). The radical initiator AIBN catalyzes the reaction with dioxygen (Floyd and Boozer, 1963). Plumb and Griffin (1963) found that at 50-55^o, air oxidizes tri-n-butyl phosphite to the phosphate with 45 % conversion in 20 hours in the dark, but with 100 % conversion in 5 hours with ultraviolet irradiation. The reaction was inhibited by hydroquinone. Very similar results were obtained with other phosphites, and by other workers (Smeykal, Baltz, and Fischer, 1963).

In contrast to trialkyl phosphites, which give the corresponding phosphate as the sole autoxidation product, trialkylphosphines give a mixture of products. And while no product distribution or kinetic studies have been reported (other than the work of Joedicke discussed below) using phosphinites or phosphonites as starting materials, it turns out that their autoxidation is involved in the phosphine autoxidation chain. An investigation by Buckler (1962) had elucidated many of the important features of trialkylphosphine autoxidation. A radical chain mechanism shown in Figure 1 was proposed for the reaction on the basis of a detailed study of the distribution of products under different reaction conditions. According to this mechanism, oxygen reacts with a hydrocarbon radical rather than directly at phosphorus.

Walling and Rabinowitz (1959) first made the postulate that trialkylphosphines react with peroxy ($RO_2\cdot$) or alkoxy ($RO\cdot$) radicals to form phosphoranylperoxy ($ROO\dot{P}R_3$) or phosphoranyl ($RO\dot{P}R_3$) radical intermediates. The phosphoranylperoxy radical decomposes to form the phosphine oxide R_3PO and an alkoxy radical $RO\cdot$ (reaction 3) while the phosphoranyl radical can decompose in two different ways (reaction 4a and 4b), forming either the phosphine oxide or the phosphinite ester R_2POR . The phosphinite ester can then react with peroxy or alkoxy radicals (reaction 5 and 6)

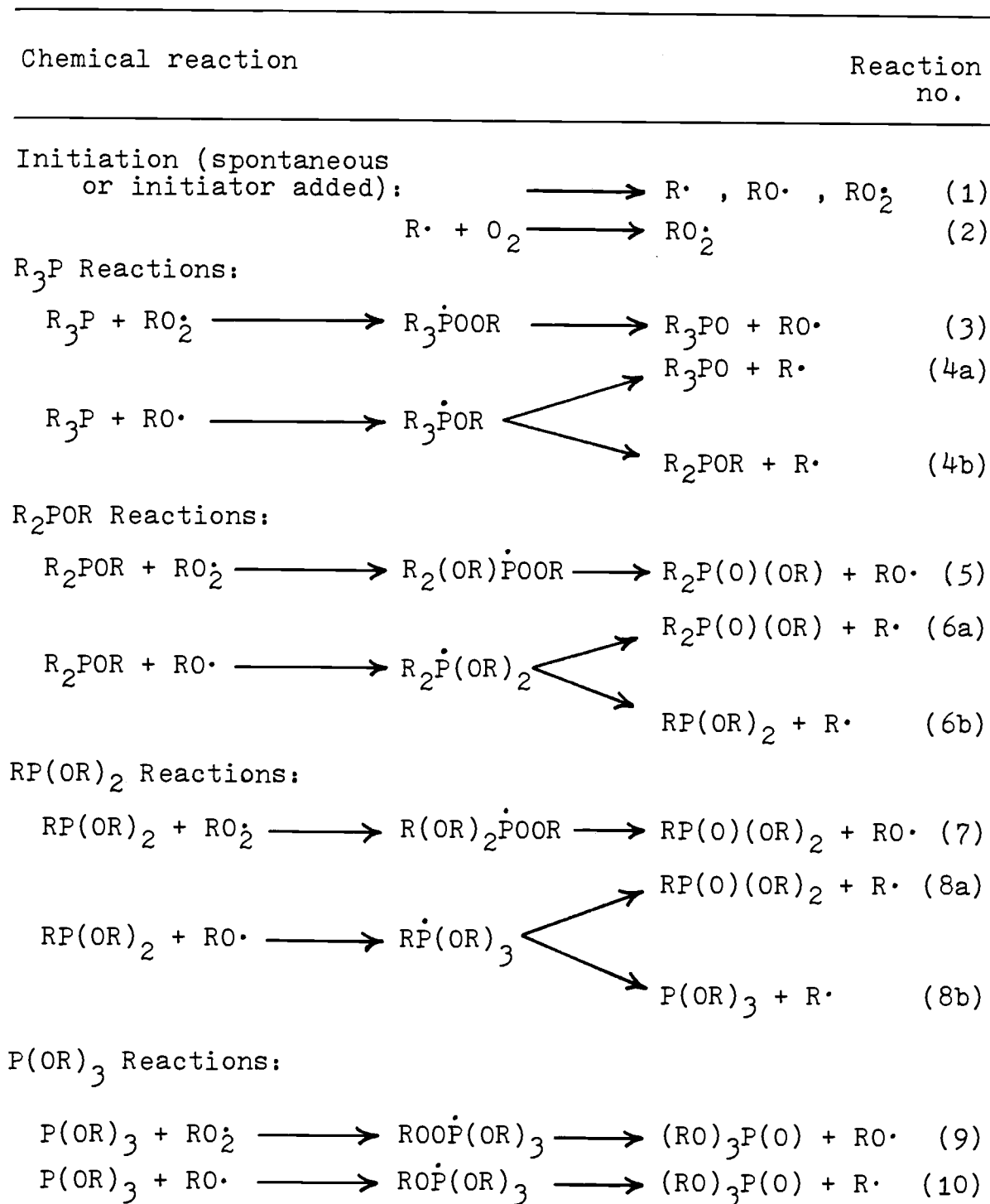


Figure 1. Mechanism of Autoxidation of Free Trialkylphosphines.

in the same manner to continue the whole chain of reactions. In this way, a mixture of products containing the P=O phosphoryl group is formed. Both Buckler, and Floyd and Boozer, found that the corresponding phosphine oxide and phosphinate $R_2P(O)(OR)$ ester were the major products with lesser amount of phosphonate $RP(O)(OR)_2$ and phosphate $P(O)(OR)_3$ esters. Also, the nature of solvent affected both the autoxidation rate and product distribution.

In order to account for the product distribution, Buckler pointed out that reaction 4b should predominate over 4a, even though the oxide forming process (4a) is favored thermodynamically. Bentrude et al (1973) indicated that the dominant decomposition pathway (reaction 4a or 4b) would be determined by the relative strength of the R-O and P-R bonds and the steric configuration of the phosphoranyl radical.

Ten years after the existence of phosphoranyl radical intermediates had been postulated (Walling and Rabinowitz, 1959), such radicals were detected experimentally by means of their esr spectra, observed when phosphines and phosphite were allowed to react with photochemically generated alkoxy radicals from peroxides (Kochi et al, 1969; Davies et al, 1971; Krusic, et al 1972). To quote Bentrude (Bentrude, et al, 1973), "the range (x=0 to 3) of alkyl-alkoxy intermediates of the type $R'_x\dot{P}(OR)_{4-x}$ from reaction of radicals with trivalent phosphorus has been detected on generation of alkoxy radicals in the presence of trivalent phosphorus

compounds. Although it is not in this way proved, the esr results are consistent with the idea that phosphoranyl radicals are in fact intermediates in the oxidations and displacements which ensue".

Using t-butylbenzene solutions saturated with dioxygen, Joedicke (1976) studied the autoxidation of the free bases $\text{Et}_n\text{P}(\text{OEt})_{3-n}$, $n = 0-2$. No initiator was used. His results are given in Table II. These product distributions were completely in accord with Buckler's mechanism. Triethyl phosphite failed to undergo autoxidation under these conditions. This is in agreement with the results of Cox and Westheimer (1958) and of Smeykal, Baltz, and Fischer (1963). Joedicke found the reactivity toward dioxygen to be in the irregular order $\text{P}(\text{OEt})_3 < \text{Et}_2\text{P}(\text{OEt}) < \text{EtP}(\text{OEt})_2$. This is different from the order postulated by Razumov et al (1952) and by Floyd and Boozer (1963). However, since no initiator was added in Joedicke's work, the initiation might be due to adventitious traces of impurities or to photoinitiation by background illumination, which might account for the irregular reactivity order.

Only very limited rate studies of phosphite autoxidation have been reported. One of these involved γ -ray initiation of air autoxidation of tri-iso-propyl phosphite (Coe, 1958). When very well-dried air was used, there was only a slow 10 % conversion. Irradiation or the lack of it made little difference. When very moist air was used, there was

Table II. Free Phosphorus Ester Autoxidation Products

0.2M in t-Butylbenzene with Added o-Dichlorobenzene.

Reactant	Autoxidation Products	Mole Percent Distribution
$P(OEt)_3$	No Reaction	--
$EtP(OEt)_2$	$EtPO(OEt)_2$	64
	$P(OEt)_3$	36
Et_2POEt	$Et_2PO(OEt)$	85
	$EtPO(OEt)_2$	15
	$P(OEt)_3$	trace

rapid and extensive hydrolysis to the secondary phosphite (hydrogen phosphonate) $HP(O)(OR)_2$. Peculiarly, when medium well-dried air was used, there was an initial rapid reaction period followed by a linear rate of formation of the $P(O)(OR)_3$ phosphate product over the approximate 30 to 60 % range of conversion; that is, the rate was independent of the phosphite concentration. The traces of water involved were stoichiometrically insignificant, and no $HP(O)(OR)_2$ was detected. Apparently, the traces of water were important to give initiating radicals on radiolysis. In another report, the u.v. photoinitiated autoxidation of tri-n-butyl phosphite was studied (Plumb and Griffin, 1963). Pure oxygen caused a much more vigorous reaction than did air. With

oxygen, the rate of formation of phosphate product was constant up to nearly 100 % conversion, i.e., again the rate was independent of phosphite concentration. However, there was no temperature control in this experiment and there was more than a 50^o thermal excursion during it. Joedicke made a preliminary kinetic study of the AIBN-initiated autoxidation of triethyl phosphite in t-butylbenzene. The data were quantitatively unsatisfactory, but ready oxidation of the phosphite to the phosphate was observed, in contrast to no reaction in the absence of initiator. Finally, a study was reported (Floyd and Boozer, 1963) of the AIBN-initiated autoxidation of tri-n-butyl phosphite at a controlled temperature (70^o) in o-dichlorobenzene solution. The reaction was found to be first order in AIBN and first order in phosphite. The only measurements were made at a constant oxygen pressure of 740 torr, so any dependence on oxygen concentration was not observed.

Reported rate measurements on trialkylphosphine autoxidation are very limited. Buckler's (1962) kinetic measurements are of no value as under his experimental conditions he found the reaction rate to be limited by the rate of diffusion of oxygen from the gas phase into the organophosphine solution. Floyd and Boozer (1963) studied the AIBN-initiated autoxidation of tri-n-butylphosphine in o-dichlorobenzene. There are some very peculiar features to their results. At constant initial tri-n-butylphosphine con-

centration and oxygen pressure, they found the reaction to be pseudo-first order in AIBN. At constant initial AIBN concentration and oxygen pressure, the reaction was pseudo-first order in the phosphine. The pseudo-first order rate constant was determined in the 38-70°C temperature range. At constant initial tri-n-butylphosphine concentration, and varying both the oxygen pressure (in the range 296-740 torr) and the initial AIBN concentration but keeping the ratio AIBN / P_{O₂} constant, the reaction rate was found to be constant within 10 %. These results were combined to give the composite rate law

$$\frac{-dO_2}{dt} = \frac{k[AIBN][(C_4H_9)_3P]}{P_{O_2}}$$

First, it is surprising the Floyd and Boozer used temperature well below 50°C with AIBN. The half-life of this initiator at 38°C, for example, is over five hundred hours, so the rate of generation of initiating radicals would be miniscule. The inverse dependence of the rate on oxygen pressure is even more surprising. It contravenes all other observations in this general area, and indeed goes against common sense. The authors offer no rationale for it, nor any mechanistic suggestions.

Finally, as a general observation about autoxidation kinetic studies, it may be noted that the solubility of dioxygen is not always known and will be different in the various solvents used. Assuming Henry's Law, the solubility

will be proportional to the oxygen partial pressure. Studies of the effect of increasing temperature on reaction rates will be made complex by the thermal variation in oxygen solubility, superimposed on the thermal variation of rates of initiation and autoxidation which may be expected.

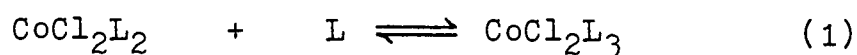
C. Cobalt(II) Halide Complexes of $\text{Et}_n\text{P}(\text{OEt})_{3-n}$
and $\text{Et}_n\text{P}(\text{O})(\text{OEt})_{3-n}$ Ligands

Divalent cobalt has the d^7 configuration and may have either three or one unpaired electrons, corresponding to quartet or doublet spin states. It forms numerous complexes of various stereochemical types depending on the nature of the ligands, concentration, nature of the solvent, temperature, etc.. Octahedral complexes, which are high-spin except in extraordinary cases, and tetrahedral complexes, which are always high-spin, are most common with cobalt(II). Five-coordinate cobalt(II) complexes, both high-spin and low-spin, and related both to the idealized trigonal bipyramidal and the square pyramidal geometries, are known. Square-planar four-coordinate cobalt(II) complexes are also known, both high-spin and low-spin, particularly with chelating ligands such as tetradentate Schiff bases and porphyrin derivatives.

The coordination chemistry of cobalt(II) with tri-valent phosphorus Lewis bases has been thoroughly reviewed by Studer (1972) and by Joedicke (1976). The various kinds of complexes CoX_2L_z which may be isolated in pure form depend on the nature of the anion X^- , the number z of phosphorus ligands bound, and the electronic and steric effects of the substituents on phosphorus in the ligands. Also, a whole host of kinds of equilibria are observed in solutions of such complexes, involving monomers and dimers, high- and low-spin states, four- and five-coordinate cobalt, addition and displacement of coordinated anions and phosphorus ligands, solvolysis, etc.

Specifically for the complexes where the anion is chloride and the phosphorus ligand is one of the series $\text{Et}_n\text{P}(\text{OEt})_{3-n}$, $n = 0 - 3$, it is known that CoCl_2L_2 is the only complex formed when $n = 3$ but that both CoCl_2L_2 and CoCl_2L_3 exist when $n = 0 - 2$. Dichlorobis(triethylphosphine)cobalt(II), first prepared by Jensen in 1936, is a typical example of a high-spin pseudotetrahedral cobalt(II) complex. It is the only complex formed in the system, both in solid-gas phase equilibrium (Hatfield and Yoke, 1962) and in solution (Boschi et al 1966). In contrast, the corresponding high-spin pseudotetrahedral complexes with ethyl diethylphosphinite and diethyl ethylphosphonite can take up an additional mole of the phosphorus ligand to give isolable low-spin five-coordinate complexes. The triethyl

phosphite-cobalt(II) chloride system gives dichlorobis-(triethyl phosphite)cobalt(II) as the only isolable complex, which exists in two polymorphic forms, but in solution in organic solvents this also will bind a third phosphorus ligand to give a low-spin five-coordinate complex. These complexes were first discovered by Studer (1972). Joedicke (1976) further characterized them, and in particular determined the equilibrium constants and thermodynamic functions for the reactions

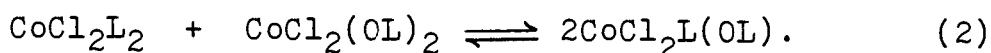


in *t*-butylbenzene (and to some extent in nitrobenzene) solution. The synthetic work and physical characterization of the complexes spectroscopically and magnetically, as well as the equilibrium studies, have been published (Joedicke, Studer, and Yoke 1976).

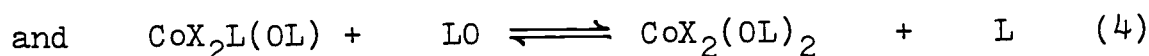
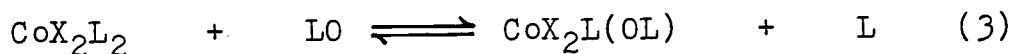
The ligands $\text{Et}_n\text{P}(\text{O})(\text{OEt})_{3-n}$ form only the bis complexes, $\text{CoCl}_2(\text{OL})_2$, in which the coordination to cobalt is through the phosphoryl oxygen. These have all been prepared in pure form and characterized physically; they are all pseudotetrahedral high-spin complexes (Schmidt 1970, Schmidt and Yoke 1970). An additional report on dichlorobis(triethylphosphine oxide)cobalt(II) has appeared (Sznajder *et al.*, 1979); its authors were unaware of the previous work. Although the triethylphosphine oxide complex ($n=3$) melts undecomposed at $76-77^\circ$, all the other

phosphoryl complexes ($n = 0-2$) are unstable thermally in the range $140 - 200^{\circ}$ with respect to loss of ethyl chloride, ultimately giving the salts $\text{Co}(\text{O}_2\text{PEt}_n(\text{OEt})_{2-n})_2$ (Schmidt and Yoke, 1970).

In his studies of the autoxidation of dichlorobis-(triethylphosphine)cobalt(II) in benzene solution, which gives dichlorobis(triethylphosphine oxide)cobalt(II) quantitatively as the product, Schmidt (1970; Schmidt and Yoke, 1971) discovered the interesting ligand redistribution



This reaction is postulated to play an important role in the mechanism of the autoxidation reaction, since the mixed ligand complex becomes a major solute species in the middle stages of the autoxidation. To put it another way, the reactant and its autoxidation product react with each other. Although phosphine phosphorus and phosphoryl oxygen have rather different donor character as far as sigma and pi bonding is concerned, it turns out that the two kinds of ligands have quite similar overall donor strength toward cobalt(II), so that energy changes in reaction (2) are small. This kind of equilibrium has attracted subsequent attention. In particular, using triphenylphosphine and triphenylphosphine oxide ligands, Rimbault and Hugel (1973) and Pierrard, et al (1977) have studied the equilibria

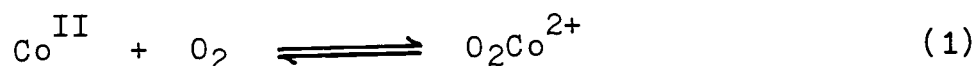


for which case the equilibrium constants $K_3/K_4 = K_2$.

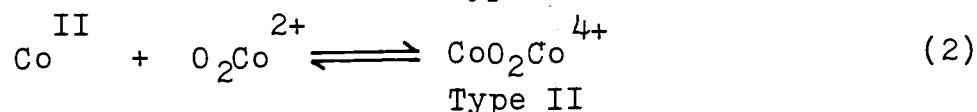
D. Cobalt(II) -Dioxygen Adducts

This topic has been reviewed extensively; for example, see Valentine (1973), Henrici-Olivé and Olivé (1974), and Vaska (1976). There has been great interest in these adducts from the biochemical standpoint, and this aspect has been reviewed (Basolo, Hoffman, and Ibers 1975). A very recent review (Jones, Summerville, and Basolo 1979) gives an excellent overview of the field and extensive citation of previous references.

Several different types of complexes can be formed in the reactions of cobalt(II) compounds with molecular oxygen. The two types thought to be of particular relevance to this research are indicated in the following scheme, in which the other ligands present (usually possessing nitrogen and oxygen donor atoms, and often chelating) are omitted for simplicity. (Any charge due to the additional ligands is also neglected).



Type I



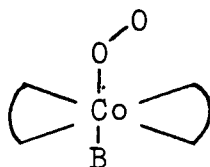
Type II

As a practical matter, reversibility of the equations shown ranges from being facile to being non-existent in various systems. Also, as a practical matter, isolability of Type I complexes in pure form or even as major solute species may depend critically on steric factors associated with the other ligands present, since both kinetic and thermodynamic factors commonly favor conversion of Type I intermediates into Type II final products (Wilkins 1971).

For simplicity of electron bookkeeping, it is common and convenient to consider Type I compounds as containing a superoxide O_2^{1-} ion coordinated to a Co^{3+} center, and Type II compounds as containing a peroxide O_2^{2-} ion bridging two Co^{3+} centers. The degree to which these descriptions are realistic has been a subject of great controversy. According to the hypotheses of Schmidt (1971) and Joedicke (1976), compounds of Type I are of relevance in the present study as postulated autoxidation reaction intermediates, so major attention will be focused on them. Compounds of Type II were postulated to be involved in an alternative autoxidation path encountered in the latter stages of the reaction.

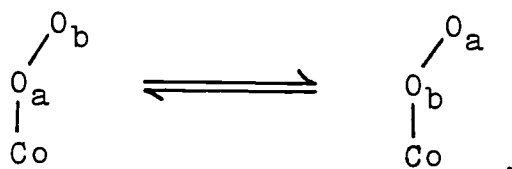
Most Type I compounds have been prepared starting with low-spin approximately square planar cobalt(II) chelates. Before oxygenation, coordination of an additional monodentate ligand B in an axial position is often important (Crumbliss and Basolo, 1970; Stynes and

Ibers 1972). Several X-ray structural determinations of Type I compounds have been reported (Rodley and Robinson 1972; Calligaris et al, 1973; Brown and Raymond 1974; Gall and Schaeffer, 1976; Huie et al, 1979). They all agree on the general type of structure,



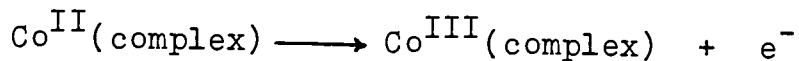
with a Co-O-O angle near 120° and an O-O distance of about 1.26 \AA .

Measurements (Melamud et al, 1974) of the epr spectra using ^{17}O in the dioxygen adducts show that the two oxygens, non-equivalent in glasses and solids, become equivalent in solution, presumably due to the rapid equilibrium

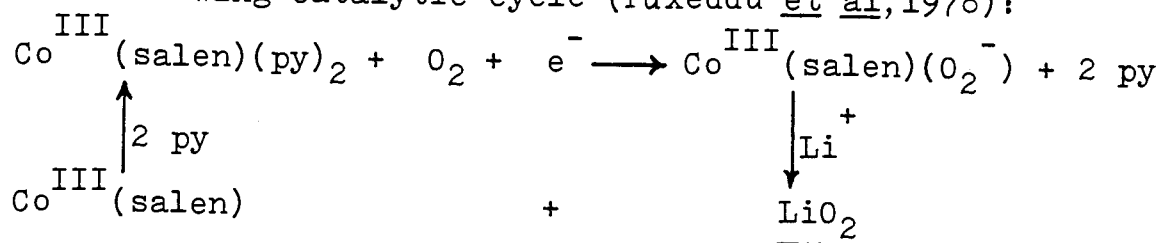


Several pieces of evidence indicate that the $\text{Co}^{\text{III}}(\text{O}_2^-)$ formulation is not a bad first approximation to describing the bonding. First, the O-O distance typically observed is about that of ionic superoxide (1.28 \AA) in contrast to the distances in molecular oxygen (1.21 \AA) and in ionic peroxide (1.49 \AA). Second, for a series of related complexes in which the equilibrium constant for equation (1) could be measured readily

(Carter et al, 1974), a linear relation was found between $\log K_{eq}$ and the polarographic half-wave potential for the reaction of the unoxygenated complexes



suggesting that the same increase in the oxidation number of the cobalt center is common to both reactions. Third, the observation of an 0-0 vibrational frequency at about 1100 cm^{-1} in the infrared and Raman spectra (Szymanski et al 1979) agrees with the frequency observed for superoxide ion (Vaska 1976). Fourth, evidence shows that reaction of superoxide ion with cobalt(III) aquocobalamin (Vitamin B_{12a}) and of molecular oxygen with borohydride-reduced cobalt(II) aquocobalamin give the same product, as determined spectroscopically (Ellis et al, 1973). Also, electrochemical synthesis of lithium superoxide by reduction of molecular oxygen in pyridine has been accomplished using the following catalytic cycle (Puxeddu et al, 1978):



Fifth, the $\text{Co}^{\text{III}}(\text{O}_2^-)$ formalism is supported by X-ray photoelectron spectroscopic results (Burness et al, 1975). Sixth, and by far the most abundant and most controversial source of information on the bonding, is the interpretation of the electron paramagnetic resonance spectra observed for Type I complexes in frozen glasses.

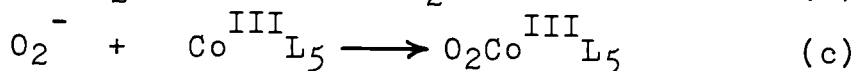
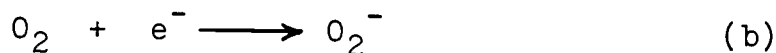
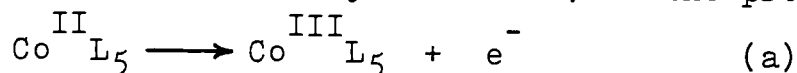
The Type I adducts all have one unpaired electron. (The one report (Willis, 1974) of a cobalt(II) dioxygen adduct with three unpaired electrons is now considered by experts in the field to be in error (Basolo, 1977)). The seminal paper in the detection and interpretation of the epr spectra is that of Hoffman, Diemente, and Basolo (1970), who studied cobalt complexes with Schiff base chelating ligands occupying four coordination positions in the xy plane and various pyridine bases in a z axial position, with the dioxygen molecule trans to it. Whereas the cobalt complexes prior to oxygenation had g_{\perp} of 2.3 - 2.45 and g_{\parallel} close to 2.0, the latter having a hyperfine splitting of about 80 G into an 8-line pattern by $^{59}\text{Co}(I=7/2, \text{ natural abundance } 100 \%)$, upon oxygenation the epr spectra undergo dramatic changes, giving a more symmetrical signal at about $g=2$ and with the hyperfine splitting greatly reduced to about 10-12 G. Their interpretation of the resolved spectrum was that the unpaired spin is located predominantly (ca. 90 %) on oxygen, whereas prior to oxygenation it was in the cobalt d_{z^2} orbital. Hence, cobalt(II) has been oxidized to cobalt(III) and dioxygen reduced to superoxide ion. The degeneracy of the $2p\pi^*$ orbitals of O_2 has been lifted, and the coordinated O_2 does not possess axial symmetry, in accord with the X-ray structural results obtained subsequently.

This interpretation has been repeatedly criticized by Drago; for example, see Drago(1979) and references therein. At first, he preferred a formulation in which a singlet state dioxygen ligand was coordinated to a cobalt(II) center. More recently, he has emphasized that the degree of electron transfer from cobalt to dioxygen on adduct formation is variable, commonly very much less than the 90% or so found by Hoffman et al, and that the unpaired spin density resides mostly on oxygen regardless of the degree of charge transfer. Drago's point of view has not been well-received nor found helpful (Getz et al, 1975), nor has it been assisted by the finding (Hoffman et al, 1975) that some of Drago's reported experimental work was incorrect. In addition, interpretation of the ^{17}O hyperfine splitting when $^{16}\text{O}^{17}\text{O}$ or $^{17}\text{O}_2$ were used to form the adduct supported the cobalt(III)-superoxide formulation (Howe and Lunsford, 1975).

A very large number of papers has been published since 1970 on epr spectra of cobalt(II) dioxygen adducts, with results and interpretations commonly along the lines given by Hoffman et al (1970). The work of Collman's group on cobalt(II) picket fence porphyrin dioxygen adducts is a particularly well-known example (Collman et al, 1974). Resolvability of the epr spectra has been

found to be very sensitive to the quality of the frozen glass, i.e., to the physical properties of the solvent (Walker 1970).

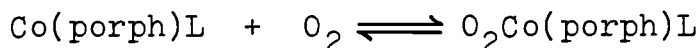
Most of the starting complexes have had cobalt(II) in the low-spin state (one unpaired electron) prior to oxygenation, but this is not a pre-requisite, as several examples have been reported of high-spin (three unpaired electrons) cobalt complex precursors to low-spin dioxygen adducts (Howe and Lunsford, 1975; Khare et al, 1976). Indeed, such adducts are intermediates in the classical syntheses of hexamminecobalt(III) ion and related Werner complexes by air oxidation of high-spin ammoniacal aqueous cobalt(II) species (Sykes and Weil 1970). Ochiai (1973) claimed that while there is no orbital (symmetry) restriction for the oxygenation of high-spin cobalt(II) complexes, the need to reorganize the spin state would be unfavorable thermodynamically. That is, in the process



the electron transfer in step (a) would be far less unfavorable in the case of a low-spin complex, thus favoring the exothermicity of the over-all process. It is not clear how such an energy comparison can be separated into kinetic and thermodynamic factors, as the need for spin reorganization in going to the transition state

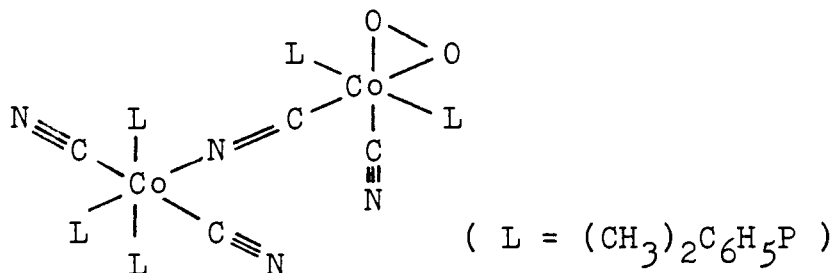
would be reflected in a large energy of activation.

Most of the complexes studied have involved ligands with nitrogen and oxygen donors rather than phosphorus ligands of the type of interest in this work, although Wayland and Abd-Elmageed (1974) did observe the epr spectra of adducts $O_2Co(TPP)L$, where TPP is the tetraphenylporphyrin dinegative ion and L is a series of ligands including triethylphosphine and triethyl phosphite. Takayanagi et al (1975) used a similar substituted porphyrin in their studies of the equilibria

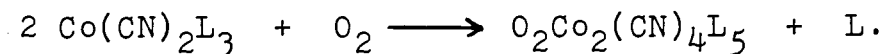


where L includes trimethyl phosphite, tributylphosphine, and triphenylphosphine.

The only work with a complex of the type CoX_2L_2 or CoX_2L_3 , where X is a halide or pseudohalide ion and L is a monodentate phosphorus donor, involved the synthesis and structural characterization of a completely atypical cyano-bridged adduct



formed by the reaction (Halpern et al, 1975)

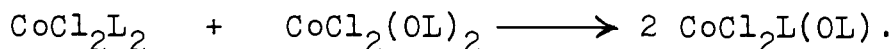


E. Autoxidation of Coordinated Phosphorus Ligands

Schmidt studied the autoxidation of dichlorobis(triethylphosphine)cobalt(II) in benzene solution (Schmidt, 1971; Schmidt and Yoke, 1971). The following facts were established:

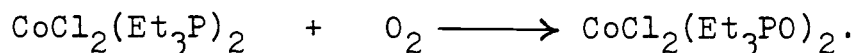
- (1) The phosphine oxide (in its cobalt chloride complex) is the sole product of the oxidation of the phosphine.
- (2) The reaction is not subject to radical initiation or inhibition.
- (3) The rate law in the initial stages of the reaction is

$$- d[O_2]/dt = k \cdot [CoCl_2L_2] \cdot [PO_2].$$
- (4) As product is formed, it reacts with starting material in a redistribution,

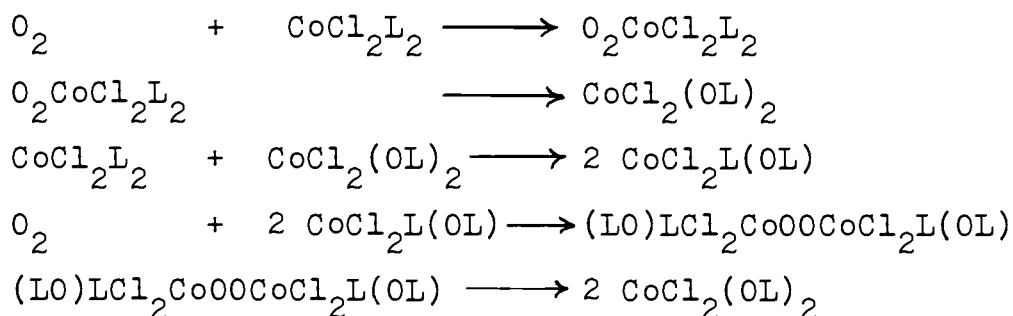


Associated with this is a slow-down in autoxidation and deviation from the simple second order rate law.

However, eventual formation of $CoCl_2(OL)_2$ is quantitative, according to the equation



The following mechanism was postulated:



Joedicke (1976) determined the products of the exhaustive autoxidation of t-butylbenzene solutions containing the $\text{Et}_n\text{P}(\text{OEt})_{3-n}$, $n = 0 - 2$, ligands at a 3:1 mole ratio to cobalt(II) chloride. At the start, the predominant solute species in these solutions were the CoCl_2L_3 complexes. After complete autoxidation, all volatile materials were pumped away from the reaction mixtures. The non-volatile residues were, in every case, the $\text{CoCl}_2(\text{OL})_2$ complexes, where OL is $\text{Et}_n\text{P}(\text{O})(\text{OEt})_{3-n}$ with no change in the value of n . It was found that the organophosphorus components in the volatile portions had been completely oxidized to phosphoryl compounds in every case. There was no change in the value of n for $n = 0$ or 1 , but for the ethyl diethylphosphinite ligand, $n = 2$, the oxidized product in the volatile portion was found to be 64 % ethyl diethylphosphinate and 36 % diethyl ethylphosphonate.

Joedicke also carried out exhaustive autoxidation reactions using nitrobenzene as solvent, but he found that because of its much lower volatility, pumping the solvent off required elevated temperatures and a much longer time. This was unsatisfactory as it led to partial thermal decomposition of the cobalt chloride phosphoryl complexes.

Joedicke also carried out some limited preliminary kinetic studies of the autoxidation reaction of dichloro-tris(diethyl ethylphosphonite)cobalt(II) in t-butylbenzene

at 1°C. The spectrophotometric experimental method was based on loss of the intense absorption at 438 nm of the green low-spin five-coordinate complex product. The mathematical analyses of the kinetic data gave ambiguous results (Joedicke, 1976).

Hanzlik and Williamson (1976) studied the catalysis of the autoxidation of tri-n-butylphosphine by bis(acetylacetonato)cobalt(II), $\text{Co}(\text{acac})_2$, in acetonitrile. Their results may be summarized as follows:

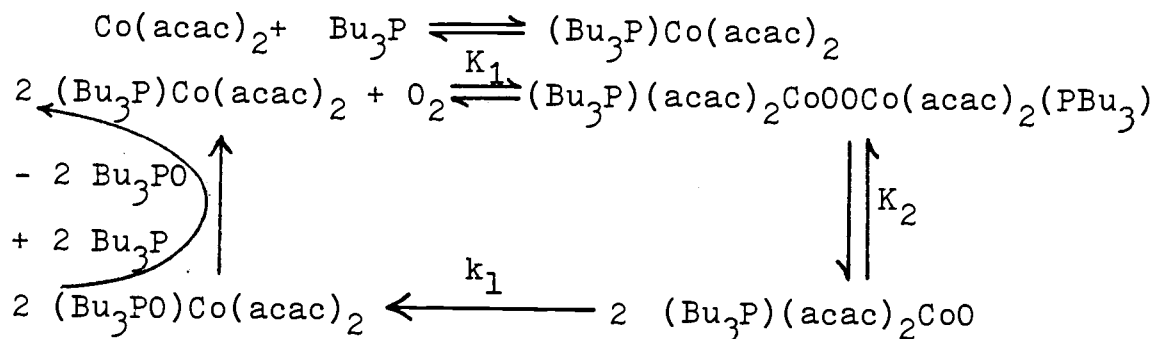
- (1) When tri-n-butylphosphine in acetonitrile at 0°C is stirred under air, three hours must pass before detectable amounts of oxidation products can be found.
- (2) When various free radical inhibitors, such as diphenylamine, are present in concentrations comparable to that of the phosphine, no reaction can be detected in days.
- (3) If, instead, catalytic amounts of $\text{Co}(\text{acac})_2$ are present, a rapid reaction ensues giving the typical free radical $\text{Bu}_n\text{P}(0)(\text{OBu})_{3-n}$ mixed products.
- (4) With both additives present simultaneously, i.e., a relatively large concentration of diphenylamine inhibitor and a catalytic amount of $\text{Co}(\text{acac})_2$, there is a very rapid reaction giving the phosphine oxide Bu_3PO as the sole product.
- (5) Various competitive ligands for cobalt hinder the above reaction. If a very powerful cobalt complexing agent, 2,2'-bipyridyl, is added, the oxidation is

instantly stopped and six-coordinate $\text{Co}(\text{acac})_2(\text{bipy})$ is formed.

- (6) In acetonitrile, chloroform, or toluene solvents, infrared difference spectra of $\text{Co}(\text{acac})_2$ show no difference in the presence versus the absence of molecular oxygen, giving no evidence for the formation of a dioxygen adduct in the absence of tri-n-butylphosphine. Spectroscopic studies in the visible region in the absence of oxygen indicate that $\text{Co}(\text{acac})_2$ and tri-n-butylphosphine form a 1:1 complex, with a formation constant of 40.
- (7) Experimentally, their rate studies involved stirring acetonitrile solutions containing 20-40 mM diphenylamine, 2 - 10 mM $\text{Co}(\text{acac})_2$, and 20-100 mM tri-n-butylphosphine under 1 atmosphere of air or of a prepared N_2/O_2 mixture. Aliquots removed at various times were quenched with 2,2'-bipyridyl and analyzed for tri-n-butylphosphine by direct injection onto a gc column, using the diphenylamine as the internal standard. Plots of $[\text{Bu}_3\text{P}]$ versus time were linear for up to two half-lives, i.e., for a given solution, $-\text{d}[\text{Bu}_3\text{P}]/\text{dt} = \text{constant}$.
- (8) For solutions of constant initial $[\text{Bu}_3\text{P}]$ and $[\text{Co}(\text{acac})_2]$, a plot of log rate versus $\log P_{\text{O}_2}$ has a slope of 0.5. For solutions of constant initial $[\text{Bu}_3\text{P}]$ and at constant oxygen pressure, a plot of log rate versus $\log [\text{Co}(\text{acac})_2]$ has a slope of 1.0.

(9) Similar $\text{Co}(\text{acac})_2$ catalyzed oxidation of chiral methylphenylpropylphosphine proceeds with retention of configuration at phosphorus.

Hanzlik and Williamson propose the following mechanism:



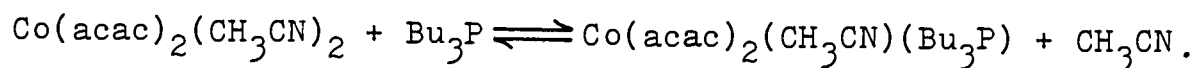
They state, "under typical conditions of a catalytic oxidation ca. 80 % of the cobalt is present as $(\text{Bu}_3\text{P})\text{Co}(\text{acac})_2$, which is assumed to be the catalytically active species, since ligands which form bis adducts of $\text{Co}(\text{acac})_2$ completely quench the catalysis. Oxygen does not interact with $\text{Co}(\text{acac})_2$ in the absence of tri-*n*-butylphosphine. Thus the rate law may be given by the expression:

$$\text{rate} = k [(\text{Bu}_3\text{P})\text{Co}(\text{acac})_2] [\text{O}_2]^{\frac{1}{2}}$$

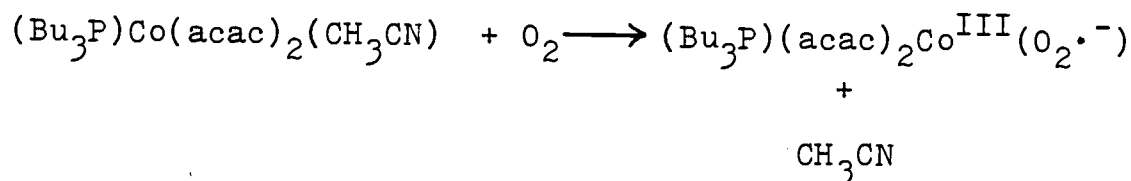
The oxidation of (R)(-)-methylphenylpropylphosphine with retention of configuration is in agreement with an intramolecular rearrangement in the product-forming step and the half order dependence on oxygen concentration can be explained if the formation of $(\text{Bu}_3\text{P})(\text{acac})_2\text{CoO}$ is reversible and k_1 is rate-limiting".

There are a number of problems with the presentation given by Hanzlik and Williamson. First, they fail to

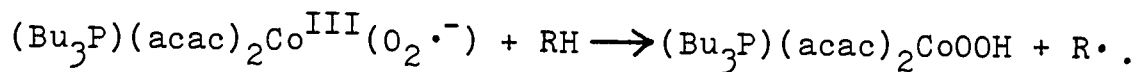
consider the nature of $\text{Co}(\text{acac})_2$ itself. This tetrameric solid is commonly, in donor solvents, a monomeric trans-disolvo six-coordinate complex (Ellern and Ragsdale, 1968). The lability of such complexes is indicated by the facile reaction with 2,2'-bipyridyl to give $[\text{Co}(\text{acac})_2\text{bipy}]$ where each chelate ring must span cis-positions. Presumably the cobalt complex equilibrium studied spectroscopically by Hanzlik and Williamson involved the high-spin six-coordinate species,



Next, they fail to comment on the vigorous free radical type initiation of the autoxidation of tri-n-butylphosphine to $\text{Bu}_n\text{P}(\text{O})(\text{OBu})_{3-n}$ mixed products by $\text{Co}(\text{acac})_2$ in the absence of diphenylamine. One possibility is that the reaction starts with

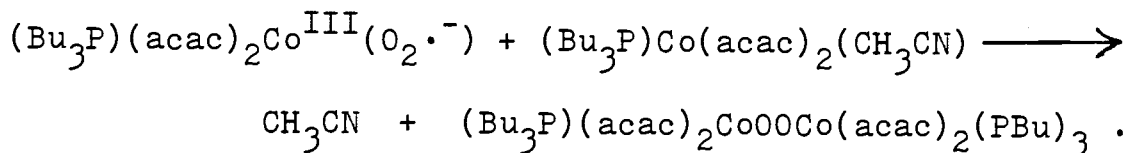


and that the cobalt(III)-superoxide somehow initiates Buckler's radical chain sequence shown in Figure I, leading to mixed products. Presumably hydrogen atom abstraction, e.g., from the solvent, would lead to initiation,



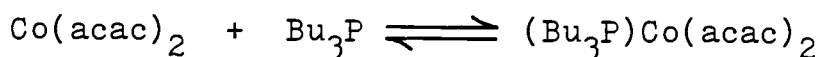
Reactions of this type have been demonstrated previously (Abel, et al 1974). Simultaneously, the mechanistic scheme of Hanzlik and Williamson given above would be brought about

by the reaction



The role of the diphenylamine inhibitor, then, would be to prevent the former but not the latter sequence.

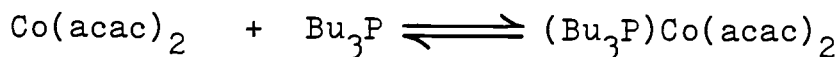
Another problem in Hanzlik and Williamson's presentation is that using $K_{\text{eq}} = 40$ and calculating the concentrations of species initially present in the equilibrium



for the actual solutions studied, one finds that almost exactly 50 % of the cobalt was present in the $\text{Co}(\text{acac})_2$ form in all cases, in contrast to their claim that it was nearly all in the $(\text{Bu}_3\text{P})\text{Co}(\text{acac})_2$ form.

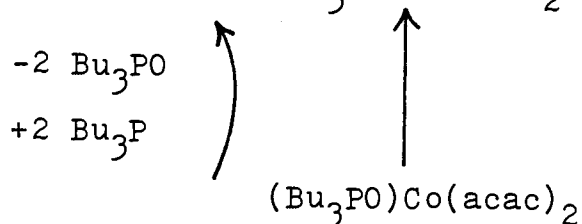
Their quantitative data are presented in the form of two graphs only, and numerical values cannot be extracted from these because of an error in labelling the ordinate units. The error is not a simple misprint, as sample calculations based on that assumption give impossible results.

Hanzlik and Williamson ignore the effect of consumption of phosphine and of the build-up of phosphine oxide on the cobalt species present. The former effect would shift the equilibrium



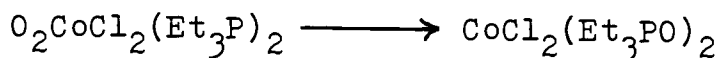
to the left, progressively inhibiting catalysis, although

phosphine concentration-time plots were said to be linear up to two half-lives. The second effect might further remove cobalt from the catalytically active species by the build-up of phosphine oxide complexes. The step shown in their mechanism as $(\text{Bu}_3\text{P})\text{Co}(\text{acac})_2$

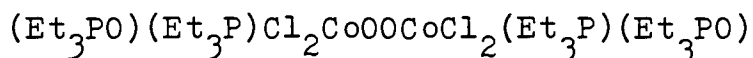
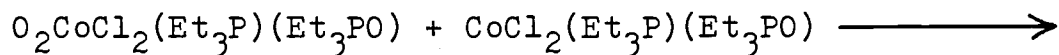
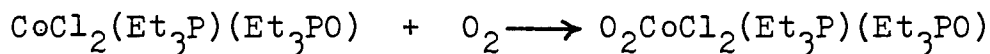


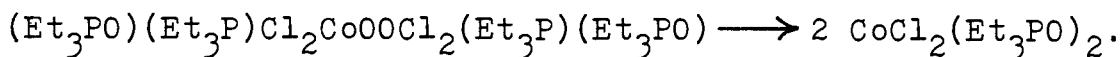
ignores this.

Finally, the equilibrium homolysis and reformation of the O-O bond shown prior to the rate determining step as $(\text{Bu}_3\text{P})(\text{acac})_2\text{CoOOC}(\text{acac})_2(\text{PBu}_3) \longrightarrow 2 (\text{Bu}_3\text{P})(\text{acac})_2\text{CoO}$ seems unreasonable. It contrasts with the emphasis placed by Schmidt on a mechanism in which the rupture of the O-O bond was compensated energetically by the formation of two P=O bonds. Thus Schmidt's complex with two oxidizable phosphine ligands could form a mononuclear O_2 adduct and undergo the reaction



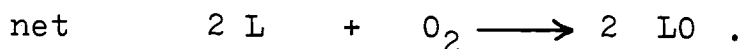
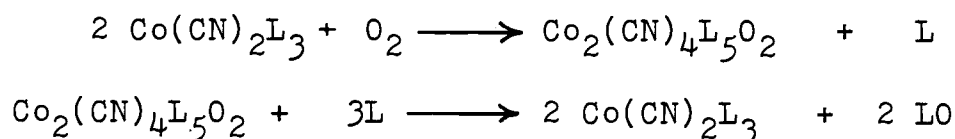
whereas a complex with only one oxidizable phosphine ligand must undergo the more complex sequence





The cleavage of the O-O bond in the last step shown was presumed to be simultaneous with the formation of the two new P=O bonds. Picturing the binuclear cobalt(II)-dioxygen adducts as having peroxide bridge two cobalt(III) centers, the species shown in Hanzlik and Williamson's mechanism as formed by the homolysis of the peroxide bridge could be written as $(\text{Bu}_3\text{P})(\text{acac})_2\text{Co}^{\text{III}}\text{O}\cdot$. Similar homolysis in $(\text{amine})_3(\text{carboxylate})_2\text{CoOOC}(\text{carboxylate})_2(\text{amine})_3$ systems was observed in the temperature range 70-110° with an activation energy of 28 kcal/mol; the cleavage product initiated copolymerization of styrene and methyl methacrylate (Henrici-Olivé and Olivé, 1973). Hanzlik and Williamson's reactions were at 0° C. If such homolytic cleavage occurred in their system, it is hard to see why the product radical would not initiate Buckler's chain leading to mixed phosphoryl products, and why it should not be quenched by reaction with diphenylamine. In addition, there is no reason why its further reaction to give the phosphine oxide should be rate determining, should be exclusively intramolecular, or should go with retention of configuration at phosphorus. The oxygen atom and phosphine ligands in the postulated $(\text{Bu}_3\text{P})(\text{acac})_2\text{CoO}\cdot$ species would presumably be trans-to each other in the coordination sphere of cobalt.

Most of the studies of autoxidation of phosphines coordinated to cobalt(II) have involved aromatic or partly aromatic phosphines. For example, the autoxidation of P, P,P',P'-tetraphenylethylenediphosphine (DPE) in the complex $[\text{Co}(\text{CN})(\text{DPE})]^+$ to the diphosphine dioxide has been reported (Rigo and Bressan, 1973). A study of catalysis of autoxidation of triphenylphosphine to triphenylphosphine oxide by various cobalt(II) chelates has been described (Hanzlik and Smith, 1974). The unique cobalt(II) cyanide-dimethylphenylphosphine(L)-dioxygen adduct of Halpern and co-workers (1975) is involved in a catalytic cycle,



Work on the autoxidation, and catalytic cycles involving the autoxidation, of triphenylphosphine coordinated to other metal centers such as in Vaska's complex $\text{Ir}(\text{PPh}_3)_2(\text{CO})\text{Cl}$ and in the coordinatively unsaturated species formed by partial dissociation of $\text{M}(\text{PPh}_3)_4$ ($\text{M} = \text{Ni}, \text{Pd}, \text{Pt}$) is very well known (for example, see Cotton and Wilkinson, 1972). Use of aromatic phosphines in research in this laboratory has always been avoided because they do not provide the opportunity, which aliphatic phosphines give, to distinguish between autoxidation of dissociated or free ligand (to mixed

products via Buckler's mechanism) and of coordinated phosphine (to a phosphine oxide product only). Indeed, it has been found that results of autoxidation studies involving aromatic phosphines may depend markedly on room illumination (Geoffroy et al, 1976). Aliphatic phosphorus ligands are certainly to be preferred.

III. EXPERIMENTAL

A. Materials

1. Solvents.

a. Benzene. Benzene (Reagent Grade) was refluxed with sodium ribbon for one hour and then distilled at atmospheric pressure under nitrogen, b. $78-79^{\circ}$. The purity of the benzene was checked by gc. It was stored over Molecular Sieves.

b. t-Butylbenzene. t-Butylbenzene (Aldrich, 99 %) was refluxed over molten sodium for several hours and then distilled under atmospheric pressure. The middle fraction (b. 166°) was collected, degassed on the vacuum line, and stored under nitrogen in the dry box.

c. Other Solvents. n-Hexane was allowed to stand over sodium ribbon and then distilled under nitrogen, b. 68° . o-Dichlorobenzene (MCB), distilled from phosphorus pentoxide, and cyclohexane, Spectroquality Grade, distilled from sodium had been purified by Joedicke (1976) and stored under nitrogen in the dry box.

2. Reagents.

a. Ethanol. Ethanol (100 % Reagent Grade) was refluxed with magnesium turnings with a few drops of ethyl

bromide added for four hours. It was then distilled from the ethoxide under one atmosphere of nitrogen. The forerun was discarded and the fraction boiling in the range 77.2 - 78.0° was collected.

b. N, N-Diethylaniline. N, N-Diethylaniline (MCB) was distilled under a reduced pressure. The fractions collected on various occasions had boiling ranges as follows: 56-58°/1 torr; 74-76°/3 torr; 68-70°/2 torr.

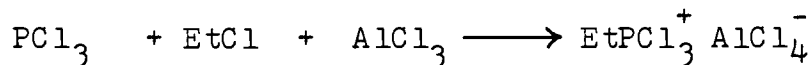
c. Cobalt(II) Chloride. Anhydrous cobalt(II) chloride was prepared from the hexahydrate (Mallinckrodt Reagent) by heating it in a stream of hydrogen chloride until the color changed from purple to light blue throughout.

d. Tetraethyl Lead. This was a gift from the Ethyl Corporation and was used as received.

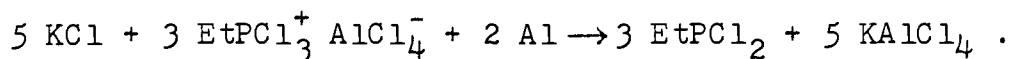
e. Phosphorus Trichloride. Phosphorus trichloride (Reagent Grade) was distilled under one atmosphere of nitrogen, b. 74-75°.

f. Ethyldichlorophosphine. Ethyldichlorophosphine, EtPCl_2 , was in part a gift from the Ethyl Corporation, used as received. Another part was prepared according to the procedure of Kharasch, et al (1949) by the reaction of tetraethyl lead with phosphorus trichloride, which has been used previously in this laboratory (Studer 1972, Joedicke 1976). Because it was felt that there was a need for a preparative route using more readily available starting materials, work was done on the preparation of additional

amounts of ethyldichlorophosphine by methods previously described in the literature and which require only phosphorus trichloride, ethyl chloride, aluminum chloride, and aluminum. The synthesis involves two steps, first (Kinnear and Perren, 1952) the preparation of ethyltrichlorophosphonium tetrachloroaluminate by the reaction



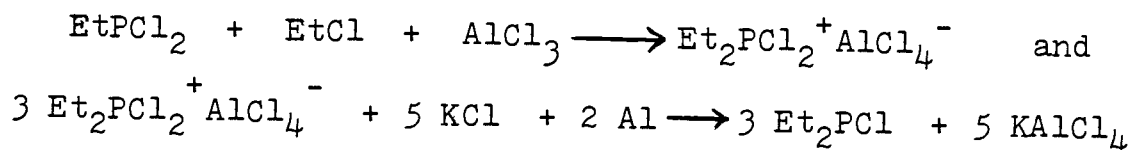
and next its reduction with aluminum (Komkov, et al 1958),



The reactions were run on various scales. In a typical synthesis, 36.1 g (0.271 mol) of anhydrous aluminum chloride (Mallinckrodt) and 34.4 g (.25mol) of phosphorus trichloride were placed in a chilled Parr bomb. A graduated cylinder was pre-cooled to about 5°, and 25.5 ml (.357 mol) of liquid ethyl chloride (b. 13°) was drained into it from an inverted pressurized cylinder (Matheson). The ethyl chloride was quickly transferred to the bomb, which was sealed and shaken mechanically for 50 minutes. It was then set in a 100° oil bath for 50 minutes. The bomb was then cooled and opened, allowing the excess ethyl chloride to vaporize and escape. The product, $\text{EtPCl}_3^+ \text{AlCl}_4^-$, was obtained as a white solid or thick slurry. The weight of this residue was typically 96-100 % of theory. It was then transferred to a 300 ml three neck round bottom flask which was fitted with a glass stirrer rod and paddle, a distilling head, condenser, and receiver leading to a mineral oil bubbler, and a solids

addition flask containing 38 g (0.5 mol) of freshly dried potassium chloride and 4.5 g (0.165 mol) of aluminum powder, thoroughly mixed. Under nitrogen, about one-tenth of the mixed powder was first added to the $\text{EtCl}_3^+\text{AlCl}_4^-$ in the flask and the stirrer rod and paddle were turned manually to mix the solids. The mixture was then heated carefully to induce the oxidation-reduction reaction, which is markedly exothermic. The mixture melted quickly and reacted vigorously, causing much of the ethyldichlorophosphine to distill into the receiver as it was formed. CAUTION: explosion and fire hazard. Gradually the rest of the potassium chloride-aluminum mixture was added in portions and the reaction mixture heated very carefully after each addition as needed to initiate reaction. After all had been added, the reaction flask was heated to cause distillation of the remaining ethyldichlorophosphine. Variable yields from zero to 87 % were obtained. The crude ethyldichlorophosphine was redistilled under nitrogen, b. 110-112°.

g. Diethylchlorophosphine. Diethylchlorophosphine, Et_2PCl , was prepared from ethyldichlorophosphine and tetraethyl lead (Beeby and Mann 1951). Yields up to 62 % were obtained, b. 80-84°/147 torr; 129-131°/760 torr of nitrogen. Attempts to prepare it by the reactions



gave very poor yields in the first step even with extended shaking and heating times. In addition, the second step tended to be uncontrollably violent (Urban 1977).

h. Azobisisobutyronitrile (AIBN). The commercial AIBN (Aldrich, 2,2'-azobis(2-methylpropionitrile)) was found to have a melting point of 102-103° (lit. 102-104°, Schmidt 1971) and so was used without further purification.

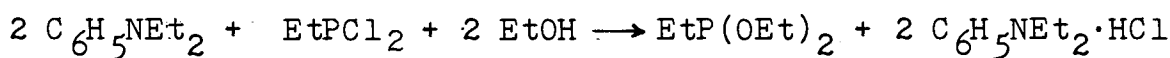
i. Oxygen. Oxygen (Airco, compressed gas) was used as received.

j. Air. Compressed air from a cylinder (Airco) was passed through a large tower of Drierite.

3. Organophosphorus Esters and Their Phosphoryl Derivatives

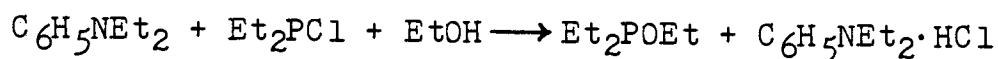
a. Triethyl Phosphite. Commercial triethyl phosphite (MCB) was refluxed over molten sodium for two hours and then distilled under nitrogen through a Vigreux column, b. 152°.

b. Diethyl Ethylphosphonite. This was prepared, using the same procedure described by Joedicke (1976), from N,N-diethylaniline, ethyldichlorophosphine, and ethanol in n-hexane solution. The reaction is



The yield was 59 %. The product was distilled; boiling ranges observed on various occasions were as follows: 47-48° / 17 torr, 52-53° / 24 torr; 137° / 760 torr of nitrogen. Lit. b. 43° / 15 torr (Joedicke 1976).

c. Ethyl Diethylphosphinite. In the same manner, this was prepared from N, N-diethylaniline, diethylchlorophosphine, and ethanol by the reaction



The yield was 61 % ; b. $80-84^\circ / 147$ torr; $130-134^\circ / 760$ torr of nitrogen; lit. $83-87^\circ / 151$ torr (Joedicke, 1976).

d. Triethylphosphine. This was recovered from the silver iodide complex $[\text{AgI} \cdot \text{Et}_3\text{P}]_4$, prepared by Schmidt (1972), by slowly heating the solid adduct on the vacuum line. The yield of recovered triethylphosphine was 77 % of theory. Its purity was established by gc.

e. Ethyl Diethylphosphinate. This was prepared by the Arbuzov isomerization of diethyl ethylphosphonite (13.2 g, 0.0879 mol) which was refluxed under nitrogen for 7 hours with ethyl iodide (10 g) (Schmidt 1971). The ethyl iodide catalyst was removed in vacuo and the remaining ethyl diethylphosphinate was purified by distillation, b. $90-90.5^\circ / 10$ torr; $207-209^\circ / 760$ torr; lit. $91^\circ / 12$ torr (Joedicke 1976). The yield was over 90 %.

f. Diethyl Ethylphosphonate. A sample which had been prepared by Joedicke (1976) was redistilled, b. $200-202^\circ$.

g. Triethyl Phosphate. A commercial sample (Eastman) was distilled, b. $87-88^\circ / 7$ torr of nitrogen (lit. $215-216^\circ$)

4. Complexes.

a. Dichlorobis(triethylphosphine)cobalt(II). As

described by Schmidt (1971), 4.2 g of triethylphosphine was condensed into a solution of 4.2 g of cobalt(II) chloride hexahydrate in 15 ml of ethanol in a flask on the vacuum line. The mixture was kept at 0° for four hours. The blue crystalline precipitate was filtered in the nitrogen-filled glove box, washed with a little chilled ethanol, and dried on the vacuum line overnight; m. 100.5-101.0° (sealed tube); lit. 101-102° (Jensen, 1963); 102° (Nicolini, et al 1965); 100-102° (Schmidt, 1970).

B. Techniques.

The phosphorus esters, their complexes and solutions, and other sensitive reagents were stored and handled under purified nitrogen in a Forma Model 3818 stainless steel drybox fitted with a #3851 evacuable interchange assembly. The nitrogen (Pre-Purified Grade) atmosphere was kept dry and oxygen-free by means of continuous circulation through Linde Molecular Sieve columns (13A, 5A, and 4A) and an oxygen scrubbing tower containing heated BTS (supported activated copper) catalyst. Entrance to the drybox was through an evacuable port.

A standard glass high vacuum line (pressure ca. 10^{-5} torr), fitted with a removable U tube, was used in parts of the syntheses, in degassing solvents and reagents, and in the separation of components of reaction mixtures. Dow Corning silicone high vacuum grease was used on

stopcocks and ground glass joints. Vapor pressures were measured using mercury manometers and a meter stick.

The preparations and distillations of air-sensitive materials were conducted under Pre-Purified nitrogen. Reduced pressure, when needed, was maintained using a mercury manostat. Vacuum distillations were conducted using a nitrogen bleed capillary. Chlorophosphines and phosphorus esters were sometimes purified by distillation using a Teflon spinning band column.

A dilatometer constructed using the stem of a 1 ml pipet graduated in 0.01 ml increments and with a calibrated 5 ml bulb was used for the determination of liquid densities as a function of temperature. The tared apparatus was loaded with the liquid to be measured in the dry box and the assembly and its contents were then weighed accurately. The stem stopcock was attached to a T-Connection with one arm leading to a nitrogen source and the other to a bubbler. The dilatometer bulb was immersed in a stirred water bath whose temperature was regulated by a Tempunit Model TU-8 controller to $\pm 0.1^{\circ}$. The stem volume V_s was measured to ± 0.001 ml at various temperatures in the range $10-45^{\circ}$. The density at temperature t is given by $d_t = M/V_{\text{total}}$ where M is the mass of sample used and $V_{\text{total}} = V_o + V_s$. Calibrations of the bulb volume V_o were described by Joedicke (1976). Satisfactory analyses of the data were obtained using the linear relationship $d_t = a - bt$ by the

method of least squares as indicated by the closeness of the linear correlation coefficients to unity.

A Haake circulator was used to regulate the temperature of the cell compartment of the Spectronic 600 spectrophotometer during kinetic studies of the decomposition of cobalt(II)-dioxygen adducts. For this purpose, methanol was circulated through a long copper coil immersed in a large styrofoam picnic cooler containing an appropriate cold bath. The cooled methanol then circulated continuously through the spectrophotometer cell block.

In kinetic studies of the autoxidation of free ligands and complexes, the Haake circulator containing water was used to provide a constant temperature. The reaction mixtures were placed in pear-shaped flasks which were immersed in a water bath containing a copper coil through which water passed from the constant temperature circulator. The temperature of the bath was measured with a mercury thermometer and was constant to $\pm 0.5^{\circ}$ at 25° or to $\pm 1^{\circ}$ at 50° . Time was measured with a Precision Time-It Model timer. The apparatus and techniques for the autoxidation studies have been described by Joedicke (1976).

C. Instrumentation

1. Melting Point Determinations.

Melting points of solid samples were determined using

a Laboratory Devices Mel-Temp apparatus (uncorrected).

Capillary melting point tubes were loaded with the powdered solid sample and capped with silicone putty in the dry box and then sealed off with a torch.

2. Gas Chromatography

An F & M Model 700 gas chromatograph with a thermal conductivity detector and a temperature programmer was used to check the purity of solvents and ligands and to analyze the products of autoxidation of free ligands and their complexes both qualitatively and quantitatively. Helium carrier gas was used. A Sargent Model SR recorder was used.

3. Infrared Spectra

Perkin-Elmer Model 621 and Model 712B spectrophotometers were used to check the solvent, phosphorus ligands, and their complexes. Infrared spectra of these compounds were compared to those tabulated by Studer (1972) to ensure the absence of hydrolysis or of Arbuzov isomerization. Spectra were obtained using thin films in sodium chloride cells. The wavelength scale was calibrated with the spectrum of a polystyrene film.

4. Visible Spectra

A Spectronic 600 spectrophotometer with a constant temperature cell holder in a large cell compartment was

used during the kinetic study of decomposition of a cobalt(II) dioxygen adduct. The cell compartment was flushed with dry nitrogen to prevent fogging at the low temperature used. Absorbance values at selected wavelengths were read directly from the Absorbance/Transmittance meter at various times. The specially designed reaction apparatus shown in Fig. 2 was used to prepare the cobalt(II) dioxygen adduct in solution on the vacuum line at a very low temperature. The apparatus could then be shut off, removed from the vacuum line, and tipped so that the solution could run into the sealed-on spectrophotometer cell. The entire assembly would then fit in the cell compartment for the kinetic study. Pure solvent was used in the reference cell.

5. Nuclear Magnetic Resonance

A varian HA-100 spectrophotometer with a C-6040 Variable Temperature Controller was used for solution paramagnetic susceptibility measurements by the Evans method. The nmr measurements were made by Susan E. Randall.

6. Electron Paramagnetic Resonance

A varian E4 (9 GHz) spectrometer was used for the attempted characterization of an dioxygen adduct

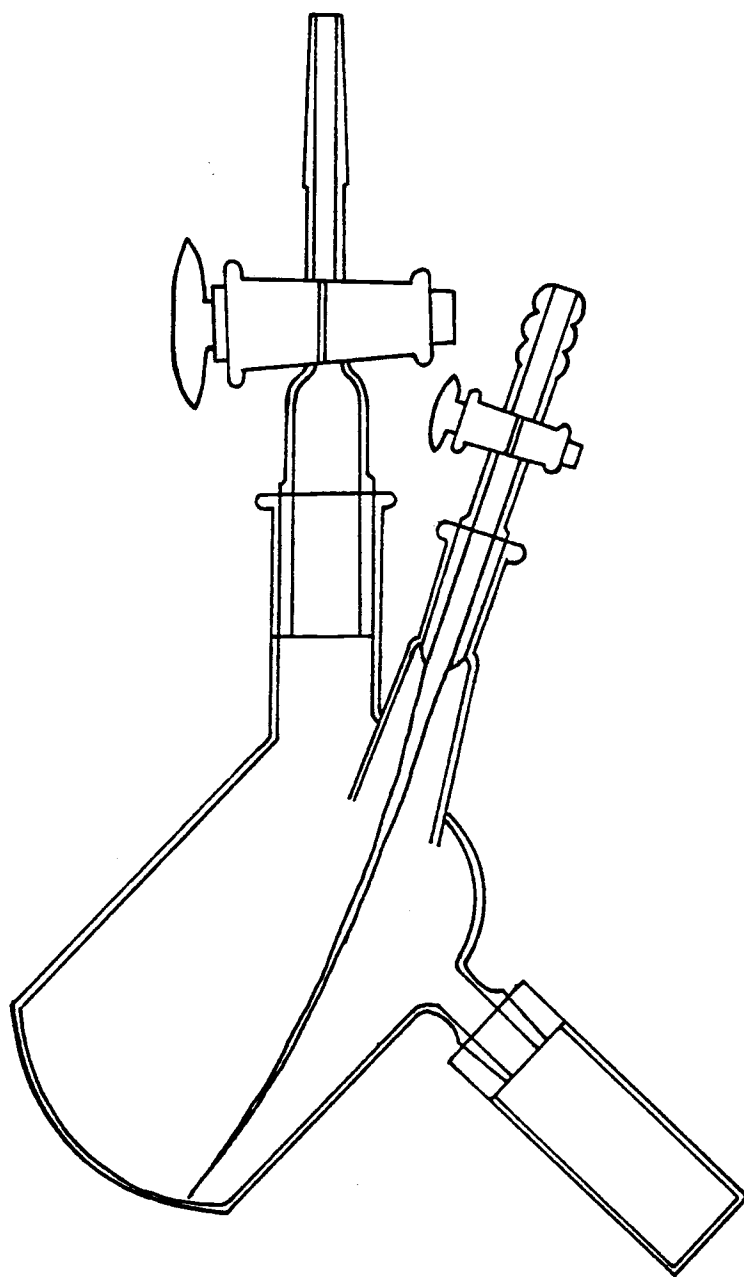


Figure 2. Reaction Apparatus for Study of O_2
Adduct Decomposition

$O_2CoCl_2L_3$. A quartz epr tube which contained the sample solution was immersed in liquid nitrogen in a Dewar flask in the cavity of the instrument for the epr measurements. Operation of the spectrometer was by the courtesy of and under the supervision of Dr. Terry L. Miller of the Department of Agricultural Chemistry.

D. Development of Gas Chromatographic Analytical Methods

1. Introduction

When this research work was initiated, no difficulty was anticipated in the qualitative and quantitative analysis of $Et_nP(OEt)_{3-n}$ and $Et_nP(O)(OEt)_{3-n}$ mixtures in benzene. Reoplex-400 on Chromosorb W columns had been found to be useful for the separation of all peaks in the complete $Bu_nP(OBu)_{3-n}$ and $Bu_nP(O)(OBu)_{3-n}$ series (Feinland, Sass, and Buckler, 1963) and for the quantitative analysis of pairs of compounds $Et_nP(OEt)_{3-n}$ and $Et_nP(O)(OEt)_{3-n}$ for each n (n=0,1,2) in *t*-butylbenzene using *o*-dichlorobenzene as the internal standard (Joedicke, 1976). However, it was quickly found that on this column the benzene solvent could not be resolved from both $EtP(OEt)_2$ and $Et_2P(OEt)$ components. Therefore, work was undertaken to find an appropriate column to bring about separation of $EtP(OEt)_2$ and $Et_2P(OEt)$ from benzene while also resolving all components of the

$\text{Et}_n\text{P}(\text{OEt})_{3-n} + \text{o-C}_6\text{H}_4\text{Cl}_2$ (internal standard) + $\text{Et}_n\text{P}(\text{O})-(\text{OEt})_{3-n}$ mixture, using the F & M instrument with a thermal conductivity detector which was available.

2. Preparation of Columns

Several columns were prepared for evaluation, using the funnel coating method and recipes for solution concentration to give the desired loading described by McNair and Bonelli (1967). A solution of the stationary phase in a suitable solvent was put in a filter flask with the solid support (e.g., 20g of 80-100M Chromosorb W). The pressure was reduced with a water aspirator for several minutes. The vacuum was then released and the flask was allowed to stand for about 15 minutes. The material was transferred to a sintered glass funnel and was allowed to drain. Then vacuum was applied for several minutes. The support was spread on filter paper and allowed to dry in air for some time before being put in an oven at 100° overnight. The coated solid support was next loaded into six-foot 0.25 inch o.d. stainless steel columns with the aid of a hand vibrator. The columns were bounced lightly to aid in the settling of the support. After being coiled, the columns were set in the instrument and conditioned at a temperature about ten degrees higher than the highest oven temperature to be used in the analysis. The exit ends of the columns were left disconnected from the detector during the conditioning.

3. Qualitative Analysis

Qualitative analysis of components of the benzene + $\text{Et}_n\text{P}(\text{OEt})_{3-n}$ + $\text{o-C}_6\text{H}_4\text{Cl}_2$ + $\text{Et}_n\text{P}(\text{O})(\text{OEt})_{3-n}$ mixture showed that the following columns were unsatisfactory for complete resolution of all components: Silicone SE-30 or UC-W 98 on Chromosorb W, Reoplex 400 (polyoxyalkylene adipate) on Chromosorb W, Carbowax 20 M on Chromosorb P, Tetraethylene-pentamine on Fluoropak 80, uncoated Fluoropak 80, uncoated Porapak Q, and STAP (steroid analysis phase) on Chromosorb W. Of these, the Reoplex 400 column satisfactorily resolved the components of a benzene + $\text{P}(\text{OEt})_3$ + $\text{o-C}_6\text{H}_4\text{Cl}_2$ + $\text{Et}_n\text{P}(\text{O})(\text{OEt})_{3-n}$ ($n=0,1,2$) mixture while the UC-W 98 column can separate the components of a benzene + $\text{Et}_n\text{P}(\text{OEt})_{3-n}$ ($n=0,1,2$) + $\text{o-C}_6\text{H}_4\text{Cl}_2$ mixture. It was finally decided to use two columns, each of which could do part of the job as indicated in Table III.

The final operating conditions were as follows. The detector temperature and injection temperature were set at 240 and 190° respectively, and the helium flow rate was adjusted to ca. 50ml/min. The instrument was used in the isothermal mode as programming caused excessive baseline drift. The UC-W 98 column was used for the first injection of sample at 100°.(The other column present in the instrument was the Reoplex 400 column.) The $\text{Et}_n(\text{OEt})_{3-n}$ compounds were analyzed

Table III. Gas Chromatographic Separations

	Silicone UC-W 98	Reoplex 400
$P(OEt)_3$	a	a
$EtP(OEt)_2$	a	d
$Et_2P(OEt)$	a	d
$\underline{o}\text{-C}_6\text{H}_4\text{Cl}_2$	a	c
$P(O)(OEt)_3$	b	c
$EtP(O)(OEt)_2$	b	c
$Et_2P(O)(OEt)$	b	c

(a) Well resolved from all other components if below 120° .

(b) Satisfactory individually but not resolved if present simultaneously with other components marked (b).

(c) Satisfactory. (d) Not resolved from benzene.

with the peaks appearing in the order C_6H_6 (3.5 min), $Et_2P(OEt)$ (10 min), $EtP(OEt)_2$ (12.4 min), $P(OEt)_3$ (15.6 min).

Then the temperature was temporarily increased to 120° and again reduced to 100° to get the $\underline{o}\text{-C}_6\text{H}_4\text{Cl}_2$ peak (ca. 25 min). At a constant temperature of 100° , it took a long time to elute the $\underline{o}\text{-C}_6\text{H}_4\text{Cl}_2$ component, while at a higher temperature the $\underline{o}\text{-C}_6\text{H}_4\text{Cl}_2$ peak was not resolved from the $EtP(O)(OEt)_2$ peak. After the $\underline{o}\text{-C}_6\text{H}_4\text{Cl}_2$ was eluted, the oven temperature was increased to 170° to elute the unresolved $Et_nP(O)(OEt)_{3-n}$ components. The polarity switch to the recorder was then reversed and a second injection of the sample was made on the Reoplex 400 column at 170° .

The unresolved benzene and combined $\text{Et}_n\text{P}(\text{OEt})_{3-n}$ components were quickly eluted, and then resolved peaks for $\text{o-C}_6\text{H}_4\text{Cl}_2$, $\text{EtP}(\text{O})(\text{OEt})_2$, $\text{P}(\text{O})(\text{OEt})_3$, and $\text{Et}_2\text{P}(\text{O})(\text{OEt})$ appeared, eluting in the order given. The chromatograms obtained from two injections are shown in Figures 3 and 4 for illustration. The trivalent phosphorus $\text{Et}_n\text{P}(\text{OEt})_{3-n}$ components were eluted on the UC-W 98 column in the same order which is the order of their boiling points (132° for $n=2$, 137° for $n=1$, 152° for $n=0$). For the phosphoryl compounds $\text{Et}_n(\text{O})(\text{OEt})_{3-n}$, good data are not available for boiling points measured at the same pressure, though it is clear that the $n=1$ compound is the most volatile of the series $n=0,1,2$. This same irregular order is in agreement with the order of elution on a Reoplex 400 column, which is $n=1,0,2$.

4. Quantitative Analysis

Aliquots of varying known concentrations (0.01M to 0.2 M) of authentic samples of pairs of components $\text{Et}_n\text{P}(\text{OEt})_{3-n}$ for each n ($n=0,1,2$) separately in benzene solution were prepared and analyzed with *o*-dichlorobenzene (0.1 or 0.2M) as an internal standard. Two Reoplex 400 columns were used for analysis of the $\text{P}(\text{OEt})_3$ and $\text{P}(\text{O})(\text{OEt})_3$ pair and UC-W 98 columns were used for the other two pairs. Peaks were cut out of the recorder chart paper carefully and weighed on an analytical balance. The standard working curves of

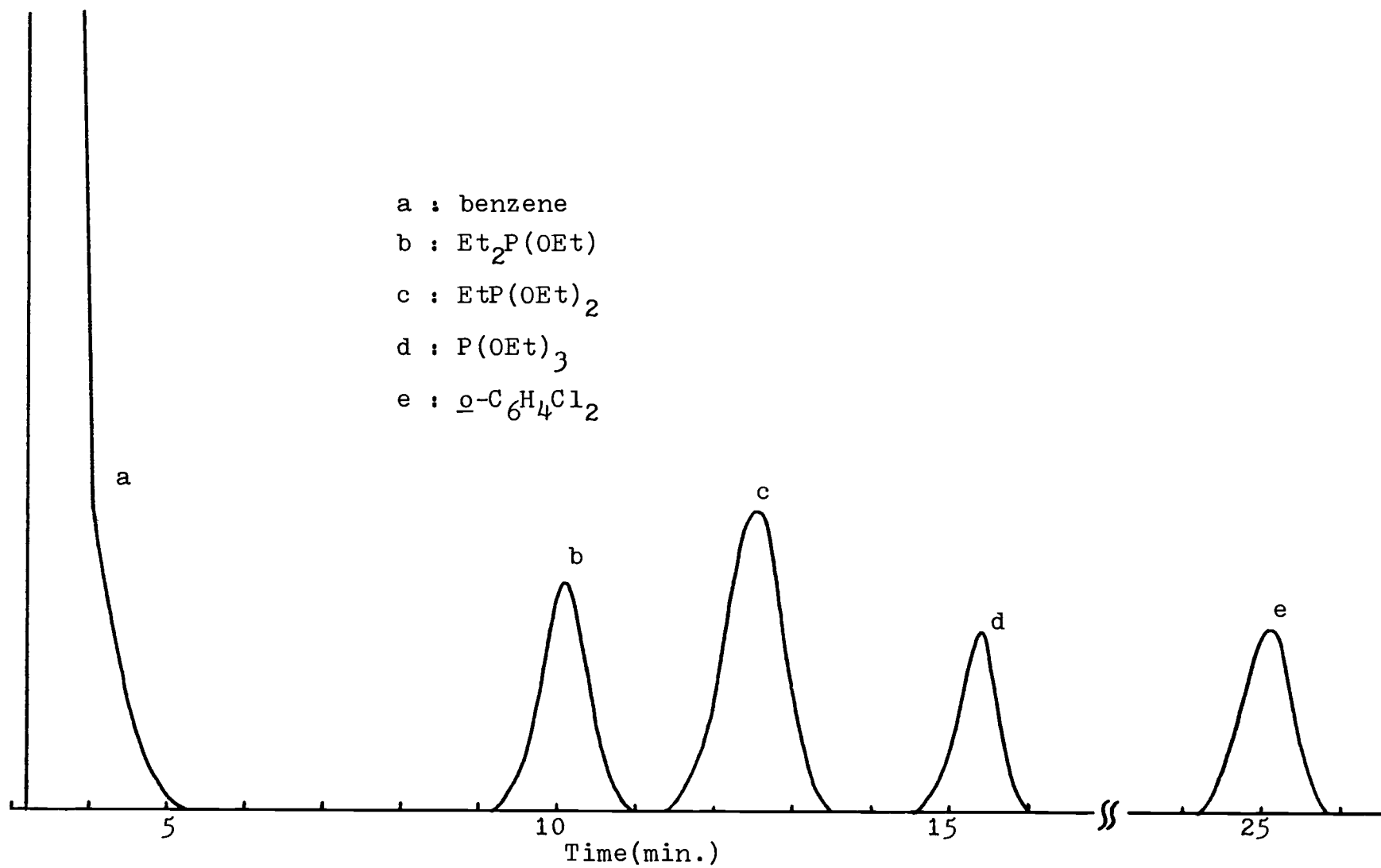


Figure 3. Qualitative G.C. Analysis on a UC-W 98 Column

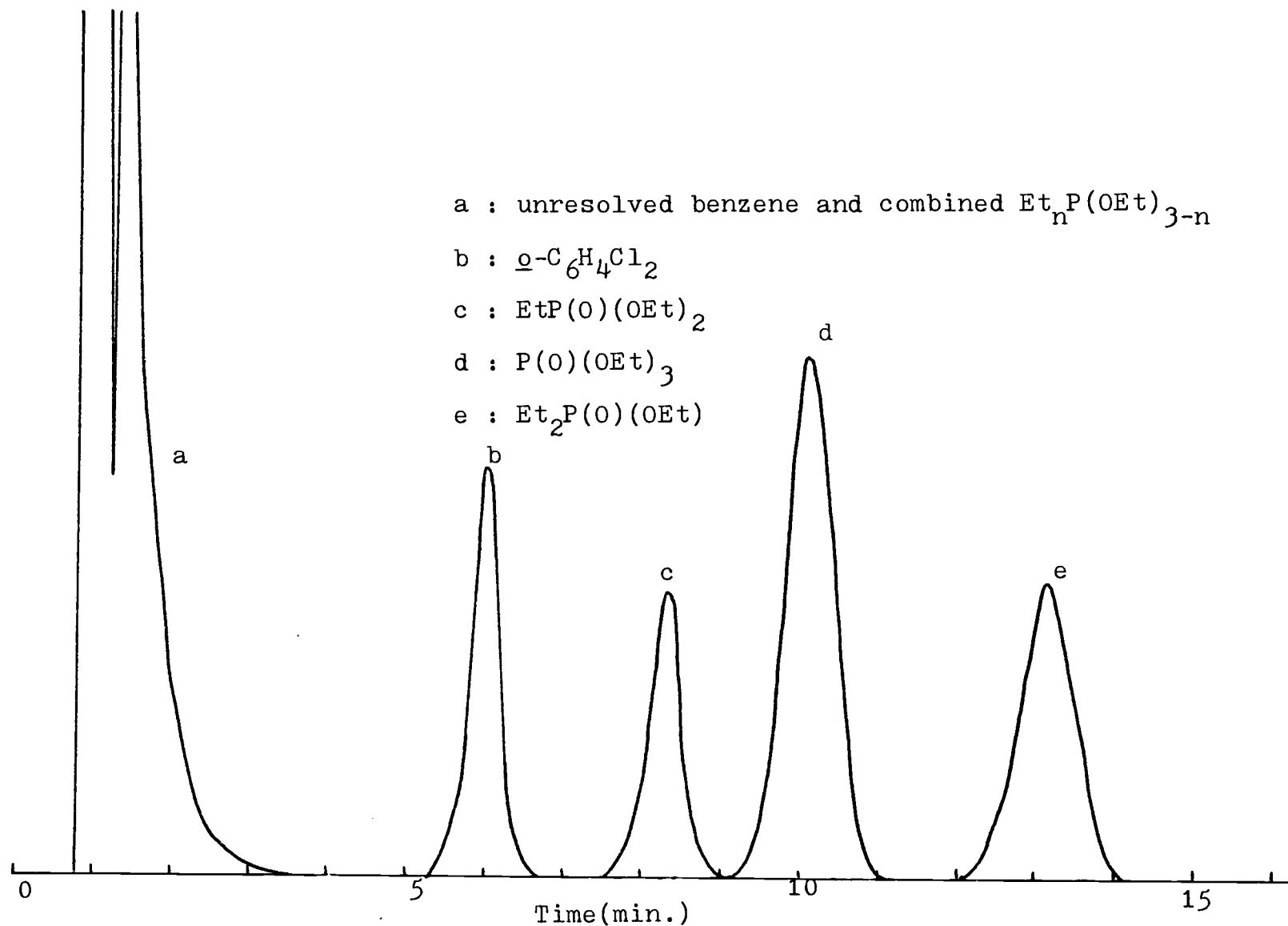


Figure 4. Qualitative G.C. Analysis on a Reoplex 400 Column

peak area vs. concentration of each component relative to the internal standard shown in Figures 5,6, and 7 were obtained. Quantitative analyses of unknown samples were accomplished by using these working curves.

However, when the two different kinds of columns are to be used simultaneously as described in the Qualitative Analysis section, the question arises if the quantitative peak area vs. concentration relation, relative to the internal standard, which was determined on one kind of column, can be used for chromatograms obtained on the other column. According to gas chromatography theory, changing the column packing, flow rate, or temperature should not change the compound : internal standard relationship. This was tested for EtP(O)(OEt)_2 standard solutions in benzene on the Reoplex 400 column. The quantitative results agreed very well with the data for the working curve obtained previously using the UC-W 98 column. Hence it is assumed that for all these compounds the quantitative relation determined on one column can be used with data on the other column, and this is further borne out by the internal consistency of the results.

Certain sources of error should be considered for the gas chromatographic quantitative analysis of the sample solutions. These include questions of the purity of reagents and the exact knowledge of concentrations, temperature, etc., especially when the sample solution was made

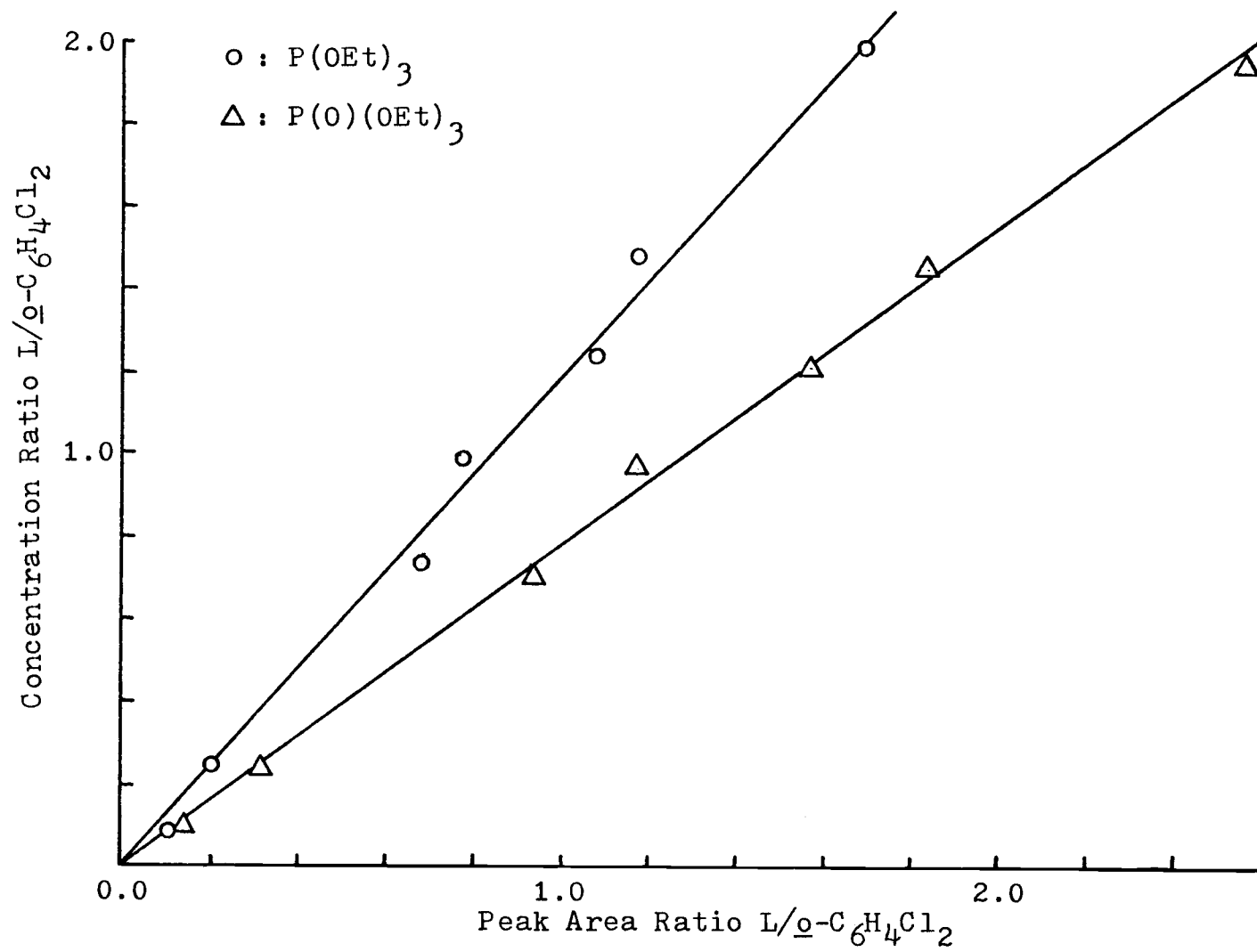


Figure 5. Quantitative G.C. Working Curves for $\text{P}(\text{OEt})_3$ and $\text{P}(\text{O})(\text{OEt})_3$

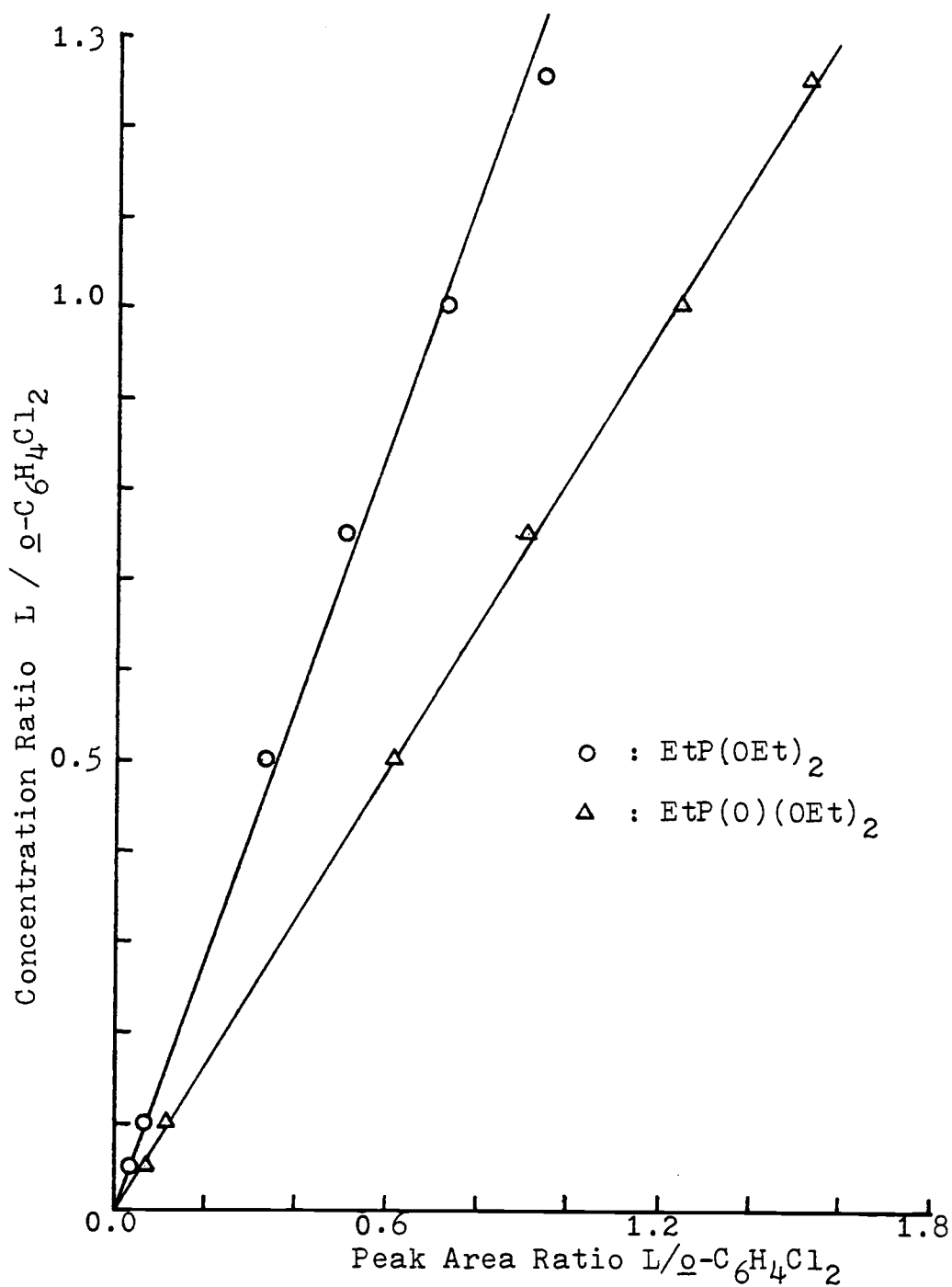


Figure 6. Quantitative G.C. Working Curves for EtP(OEt)₂ and EtP(O)(OEt)₂

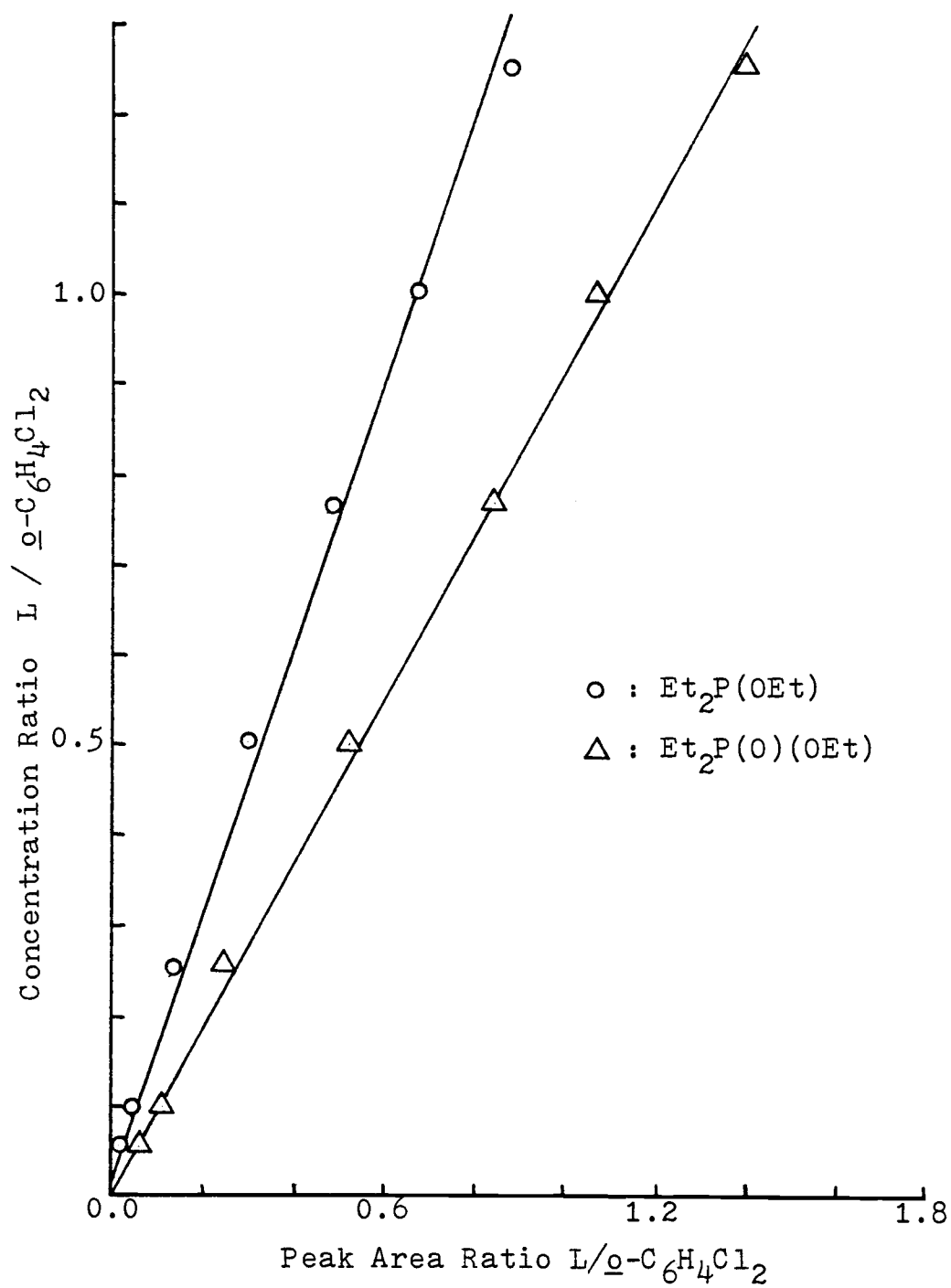
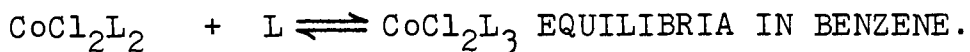


Figure 7. Quantitative G.C. Working Curves for Et₂P(OEt) and Et₂P(O)(OEt)

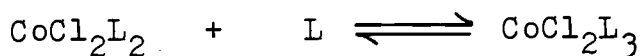
using previously prepared stock solutions. One important source of error lies in the method of handling g.c. data. The cut and weigh method which had been used for this research work is one of the earliest methods of peak area measurement. A time consuming technique at best, it also destroys the chromatogram. The relative precision is 1 to 2 %, which may be compared to the error in integration using electronic integrators and computers(0.1 -0.2 %). This error, if applied to the kinetic work, would cause an error of about 6 % in the rate constant calculation. Also, the baseline shift in some chromatographic processes would cause another error in the peak area measurement.

IV. DETERMINATION OF THE THERMODYNAMIC FUNCTIONS FOR THE



A. Introduction

The coordination chemistry of cobalt(II) chloride with trivalent phosphorus bases has been reviewed in Chapter II Section C. The high-spin complexes CoCl_2L_2 and low-spin complexes CoCl_2L_3 ($\text{L} = \text{Et}_n\text{P}(\text{OEt})_{3-n}$, $n = 0 - 2$) have been prepared and characterized thoroughly in this laboratory by Studer (1972) and Joedicke (1976). They exist in equilibrium,



in solution in organic solvents (Joedicke, Studer, and Yoke, 1976). The equilibrium constants were determined spectrophotometrically in nitrobenzene and in t-butylbenzene, but the results showed poor precision. In further work using t-butylbenzene, it was found that much more satisfactory quantitative results could be obtained using as the experimental method the determination of the paramagnetic susceptibilities of the equilibrium mixtures. Susceptibilities were determined over a range of temperature by the Evans nmr method, permitting calculation of the equilibrium constants and thermodynamic functions for the reactions.

Since the paramagnetism and geometry of these cobalt

complexes are expected to be an important factor in their reaction with the paramagnetic dioxygen molecule, prior knowledge of the distribution of species present in the reaction mixture is a pre-requisite to kinetic studies of autoxidation. Therefore, the equilibrium constants are to be determined in the solvent benzene to be used in the autoxidation reactions, by the same Evans nmr shift method which was worked out in detail by Joedicke.

B. Theory

The molar susceptibility of a single paramagnetic complex in solution can be calculated from the Evans (1959) equation, which when expressed on a molar basis is

$$\chi_M^{\text{cor}} = \frac{3}{2} \frac{\Delta\nu (10^3)}{\pi \nu M} + \chi_o(\text{MW}) + \frac{\chi_o(d_o - d_s)(10^3)}{M} + \text{DC} \quad (1)$$

Here, $\Delta\nu$ is the shift in nmr frequency of a proton resonance of an inert reference compound in the solution due to the presence of the paramagnetic solute, relative to the resonance frequency it would have in the absence of that solute. In addition, ν is the frequency of the spectrometer, χ_o is the diamagnetic gram susceptibility of the solvent, M is the molarity of the complex, MW is the molecular weight of the complex, d_o and d_s are the densities (g/ml) of the solvent and the solution respectively, and DC is the (inherently negative) diamagnetic correction for the complex. Of the four terms on the right hand side of

equation (1) the first is predominant. Joedicke (1976) showed that all three of the minor terms must be included for accuracy.

For an unknown equilibrium mixture of the two complexes CoCl_2L_2 (or A) and CoCl_2L_3 (or B), which have very different magnetic susceptibilities, the observed molar susceptibility

$\chi_{\text{M}_{\text{obs}}}^{\text{cor}}$ of the mixture can be expressed in terms of the solute mole fractions N_A and N_B (which equals $1-N_A$) and the molar susceptibilities $\chi_{\text{M}_A}^{\text{cor}}$ and $\chi_{\text{M}_B}^{\text{cor}}$ of the two individual complexes A and B, i.e.,

$$\chi_{\text{M}_{\text{obs}}}^{\text{cor}} = N_A \chi_{\text{M}_A}^{\text{cor}} + N_B \chi_{\text{M}_B}^{\text{cor}} \quad (2)$$

or

$$\chi_{\text{M}_{\text{obs}}}^{\text{cor}} = \chi_{\text{M}_B}^{\text{cor}} + N_A (\chi_{\text{M}_A}^{\text{cor}} - \chi_{\text{M}_B}^{\text{cor}}) \quad (2a)$$

Therefore, the mole fraction N_A can be expressed as

$$N_A = \frac{\chi_{\text{M}_{\text{obs}}}^{\text{cor}} - \chi_{\text{M}_B}^{\text{cor}}}{\chi_{\text{M}_A}^{\text{cor}} - \chi_{\text{M}_B}^{\text{cor}}} \quad (3)$$

A major advantage of the Evans method is that, in the absence of specific solvent - solute interactions, the susceptibilities of individual complexes are solvent independent and can be used interchangeably in different solvents. Thus, susceptibilities previously obtained in t-butylbenzene for the individual pure complexes CoCl_2L_3

and CoCl_2L_3 can now be used in calculations with data for their equilibrium mixtures in benzene.

The value of $\chi_{\text{M}_{\text{obs}}}^{\text{cor}}$ is to be calculated using equation (1) from the observed $\Delta\nu$ for the equilibrium mixture. However, for that system the values of MW and DC are weighted averages,

$$\text{MW} = N_A (\text{MW})_A + N_B (\text{MW})_B \quad (4)$$

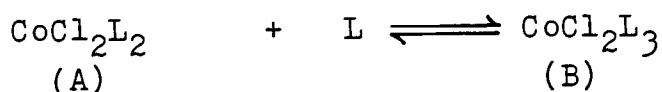
$$\text{and DC} = N_A (\text{DC})_A + N_B (\text{DC})_B \quad (5)$$

where N_A and N_B are not yet known. Therefore, it is necessary to use an approximation, i.e., to calculate a trial value of N_A using only the dominant first term of equation (1), by

$$N_A^{\text{trial}} = \frac{\Delta\nu_{\text{obs}} - \Delta\nu_B}{\Delta\nu_A - \Delta\nu_B} \quad (6)$$

This can be used to calculate trial values of MW and DC using equations (4) and (5), and these are then used in equation (1) to get a trial value of $\chi_{\text{M}_{\text{obs}}}^{\text{cor}}$. An improved value of N_A is next obtained from equation (3) and reiteration is continued until N_A becomes constant.

For our particular equilibrium system,



the equilibrium constant can be expressed as

$$K_{\text{eq}} = [\text{B}] / [\text{A}][\text{L}] \quad (7)$$

The total cobalt concentration M and the free ligand concentration L are given by

$$[M] = [A] + [B]$$

$$\text{and } [L] = [C_L] - 2[A] - 3([M] - [A])$$

where C_L is the total ligand concentration in the solution.

In terms of the solute mole fractions N_A and $N_B (= 1 - N_A)$,

$$[A] = N_A[M]$$

$$[B] = (1 - N_A)[M]$$

$$[L] = \frac{[C_L]}{[M]} - 2N_A - 3(1 - N_A) = MR + N_A - 3 \quad [M]$$

where MR is the ligand: cobalt mole ratio $[C_L]/[M]$ as determined by the initial preparation of the solution.

Substitution into equation (7) gives

$$K_{eq} = (1 - N_A) / N_A[M] (MR + N_A - 3) \quad (8)$$

This may be arranged to give

$$MR + N_A - 3 = \frac{1}{K_{eq}} \left(\frac{1 - N_A}{N_A M} \right) \quad (9)$$

which is of the form $y = (1/K_{eq})x$. Thus, the equilibrium constants at various temperatures can be obtained from the reciprocal of the slope of a plot of this function, using the refined values of N_A for solutions of known MR and M . The data are fitted by linear least squares; the closeness of the linear correlation coefficient to unity and of the intercept to zero are a test of the method. Next, the thermodynamic functions may be calculated according to the

Van't Hoff equation,

$$\ln K_{eq} = -\Delta G^{\circ}/RT = -\Delta H^{\circ}/RT + \Delta S^{\circ}/R \quad . \quad (10)$$

In a plot of $\ln K_{eq}$ versus $1/T$, linear least squares are used to give best values of the slope $-\Delta H^{\circ}/R$ and the intercept $\Delta S^{\circ}/R$. The closeness of the linear correlation coefficient to unity serves as a test of the method.

C. Methodology

The nmr cell used for this study was a Wilmad Precision No. 517 coaxial cell as described by Joedicke (1976). The benzene sample solution containing the cobalt(II) chloride, the phosphorus ester, and cyclohexane as the inert reference was placed in the central tube by means of a narrow dropping pipet. A flared end sealed capillary containing TMS was inserted and the tube was capped with a Teflon stopper. The reference benzene solution containing cyclohexane and (when appropriate) phosphorus ester was placed in the outer tube and the liquid levels made equal. The proton resonance spectrum of the cyclohexane was recorded for both the sample and the reference solution in a single sweep of the nmr spectrometer. The resonance of the sample solution appeared upfield from that of the reference solution. The difference between the two peaks $\Delta\nu$ is determined by measuring with an accurate ruler the distance on the chart paper between the peak maxima of the inert reference in the two solutions. After multiplying by a scaling factor

(determined from two frequency reference lines), the value of $\Delta\nu$ was obtained with a precision of ± 0.001 Hz.

The samples used were 0.01 M cobalt(II) chloride in benzene containing 5.00 vol % cyclohexane. Values of $\Delta\nu$ were measured from 10° to 45°C for solutions with varying phosphorus ester: cobalt mole ratios. The diamagnetic contribution due to excessive amounts of uncoordinated ligand in the sample solution was compensated by including a corresponding concentration in the reference solution.

Molar susceptibilities of the complexes were calculated from $\Delta\nu$ data using equation (1). Densities were determined as described in Chapter III Section B for the solvents and solutions of several mole ratios. Densities of solutions of other mole ratios were calculated by interpolation. Molarities were corrected for the variation in solution volume with temperature. Values of the "solvent" χ_0 used included contributions from the benzene, the cyclohexane reference, and the excess ligand present. The diamagnetic susceptibilities of benzene and cyclohexane were taken from the Handbook of Chemistry and Physics (CRC, E-127-128). Values of the diamagnetic corrections for the phosphorus esters were taken from Studer (1973), and for the cobalt(II) chloride from Lewis and Wilkins (1960).

D. Results and Discussion

Dilatometrically measured densities as a function of temperature of the solvents and solutions used in the nmr studies are presented in Table IV.

The determination of the paramagnetic susceptibilities of the equilibrium systems was made over the temperature range 10° to 45° using benzene solutions of cobalt(II) chloride containing added ligand such that the ligand: cobalt mole ratios encompassed the following ranges: 3.100 to 3.400 with triethyl phosphite, 2.800 to 3.400 with diethyl ethylphosphonite, and 3.000 to 3.400 with ethyl diethylphosphinite. The values of $\Delta\nu$ observed and the other quantities needed in the equilibrium constant calculations are presented in the Tables of Appendix I. The values of $\Delta\nu_A$, $\Delta\nu_B$, $\chi_{M_A}^{cor}$, and $\chi_{M_B}^{cor}$ were determined from Joedicke's experimental data with correction to each temperature under study.

In each system, trial values of K_{eq} at each individual temperature were obtained from the reciprocal of the slope of the function of equation (9). On only one out of 24 occasions was one sub-set of data rejected at this stage because for it the least squares intercept for function (9) did not include zero within three standard deviations; in every case the linear correlation coefficients exceeded .94.

Table IV. Densities as a Function of Temperature

Solutions	d = a - bt		$10^4 b$	Linear Correlation Coefficient
		a		
Benzene + 5.00 vol. % Cyclohexane--Solvent(S)		.8921	9.98	-0.9999
.04751 M P(OEt) ₃ in S		.8967	10.40	-0.9999
.1200 M EtP(OEt) ₂ in S		.8920	10.19	-0.9999
.3200 M Et ₂ POEt in S		.8926	10.17	-0.9999
.01000 M CoCl ₂ + .03100 M P(OEt) ₃ in S		.8944	10.25	-0.9999
.01000 M CoCl ₂ + .03500 M P(OEt) ₃ in S		.8943	10.08	-0.9999
.01001 M CoCl ₂ + .03003 M EtP(OEt) ₂ in S		.8946	10.08	-0.9963
.009996 M CoCl ₂ + .1501 M EtP(OEt) ₂ in S		.8936	10.02	-0.9999
.010206 M CoCl ₂ + .02052 M Et ₂ POEt in S		.8944	9.83	-0.9999
.01000 M CoCl ₂ + .03000 M Et ₂ POEt in S		.8976	10.34	-0.9960
.01000 M CoCl ₂ + .3000 M Et ₂ POEt in S		.8907	9.98	-0.9999

The thermodynamic quantities ΔH° and ΔS° reported in Table V were obtained by least squares fit of the function of equation (10), using the trial values of K_{eq} . Then the final values of the equilibrium constants to be used in each system at any specified temperature were calculated from the values of ΔH° and ΔS° using equation (10), so that such values would be based on an entire set of data rather than an individual point. These values of K_{eq} (and ΔG°) calculated for 25°C are given in Table V as examples for discussion. Corresponding values of the same quantities for the same reactions in t-butylbenzene, as determined by Joedicke, are also included in Table V as examples for discussion.

The reactions are exothermic in every case, and the equilibrium constants decrease with increasing temperature. The entropy change is negative in every case, corresponding to the formation of a more ordered system in the reaction. The decrease in spin multiplicity makes a contribution of -2.2 entropy units to ΔS° .

In every case, the values of ΔG° and of K_{eq} are less in benzene than in t-butylbenzene, but the ΔH° and ΔS° comparisons show an irregular solvent effect. While for the triethyl phosphite and diethyl ethylphosphonite systems ΔH° and ΔS° are both more negative in benzene than in t-butylbenzene, the converse is true for the ethyl diethylphosphinite system.

Table V. Thermodynamic Functions ^a for $\text{CoCl}_2\text{L}_2 + \text{L} \rightleftharpoons \text{CoCl}_2\text{L}_3$

Ligand	^b In Benzene				^c In t-Butylbenzene			
	ΔH^{od}	ΔS^{oe}	$\Delta G_{298}^{\text{od}}$	$K_{\text{eq } 298}$	ΔH^{od}	ΔS^{oe}	$\Delta G_{298}^{\text{od}}$	$K_{\text{eq } 298}$
$\text{Et}_2\text{P}(\text{OEt})$	-12.0±.3	-29.1±.8	-3.27	2.50×10^2	-13.9±.2	-33.2±.7	-4.00	8.54×10^2
$\text{EtP}(\text{OEt})_2$	-10.6±.2	-20.6±.8	-4.45	1.82×10^3	- 8.6±.1	-11.9±.3	-5.02	4.79×10^3
$\text{P}(\text{OEt})_3$	- 6.2±.7	-11.6±2.2	-2.72	9.9×10^1	- 5.9±.3	- 8.5±.9	-3.33	2.8×10^2

(a) Errors shown are based on one standard deviation of the slope and intercept in the linear regression.

(b) This work

(c) Joedicke, 1976

(d) Kcal/mol

(e) cal/mol·deg

Ethyl diethylphosphinite is the most sterically demanding of all three ligands studied. It has been noted previously (Joedicke, Studer, and Yoke, 1976) that its system seems out of line compared to the other two in several ways, magnetically, spectroscopically, and in the much more negative value for ΔS° for it in the above reaction, suggestive of steric crowding on going from the four- to the five-coordinate complex. Thus, even though ΔH° is most negative with this ligand, the entropy factor causes the equilibrium constant for it to be smaller than for the middle member of the $\text{Et}_n\text{P}(\text{OEt})_{3-n}$ series. The result that ΔH° is most negative in the ethyl diethylphosphinite system suggests that the new bond being formed in the reaction is strongest for it. Since the effect of the electronegativity of ethyl- and ethoxy- substituents on phosphorus should make ethyl diethylphosphinite the best sigma donor and poorest pi acceptor, the observed ΔH° values suggest that sigma bonding is the more important. The dominant effect of steric hindrance is, of course, emphasized by the total non-existence of a tris(triethylphosphine) complex; triethylphosphine would be the extreme case of a large steric requirement.

In the previous work (Joedicke, Studer, and Yoke, 1976) it was noted that the equilibrium constants are one to two orders of magnitude less in nitrobenzene than in *t*-butylbenzene (dipole moments 4.27 and 0.83 Debye, respectively).

This was attributed to a more favorable interaction of the more polar solvent with the presumably more polar four-coordinate complexes, stabilizing them with respect to the five-coordinate complexes. That hypothesis can no longer be sustained, since in the benzene versus t-butylbenzene comparison, the equilibrium constants are uniformly larger in the more polar solvent.

V. AUTOXIDATION OF FREE $\text{Et}_n\text{P}(\text{OEt})_{3-n}$ LIGANDS IN BENZENE.

A. Methodology

The autoxidation of free $\text{Et}_n\text{P}(\text{OEt})_{3-n}$ ligands in benzene was carried out using the apparatus described by Joedicke (1976). Benzene solutions which were equimolar (ca. .2 M) in the free ligand and in o-dichlorobenzene and with AIBN initiator (ca. .01 or .02 M) added were prepared in the dry box and placed in a 50 ml pear-shaped flask. The reaction temperature was controlled by immersing the flask in a water bath containing a copper coil through which was passed water from a Haake constant temperature circulator. The temperature of the water bath was measured to $\pm 0.5^\circ\text{C}$ with a mercury thermometer. Nitrogen, oxygen, or dry air could be introduced from the appropriate compressed gas cylinder by turning stopcocks in a gas manifold. The gas passed through an inlet tube which was inserted into the reaction solution and which terminated in a glass frit for the dispersion of fine bubbles. Unconsumed gas flowed out through two six inch reflux condensers in series and then through tubing to a mineral oil bubbler. The three way connecting tube bearing the gas inlet tube and the reflux condensers was mounted on the center joint of the reaction flask. The flask had an auxiliary side neck which allowed the removal of samples with a syringe

at various times for the kinetic studies. At time zero, a stopcock was turned in the manifold to switch the inlet gas from nitrogen to oxygen or air. The systematic error corresponding to the time necessary to saturate the solutions with oxygen was relatively small, as indicated by the instantaneous decrease in, and rapid recovery of, the rate of bubbling of escaping gas in the mineral oil bubbler. The samples withdrawn at various times were analyzed by gas chromatography as described in Section III D.

B. Results.

Triethyl phosphite differs from the other two phosphorus esters in that its autoxidation gives only a single product, triethyl phosphate, while the others give a distribution of products. The present kinetic results show another major difference in kind-autoxidation is zero order in triethyl phosphite, but first order in each of the other phosphorus esters.

Plots of time versus the decreasing concentration of triethyl phosphite and the increasing concentration of triethyl phosphate are shown in Figures 8, 9, 10 for the autoxidation of 0.2 M triethyl phosphite in benzene at 50°. In Figure 8, it is seen that the decrease in concentration of triethyl phosphite with time is linear (correlation coefficient -0.993) over 100 % of the course of the reaction, and that it is quantitatively matched within the

$$\circ : \frac{d[P(OEt)_3]}{dt} = -(5.47 \pm .20) \times 10^{-6} \text{ mol/l-sec}$$

$$\triangle : \frac{d[P(O)(OEt)_3]}{dt} = (5.40 \pm .09) \times 10^{-6} \text{ mol/l-sec}$$

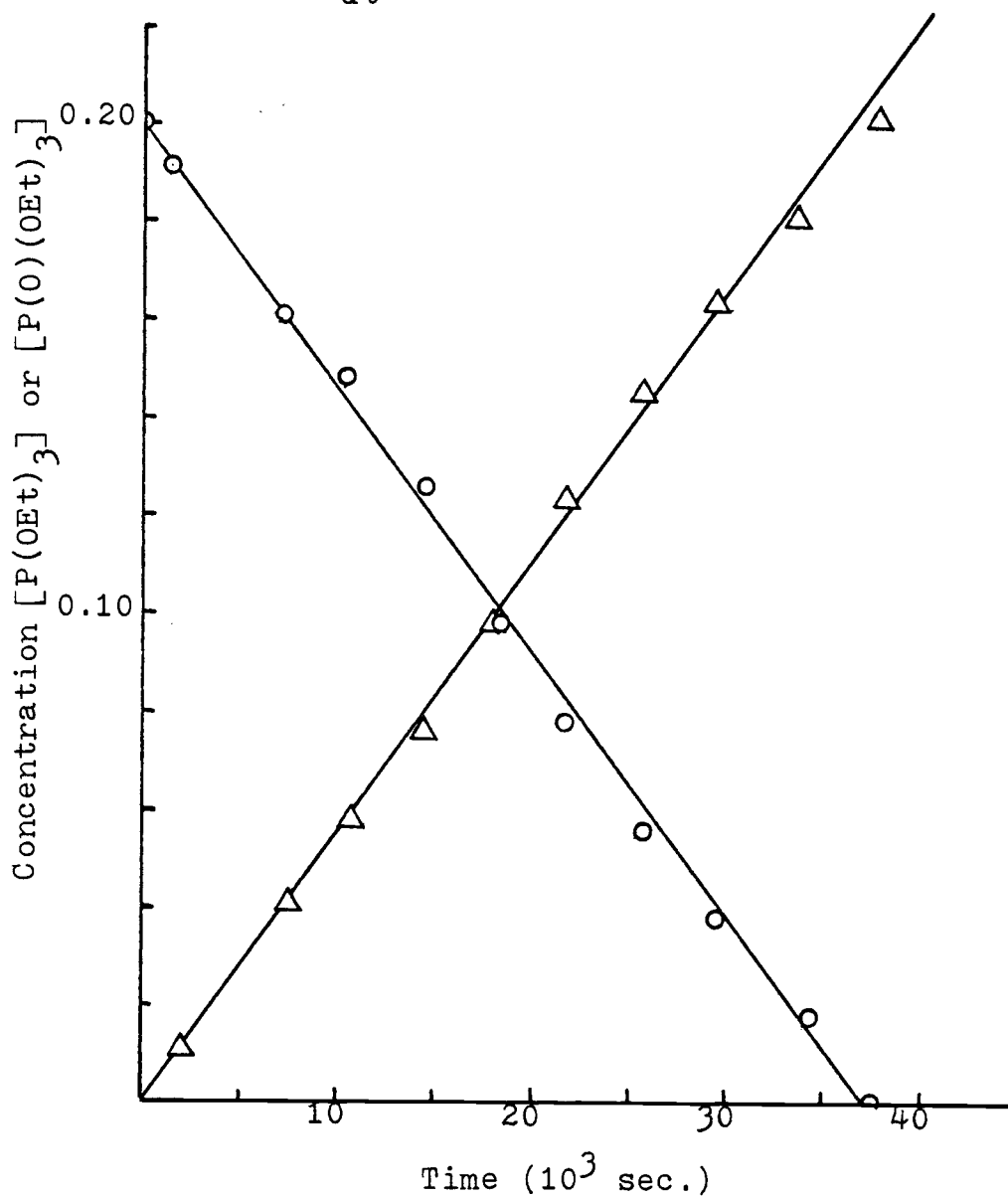


Figure 8. Autoxidation of 0.2M Triethyl Phosphite in Benzene with 0.02931M AIBN under 1.00 Atm. of Oxygen

$$O, \Delta : \frac{d[P(OEt)_3]}{dt} = -(2.29 \pm .11) \times 10^{-6} \text{ mol/l-sec}$$

$$\bullet, \blacktriangle : \frac{d[P(O)(OEt)_3]}{dt} = (1.85 \pm .07) \times 10^{-6} \text{ mol/l-sec}$$

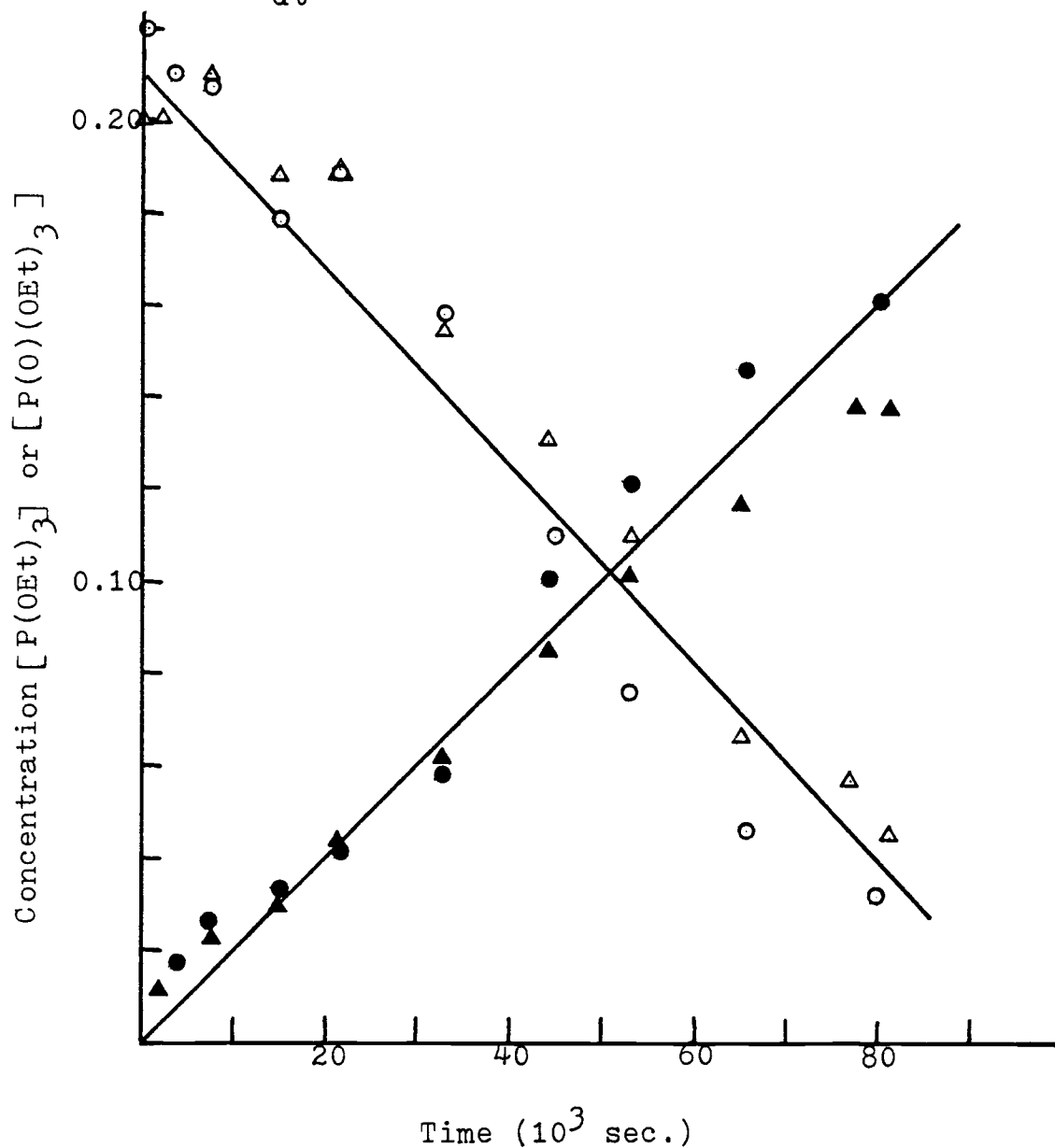


Figure 9. Autoxidation of 0.2M Triethyl Phosphite in Benzene with 0.0105M AIBN under 1.00 Atm. of Oxygen.

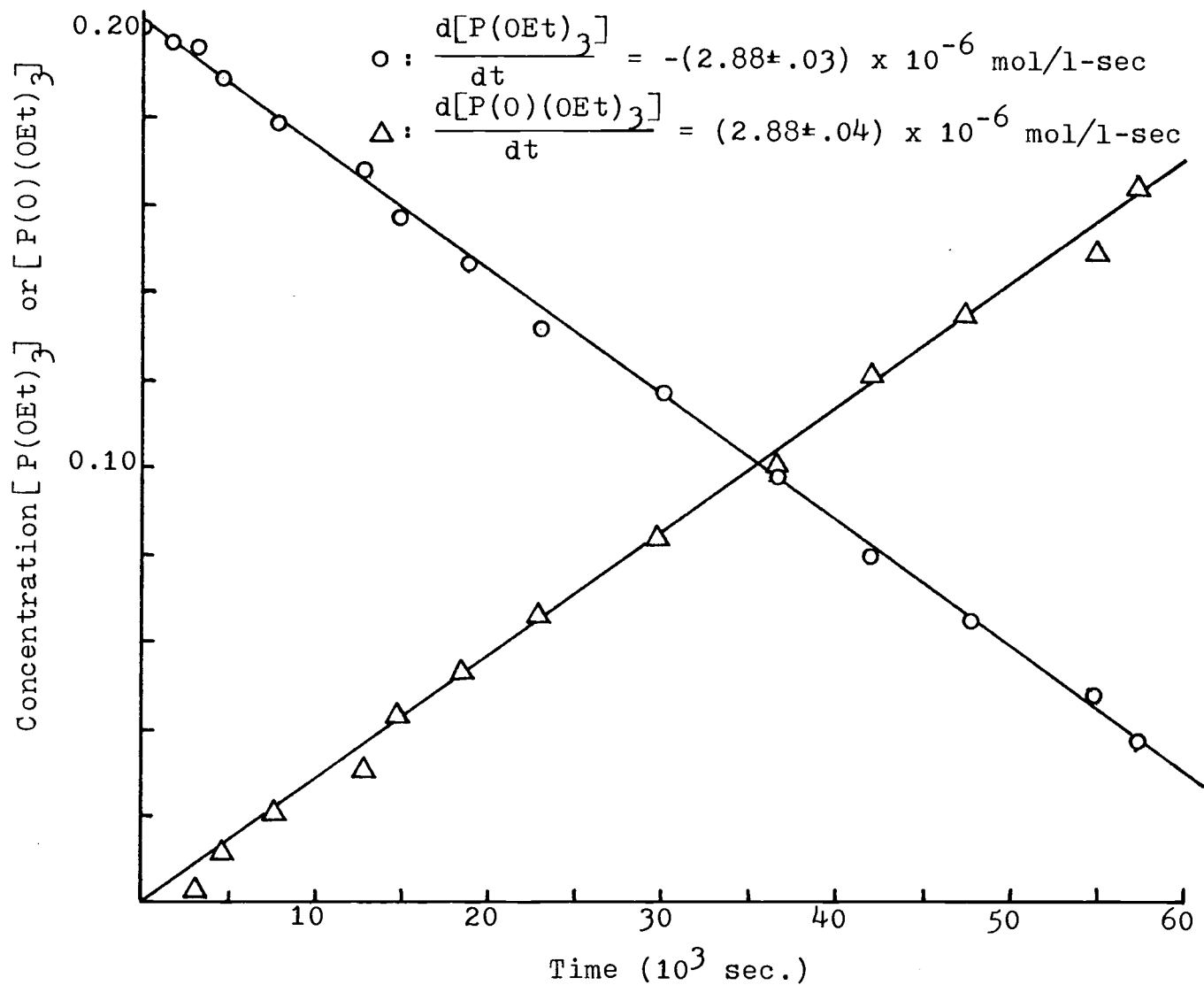


Figure 10. Autoxidation of 0.2M Triethyl Phosphite in Benzene with 0.6414M AIBN under 1.00 Atm. of Dry Air.

experimental error with the linear increase in concentration of triethyl phosphate with time (correlation coefficient +0.993). Similar results are shown in Figure 9, which represents a combination of data from separate but duplicate runs, so that there is a good deal more scatter of the data points (linear correlation coefficients -0.978 and +0.985, respectively). The data of Figures 8 and 9 were both obtained at 1.00 atm oxygen pressure, but with different concentrations of AIBN initiator. As will be shown in the Discussion, each AIBN concentration remains effectively constant during each of the reaction times involved. Next, data obtained using 1.00 atm of dry air are shown in Figure 10 (linear correlation coefficients -0.999 and +0.999). Dry air is 20.9 vol % oxygen (Handbook of Chemistry and Physics).

All these data are summarized in Table VI, where the rate of reaction in each case is calculated as the average of the absolute magnitudes of the least squares slopes of Figures 8, 9, and 10. Assuming the rate law

$$\text{Rate} = -d[\text{P(OEt)}_3] / dt = +d[\text{P(O)(OEt)}_3] / dt = k[\text{AIBN}] \text{P}_{\text{O}_2}$$

permits calculation of the second order rate constant values shown in the final column of Table VI.

Data for the AIBN-initiated autoxidation of diethyl ethylphosphonite in benzene at 50° under 1.00 atm of oxygen are displayed in Figure 11. The curve showing the pseudo-first

Table VI. Kinetic Data for Triethyl Phosphite Autoxidation in Benzene at 50°

$$2 \text{ P(OEt)}_3 + \text{O}_2 \longrightarrow 2 \text{ P(O)(OEt)}_3$$

$$\text{Rate} = k[\text{AIBN}] (\text{P}_{\text{O}_2})$$

P_{O_2} , atm	[AIBN]	Rate, mol l ⁻¹ sec ⁻¹	k, atm ⁻¹ sec ⁻¹
1.00	0.0105	2.07×10^{-6}	1.97×10^{-4}
1.00	0.2913	5.44×10^{-6}	1.87×10^{-4}
0.209	0.06414	2.88×10^{-6}	2.15×10^{-4}
		Mean	2.0×10^{-4}

order decrease in diethyl ethylphosphonite concentration is faithfully matched by the mirror image curve showing the increase in the sum of the concentrations of all the oxidation products. All three oxidation products predicted by Buckler's chain mechanism (Figure 1) are observed, diethyl ethylphosphonate, triethyl phosphite, and (from further oxidation of the latter) triethyl phosphate.

Data for the AIBN-initiated autoxidation of ethyl diethylphosphinite in benzene at 50° under 1.00 atm of oxygen are similarly shown in Figure 12. In this Figure, data points from two runs involving two different concentrations of AIBN fall on the same curves. The curve showing the pseudo-first order decrease in ethyl diethylphosphinite is well matched by the curve

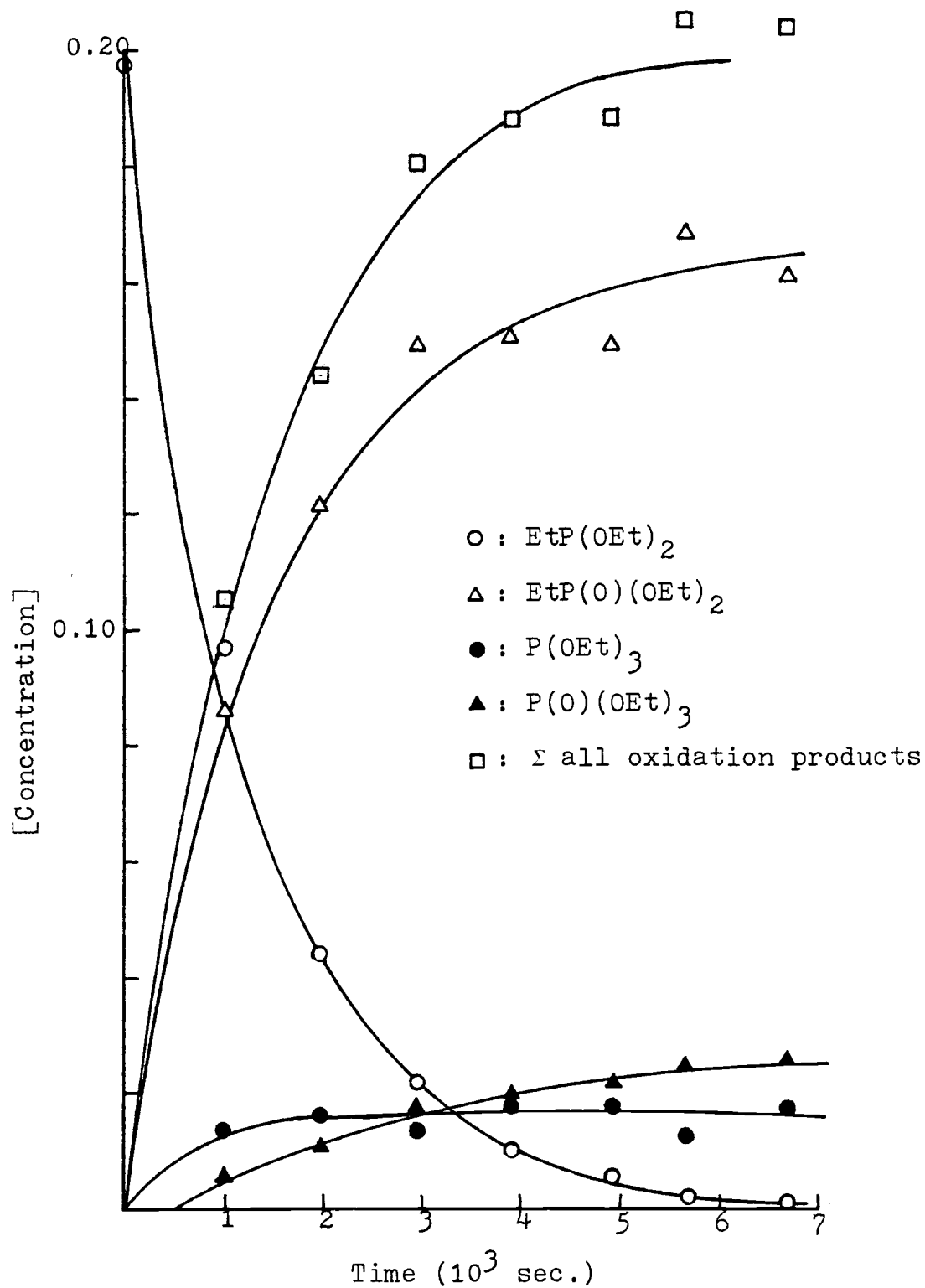


Figure 11. Autoxidation of 0.2M Diethyl Ethylphosphonite in Benzene

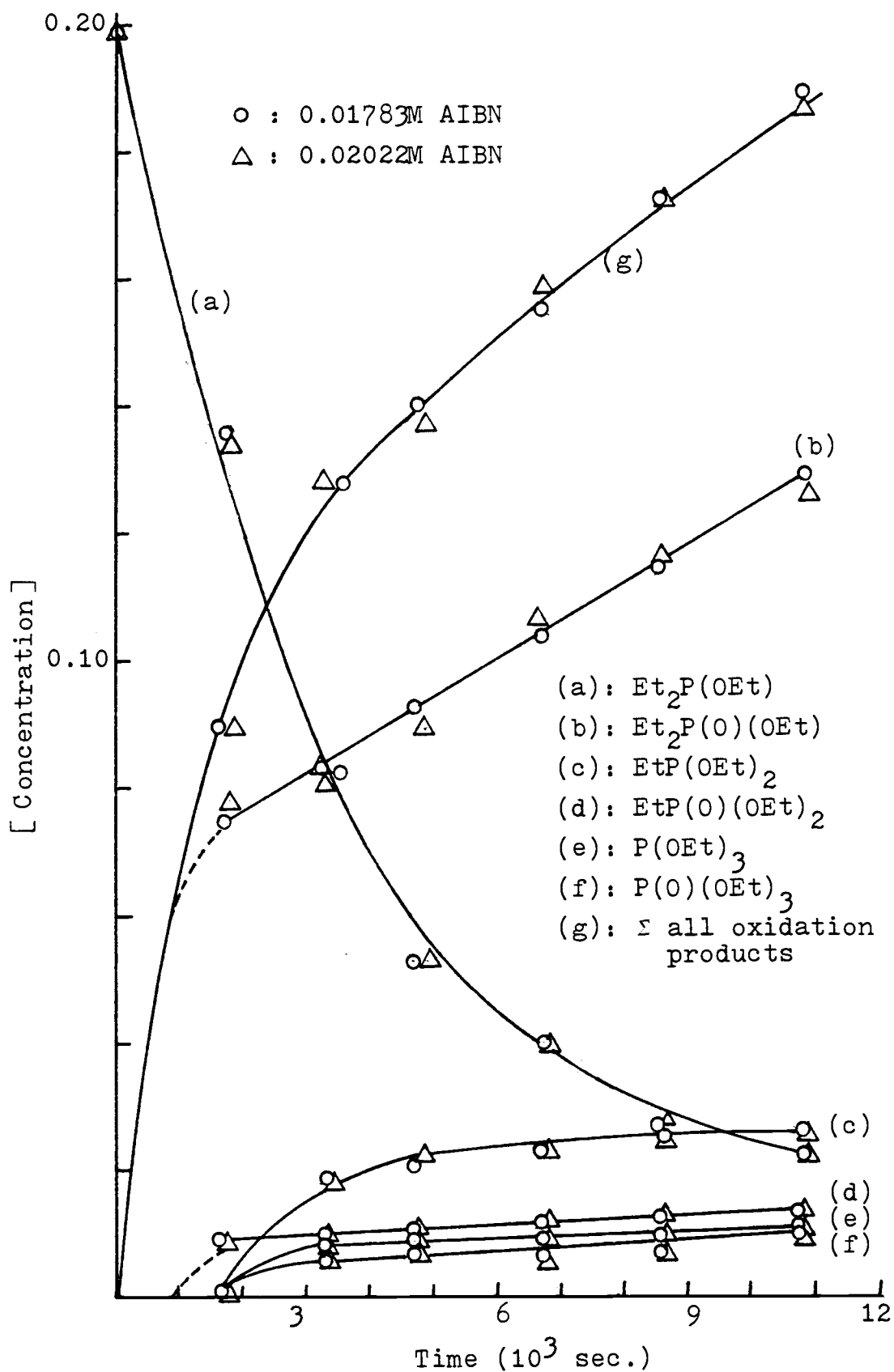


Figure 12. Autoxidation of 0.2M Ethyl Diethylphosphinite in Benzene.

showing the increase in the sum of the concentrations of all the oxidation products. All five oxidation products predicted by Buckler's chain mechanism (Figure 1) are observed, ethyl diethylphosphinate, diethyl ethylphosphonite, and the three oxidation products of the latter. After an initial period of about 2×10^3 seconds, the major product, ethyl diethylphosphinate, is formed at a constant rate for the next 9×10^3 seconds, after which time 90 % of the starting material has been consumed. During much of this time interval the concentration of the other breakdown product of the $\text{Et}_2\text{P}(\text{OEt})_2$ phosphoranyl radical, diethyl ethylphosphonite, remains at a nearly steady state, as does the concentration of the other trivalent phosphorus compound derived from it, triethyl phosphite.

If, for the AIBN-initiated autoxidation of $\text{L} = \text{diethyl ethylphosphonite}$ or of $\text{L} = \text{ethyl diethylphosphinite}$, under a constant pressure of oxygen, one assumes the rate law

$$\text{Rate} = -d[\text{L}]/dt = k[\text{L}](\text{P}_{\text{O}_2}) = k'[\text{L}]$$

then a plot of $\ln [\text{L}]_0/[\text{L}]_t$ versus time should give a straight line whose slope is the pseudo-first order rate constant k' . Such plots are shown in Figure 13 for diethyl ethylphosphonite ($k' = 7.49 \times 10^{-4} \text{ sec}^{-1}$) and for ethyl diethylphosphinite ($k' = 2.37 \times 10^{-4} \text{ sec}^{-1}$). Again, for the latter, data points from experiments using two different concentrations of AIBN fall on the same line.

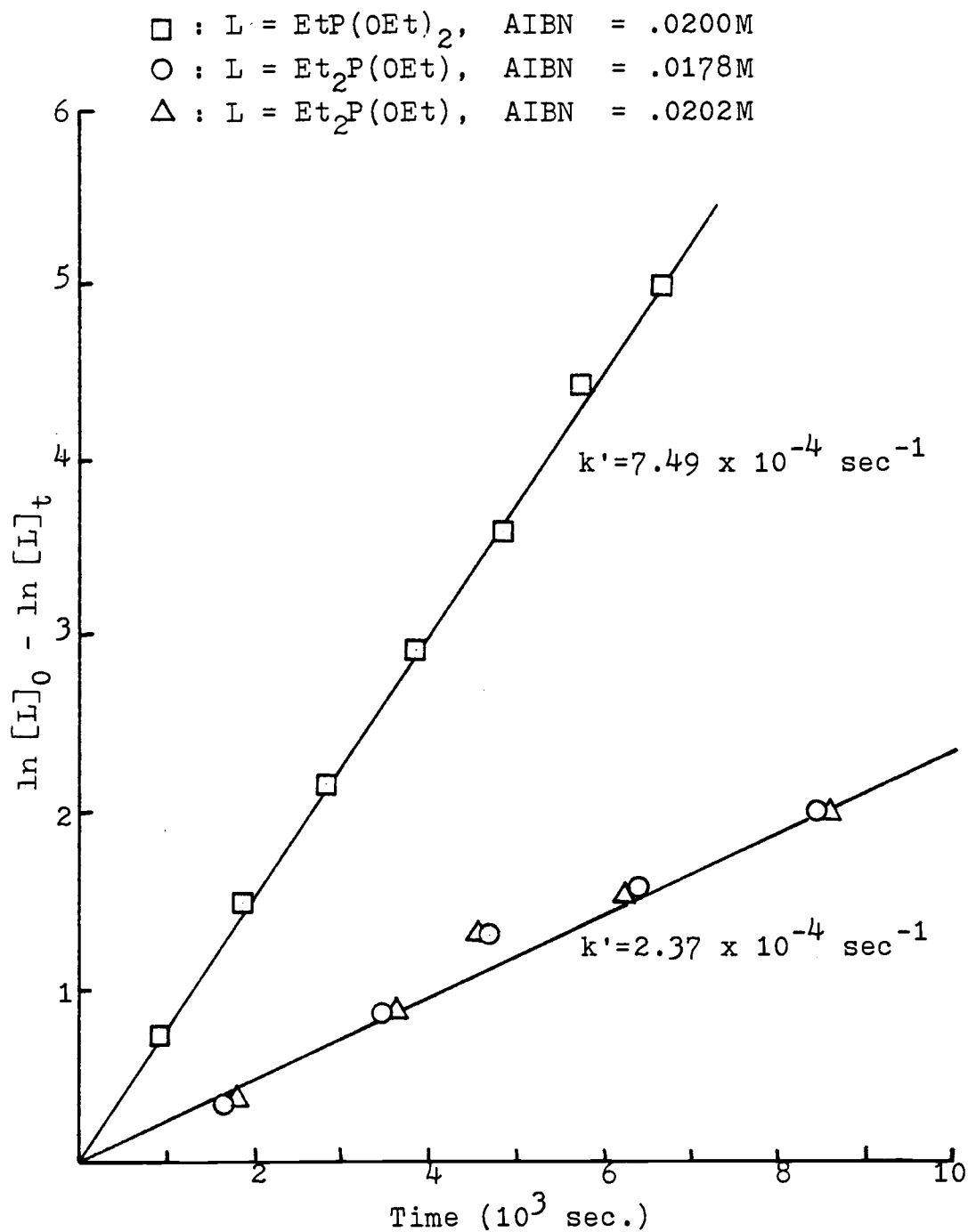
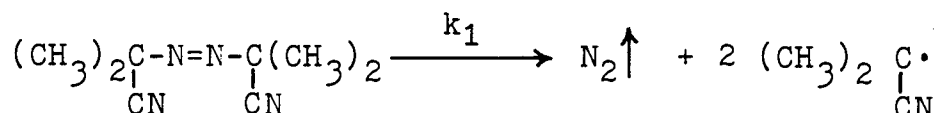


Figure 13. Pseudo-First Order Kinetic Plots for the Autoxidation of EtP(OEt)₂ and Et₂P(OEt).

Discussion

Azobisisobutyronitrile (AIBN), a commonly used initiator, generates radicals on thermolysis by the equation



for which Huyser (1970) gives $\Delta E^\ddagger = 31.3 \text{ Kcal/mol}$ and $t_{\frac{1}{2}} = 4.32 \times 10^2 \text{ sec}$ at 373° K , so that $k_1 = 1.60 \times 10^{-3} \text{ sec}^{-1}$ at 373° K . At any other temperature $T(^{\circ}\text{K})$, k_1 may be calculated from

$$\ln \left(\frac{1.6 \times 10^{-3} \text{ sec}^{-1}}{k_1 \text{ at } T} \right) = \left(\frac{31.3 \times 10^3 \text{ cal/mol}}{1.987 \text{ cal/mol deg}} \right) \left(\frac{373 - T}{373T} \right) .$$

For example, at 50° C , $k_1 = 2.25 \times 10^{-6} \text{ sec}^{-1}$ and $t_{\frac{1}{2}}$ is 85.6 hours. Considering typical conditions used in the 50° C kinetic studies just described, one can calculate that in 10^4 seconds an initial AIBN concentration of 0.0200M would be reduced to 0.0196 M. This is the basis of the previous statement that the AIBN concentration is effectively constant in each run.

The curves in Figures 12 and 13 show that the rate of autoxidation of ethyl diethylphosphinite is apparently independent of AIBN concentration (although it must be noted that the experimental variation in AIBN concentration was only 12 %). This may tentatively be assumed to be true also for diethyl ethylphosphonite, which has similar

autoxidation behavior. In contrast, the data in Table VI demonstrate that autoxidation of triethyl phosphite is first order in AIBN. It is instructive to calculate the rate of generation of initiating radicals (2 per AIBN decomposed), or rate of initiation, by the equation

$$d[(\text{CH}_3)_2(\text{CN})\text{C}\cdot]/dt = 2 k_1[\text{AIBN}]$$

for each of the experiments at 50° and 1.00 atm of oxygen, and to compare this with the (constant) rate of autoxidation of triethyl phosphite and the (initial) rate of autoxidation of diethyl ethylphosphonite and ethyl diethylphosphinite. These values are given in Table VII.

Table VII. Comparison of Rates^a of Initiation and Autoxidation in Benzene at 50°, 1.0 Atm. O₂

Compound	Rate of Autoxidation	[AIBN] M	Rate of Initiation	Ratio of Rates
P(OEt) ₃	2.07 x 10 ⁻⁶	0.0105	4.73 x 10 ⁻⁸	43.8
P(OEt) ₃	5.44 x 10 ⁻⁶ ^b	0.02913	1.31 x 10 ⁻⁷	41.5
EtP(OEt) ₂	1.50 x 10 ⁻⁴ ^b	0.0200	9.00 x 10 ⁻⁸	1670
Et ₂ POEt	4.74 x 10 ⁻⁵ ^b	0.01783	8.02 x 10 ⁻⁸	591
Et ₂ POEt	4.74 x 10 ⁻⁵ ^b	0.02022	9.10 x 10 ⁻⁸	521

(a) mol lit⁻¹ sec⁻¹

(b) initial rates

The ratio of the rates, i.e., the number of moles of phosphorus ester oxidized per mole of initiating radical generated, should be an approximate relative measure of the chain length, assuming comparable efficiencies of initiation. It is noteworthy that this ratio is an order of magnitude smaller for triethyl phosphite autoxidation, which has a first order dependence on AIBN, than it is for ethyl diethylphosphinite autoxidation, which appears to be independent of AIBN concentration. For diethyl ethylphosphonite, the radical chain length appears to be about three times greater by this measure than it is for ethyl diethylphosphinite, based on the three-fold greater reaction rate constant for its autoxidation.

The present results on the kinetics of triethyl phosphite autoxidation

$$-d[P(OEt)_3]/dt = + d[P(O)(OEt)_3]/dt = k[AIBN](P_{O_2})$$

disagree with those of Floyd and Boozer on the AIBN-initiated autoxidation of tri-n-butyl phosphite in o-dichlorobenzene at 70°. They reported first order dependence on the phosphite concentration as well as on the AIBN concentration. It was noted in the discussion of the work of Floyd and Boozer in Section II B that there are a number of peculiarities in their results and their experimental method. They did not study the dependence of the rate on the oxygen pressure, but in a simultaneous study of tri-n-butylphosphine autoxidation they did claim an inverse

first order dependence on oxygen. This contrasts with the direct first order dependence observed in this work (Table VI) and in Schmidt's (1971) study of the autoxidation of triethylphosphine coordinated to cobalt(II) chloride.

The autoxidations of L = diethyl ethylphosphonite and L = ethyl diethylphosphinite are also probably first order in the concentration (or pressure) of oxygen, although no evidence has yet been obtained to demonstrate this.

Therefore, in the rate law

$$- d[L]/dt = k'[L]$$

the reaction rate constants k' are called pseudo-first order rate constants and it is presumed that the true rate law is

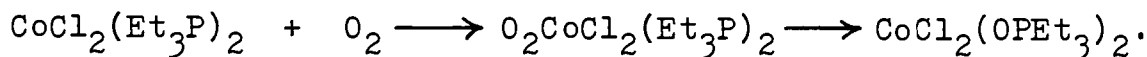
$$- d[L]/dt = k_2[L] (P_{O_2}) \quad .$$

Citations on the solubility of oxygen in benzene given in the solubility compendia of Seidell and of Stephen and Stephen refer to the work of Horiuti in 1931 as giving the "best" data. At 1.00 atm pressure, the solubility increases very slightly in the range 10° to 60°C. It is 0.00911 M at 25° and 0.00936 M at 50°C. Reviews on the solubility of oxygen in organic solvents are given by Wilhelm and Battino (1973) and by Field, et al (1974). No data are available for t-butylbenzene, the solvent used by Joedicke (1976), but only a small variation in oxygen solubility is observed in the group benzene, toluene, and m-xylene.

VI. STUDIES OF A COBALT DIOXYGEN ADDUCT INTERMEDIATE

A. Introduction

In previous work in this laboratory, Schmidt (1970) postulated that a dioxygen adduct might be an intermediate or a transition state in coordinated triethylphosphine autoxidation, viz.



In his preliminary kinetic study of the autoxidation of dichlorotris(diethyl ethylphosphonite)cobalt(II) in t-butylbenzene, Joedicke(1976) postulated the existence of a dioxygen adduct stable at 0°C but not at room temperature to explain some peculiar spectrophotometric results.

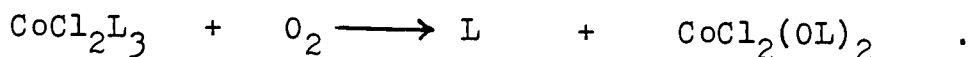
Part of the present work was devoted to finding out if such adducts are in fact involved as reaction intermediates, and to characterize them if possible. An attempt to isolate a dioxygen adduct from solution by crystallization was not successful. However, experiments have been carried out on dichlorotris(diethyl ethylphosphonite)-cobalt(II) which demonstrate the existence of such an adduct in solution at low temperatures. A low temperature epr study was made of such a solution. The key experiment involved a determination of reaction stoichiometry under a sequence of special conditions. Finally, a series of kinetic measurements of the decomposition of the adduct

was carried out by spectrophotometric methods. These results provide a useful basis for the interpretation of the catalytic autoxidation of the phosphorus esters at room temperature.

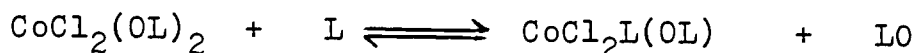
B. Chemical Evidence for the Dioxygen Adduct

The low temperature work was done in t-butylbenzene (m.p. -58°) solution, since benzene freezes at $+5^{\circ}$. The ligand L was diethyl ethylphosphonite. In a flask attached to the high vacuum line, a solution of CoCl_2L_3 at -46° (chlorobenzene slush bath) was stirred for about 2.5 hours under a large volume of oxygen gas initially at 1.00 atm until the pressure stopped dropping. The solution remained green. The reaction mixture was then frozen at -196° and the apparatus evacuated. This was followed by thawing and warming the reaction mixture to -23° (carbon tetrachloride slush bath) in vacuo to remove physically dissolved oxygen, which was pumped off. Later, on being warmed to room temperature, the green solution turned blue within a couple of minutes. This change was irreversible. All volatile material was pumped off and analyzed qualitatively by gc; it was found that only solvent and unoxidized diethyl ethylphosphonite were present. The blue non-volatile residue consisted of $\text{CoCl}_2(\text{OL})_2$, as indicated by its intense $\text{P}=\text{O}$ absorption in

the ir. Thus, the net reaction under this sequence of operations was



(Since L is much more volatile than L₀, any equilibrium

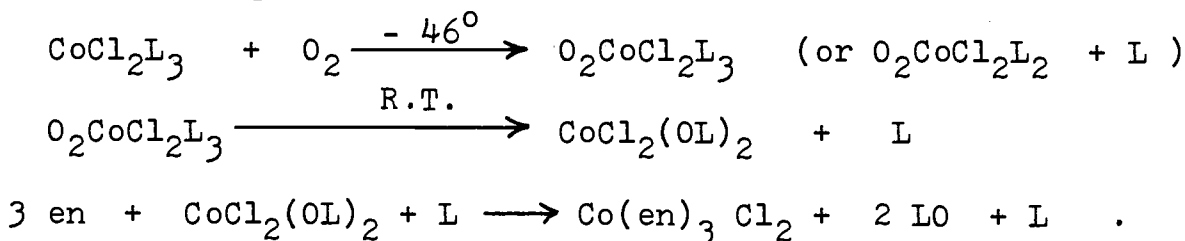


would be shifted completely to the left on pumping the residue to dryness).

Quantitatively, a solution of 0.08944 M CoCl_2L_3 and 0.2000 M in o-dichlorobenzene (internal standard) at -46° was bubbled with 1.00 atm oxygen gas for three hours. After being degassed by two -196° to -23° freeze-pump-thaw cycles to remove physically dissolved oxygen, the solution was allowed to warm to room temperature and was moved into the dry box. An excess amount of ethylenediamine was added and the solution was stirred; this causes all organo-phosphorus ligands to become displaced. All volatile material was next pumped off on the vacuum line and was analyzed by gc. The concentrations of diethyl ethylphosphate and diethyl ethylphosphonite were determined to be 0.1804 M and 0.08897 M, respectively. These numbers are in the ratio 2.03:1 and their sum is 0.269, while three times the initial concentration of CoCl_2L_3 is 0.268.

These experimental results constitute chemical proof for a 1:1 cobalt dioxygen adduct which can be formed at -46° and whose formation is not reversed at -23° by

pumping off all the physically dissolved oxygen. The adduct is thermally stable at -23° but decomposes in the course of being warmed to room temperature. The following reactions are quantitative:



C. Low Temperature EPR Studies

A cold *t*-butylbenzene solution of the $\text{O}_2\text{CoCl}_2\text{L}_3$ (or $\text{O}_2\text{CoCl}_2\text{L}_2 + \text{L}$) adduct was prepared as described above, i. e., oxygen gas was bubbled through the green 0.09 M CoCl_2L_3 ($\text{L} = \text{EtP}(\text{OEt})_2$) solution at -46° . The solution was then degassed by a -196° freeze, pump, -46° thaw cycle. The portion of the solution to be used for the epr measurement was transferred by being forced under nitrogen pressure through a pre-chilled double-pointed stainless steel needle using rubber septa and syringe techniques. The needle was inserted through the bore of a stopcock attached to the reaction flask. The other part of the needle passed through a glass stopcock on a three-way brass Swagelok adapter fitted with Teflon ferrules. The needle dipped nearly to the bottom of an attached quartz epr tube cooled to -46° (chlorobenzene slush bath). The nitrogen gas exited through a second stopcock on the adapter which

led to a mineral oil bubbler. The needle was kept cold with occasional applications of powdered Dry Ice wrapped in cloth. After the transfer, the needle was pulled out, all the stopcocks were closed, and the quartz tube was immersed in liquid nitrogen for transport and subsequent insertion into the cavity of a Varian E4 spectrometer. The instrument was calibrated using the signal of DPPH ($g = 2.00345$, $\nu = 9.078 \times 10^9 \text{ sec}^{-1}$, resonance centered at $3.237 \times 10^3 \text{ gauss}$). The spectrum of the frozen *t*-butylbenzene solution of the oxygen adduct was scanned at -196° and again as the sample was allowed to warm up in the cavity of the instrument. Unfortunately, no resolution of components or hyperfine splitting of the resonance could be observed. The spectrum consisted only of a broad (200 gauss wide) resonance centered at $g = 2.08$, as shown in Figure 14. This is attributed to the low quality of the frozen *t*-butylbenzene glass. As noted in Section II D, resolvability of dioxygen adduct epr spectra depends critically on the physical properties of the solvent (Walker 1970).

D. Kinetics of the Decomposition of the Dioxygen Adduct

The equipment described in Section III C 2 and the special glass apparatus shown in Figure 2 were used in this spectrophotometric study. The vessel had a stopcock-fitted gas inlet tube dipping nearly to its bottom. It had a second stopcock with joints for attachment to the vacuum

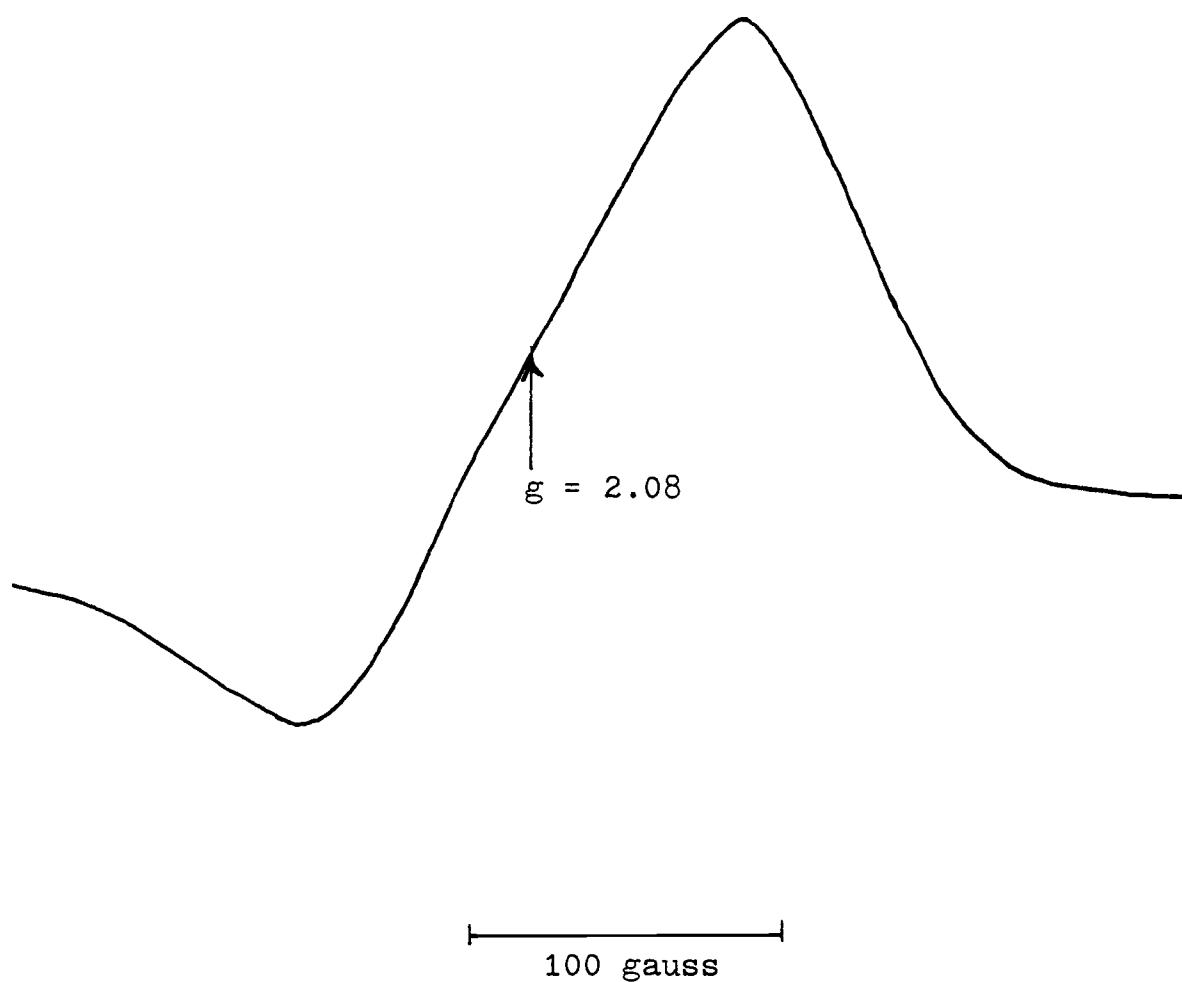


Figure 14. Electron Paramagnetic Resonance Spectrum of the Dioxygen Adduct in Frozen t-Butylbenzene.

line. It was loaded with the solution of dichlorotris-(diethyl ethylphosphonite)cobalt(II) in t-butylbenzene in the dry box under nitrogen. It was then connected to the vacuum line and cooled to -46° . Next, oxygen gas at 1 atm was bubbled through the solution for 50 minutes. The solution containing the oxygen adduct was then degassed by two -196° freeze, pump, -46° thaw cycles, and it was stored in Dry Ice for subsequent study.

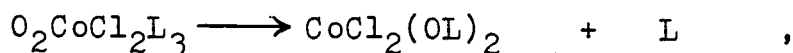
When rotated on its side, the entire apparatus would fit into the sample chamber of the Spectronic 600 spectrophotometer. This rotation caused the reaction mixture to flow into the cuvette. The temperature of the instrument cuvette holder was controlled by pumping methanol through it and through a copper coil immersed in an appropriate bath, using a Haake circulator. Temperatures were measured with a mercury thermometer immersed in a cuvette containing pure solvent in the reference cell.

At first, repeated scans of the solution at 2° were made in the range 360 -580 nm. A rapid decrease in absorption in the 400 -440 nm region and a steady increase in absorption at 550 nm were observed as the green solution turned blue. The latter wavelength was chosen for kinetic runs at various temperatures in the range -9 to $+11^{\circ}\text{C}$

The spectrophotometric absorbance measurements and related data are tabulated in Appendix II. Time $t = 0$ was taken as the moment when the apparatus was rotated and

fitted into the temperature controlled cell compartment; it is, of course, subject to considerable error in that some time would be required for the solution to warm up from -78° and for the apparatus to equilibrate at the temperature of the experiment. This uncertainty was eliminated in the way that the data were actually worked up.

Curves of absorbance versus time were plotted. For the analysis of data, points were selected from the middle ranges of these curves only. For each run, assuming first order decomposition of a dioxygen adduct,



first order constants were calculated as the slopes of the function

$$\ln((A_{\infty} - A_1) / (A_{\infty} - A_t)) = k (t - t_1)$$

where t_1 is the time of the first data point selected for use and A_1 , A_t , and A_{∞} are the absorbances at t_1 , t , and t_{∞} , respectively. The data were fitted to this function by linear least squares and gave correlation coefficients of 0.9991 or higher. The results are given in Table VIII.

Next, to fit the Arrhenius function,

$$k = A e^{-\Delta E^{\ddagger}/RT} \quad \text{or} \quad \ln k = \ln A - \Delta E^{\ddagger}/RT$$

the $\ln k$ versus $\frac{1}{T}$ data were fitted by linear least squares, giving a correlation coefficient of 0.999. The resulting values of slope and intercept give for ΔE^{\ddagger} 20.79 Kcal/mol and for A 5.715×10^{13} . From these, one may calculate

Table VIII. First Order Rate Constants for Thermal Decomposition of $O_2CoCl_2L_3$, $L = EtP(OEt)_2$

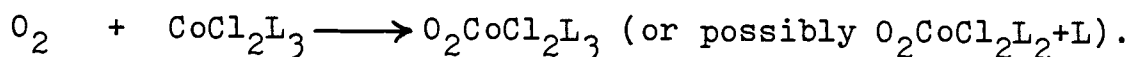
Temperature, $^{\circ}K$	k, sec^{-1}
264	3.587×10^{-4}
271	9.080×10^{-4}
276	1.965×10^{-3}
280	3.420×10^{-3}
284	5.696×10^{-3}

that at $25^{\circ}C$ the first order reaction rate constant k is $3.226 \times 10^{-2} sec^{-1}$ and that the half life of the dioxygen adduct would be 21.5 seconds. Other calculated values are $\Delta H^{\ddagger} = 20.2$ Kcal/mol, $\Delta G^{\ddagger} = 19.48$ Kcal/mol, and $\Delta S^{\ddagger} = 2.42$ cal/mol·deg.

E. Discussion

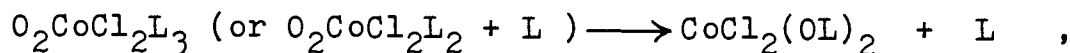
The chemical evidence for the existence of a 1:1 cobalt dioxygen adduct in solution at low temperatures is absolutely conclusive. A solution of $CoCl_2L_3$ (where $L = EtP(OEt)_2$) in *t*-butylbenzene at -46° was allowed to react with an excess of oxygen gas, and the mixture was then degassed using -196° freeze/pump/ -23° thaw cycles to remove all physically dissolved oxygen. When the resulting green solution was allowed to warm to room temperature, it turned blue irreversibly. Analysis proved that, of the three moles

of phosphonite ligand per cobalt, two were quantitatively oxidized to phosphonate and one was not oxidized. Thus, exactly one mole of dioxygen is bound per cobalt in an adduct whose formation is not reversed on pumping and which is stable for many minutes at and below -23°C .



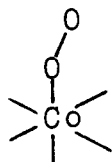
Unfortunately, attempts at physical characterization of the adduct were not successful. The adduct did not crystallize from the solution when the latter was cooled. Rapid freezing (by plunging into liquid nitrogen) caused transformation of the whole mixture to a glass, but this was physically of poor quality. Its broad and unresolved epr spectrum at $g = 2.08$ proved only that the adduct had one unpaired electron, as expected. No attempt was made to look for a O-O stretching vibration at about 1100 cm^{-1} , which would be expected for the dioxygen adduct, because it is known (Studer 1972) that this is a region of strong P-O- C_2H_5 absorption in all of these complexes, and the O-O absorption is described as being very weak (K. Nakamoto, private communication, 1979).

The assumption that the thermal decomposition reaction would be first order,

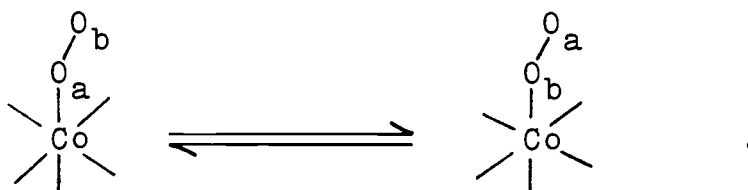


is confirmed by the excellent linearity of first order log plots of the spectrophotometric data obtained in five runs. These runs were carried out in the temperature range -9 to $+11^{\circ}\text{C}$, and the first order constants were fitted to an Arrhenius function. The activation process is endothermic by some 20 Kcal/mol and there is a fairly small positive entropy of activation, 2.4 e.u.

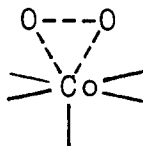
As was pointed out in Section II D, the two oxygens which are structurally non-equivalent in the solid state of adducts of this type,



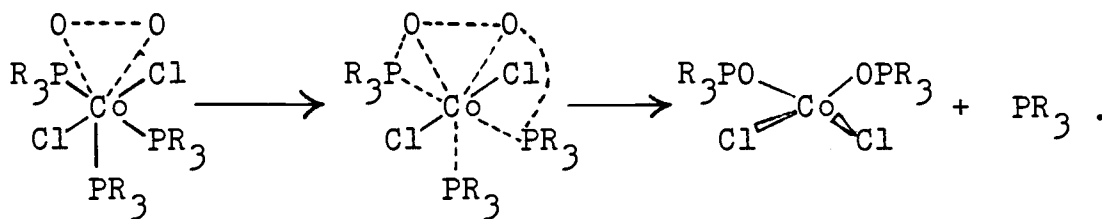
appear equivalent in the solution phase (according to epr studies of ^{17}O - tagged adducts). This was attributed to a rapid equilibrium,



It seems reasonable that the transition state for this facile reversible process would have the symmetrical side-on structure,



which in turn would lead to an attractive candidate for the transition state for thermal decomposition,



VII. AUTOXIDATION OF CoCl_2 COMPLEXES WITH $\text{Et}_n\text{P}(\text{OEt})_{3-n}$
LIGANDS IN BENZENE.

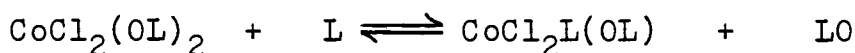
A. Methodology

The same apparatus and procedures which were employed for the autoxidation of the free $\text{Et}_n\text{P}(\text{OEt})_{3-n}$ ligands were used for the autoxidation of the complexes. Benzene solutions containing cobalt(II) chloride were made in the dry box with added phosphorus ester to give the desired ligand : cobalt mole ratio and with o-dichlorobenzene, the internal standard for g.c. analysis. The autoxidation reactions were conducted at 25°C .

During the reactions at mole ratios 2 and 3, the samples withdrawn at various times were treated with an excess of ethylenediamine so that all organophosphorus ligands would be displaced from the cobalt ion. All volatile materials were then pumped off quantitatively and collected at -196° in a detachable U trap on the vacuum line. The volatile mixture containing unoxidized and oxidized forms of the organophosphorus ligands, benzene, o-dichlorobenzene, and ethylenediamine, was analyzed quantitatively by g.c.

For those samples withdrawn from reaction mixtures with very high ligand : cobalt mole ratios, the ethylenediamine method was not used. Instead, the aliquots were pumped on

directly in the vacuum line until their non-volatile residues reached constant weight. The volatile materials, trapped quantitatively at -196° , were then analyzed. Two moles of organophosphorus ligand would be retained per mole of cobalt(II) chloride in the non-volatile residue and thus the g.c. analysis would be only for the other part of the organophosphorus ligand present in the solution. In the case that both oxidized and unoxidized forms of the ligand would be present, the non-volatile residue would quantitatively preferentially bind the much less volatile oxidized form, i.e., any equilibrium



would be quantitatively shifted to the left when the systems were pumped to constant weight.

B. Autoxidation Using a Ligand : Cobalt(II) Chloride Mole Ratio of 2.00

Each of the complexes CoCl_2L_2 , where $\text{L} = \text{Et}_n\text{P}(\text{OEt})_{3-n}$, $n = 0 - 2$, was oxidized in benzene solution under 1.00 atm. oxygen pressure. In addition, the bis(triethylphosphine) complex, where $n = 3$, whose autoxidation had been studied previously by Schmidt (1971), was prepared and the kinetics of its autoxidation were studied under the same conditions for purposes of comparison.

In each case, quantitative g.c. analysis showed that the only organophosphorus ligands present in samples

withdrawn during the progress of a given reaction were a single pair of compounds for each value of n , $\text{Et}_n\text{P}(\text{OEt})_{3-n}$ and $\text{Et}_n\text{P}(\text{O})(\text{OEt})_{3-n}$ with no change in the value of n during the autoxidation. The sum of the concentrations of each member of the pair of compounds remained constant for all reaction times sampled, indicating the quantitative conversion of one to the other. These results prove that the stoichiometry of the autoxidation at mole ratio 2.0 is

$$\text{CoCl}_2 \cdot 2\text{Et}_n\text{P}(\text{OEt})_{3-n} + \text{O}_2 \longrightarrow \text{CoCl}_2 \cdot 2\text{Et}_n\text{P}(\text{O})(\text{OEt})_{3-n},$$

as had been demonstrated earlier by Schmidt for the particular case $n = 3$.

The assumed pseudo-first order rate law under a constant pressure of oxygen can be expressed as

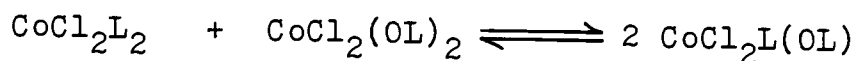
$$-d[\text{CoCl}_2\text{L}_2]/dt = k[\text{CoCl}_2\text{L}_2]\text{P}_{\text{O}_2} = k'[\text{CoCl}_2\text{L}_2]; k' = k\text{P}_{\text{O}_2}.$$

Since the analytical method involves the displacement of all organophosphorus ligands with excess ethylenediamine and their subsequent isolation, the actual experimental data consist of measurements of unoxidized and oxidized ligand concentrations as a function of time. Hence,

$$-d[\text{CoCl}_2\text{L}_2]/dt = .5(-d[\text{L}]/dt) = .5k[\text{L}]\text{P}_{\text{O}_2} = .5k'[\text{L}].$$

In a plot of $\ln([\text{L}]_0/[\text{L}]_t)$ versus time, the factor .5 has cancelled in the numerator and denominator of the logarithmic term; such a plot would give a straight line of slope k' and intercept zero. However, such simple first order kinetics would be obeyed only to the extent that the additional and

complicating mechanistic path involving the redistribution equilibrium



can be neglected, i.e., only in the early stages of the reaction. As shown in Figure 15, the experimental lines appear fairly linear up to ca. 60 %, 50 %, 60 %, and 35 % of completion of reaction for $n = 0, 1, 2$, and 3, respectively. The plots then curve downward steadily. This same behavior was observed earlier by Schmidt in his work with dichlorobis(triethylphosphine)cobalt(II), and was attributed by him to the redistribution reaction. The values of the pseudo-first order rate constants k' obtained from the slopes in the early stages of the reactions are given in Table IX.

For the autoxidation of dichlorobis(triethylphosphine)-cobalt(II) in benzene at 25° under 760 torr of oxygen, the value of the pseudo-first order rate constant, $3.5 \times 10^{-4} \text{ sec}^{-1}$, is in reasonable agreement with the value which can be calculated from the data of Schmidt (1971) for the same reaction in *t*-butylbenzene at 36° and 678 torr of oxygen; the latter value is $4.8 \times 10^{-4} \text{ sec}^{-1}$. (Schmidt actually reported an incorrect value in his Dissertation, presumably due to a computational error). It may be noted that Schmidt used a completely different analytical method to follow the kinetics of the reaction, namely measurement of the

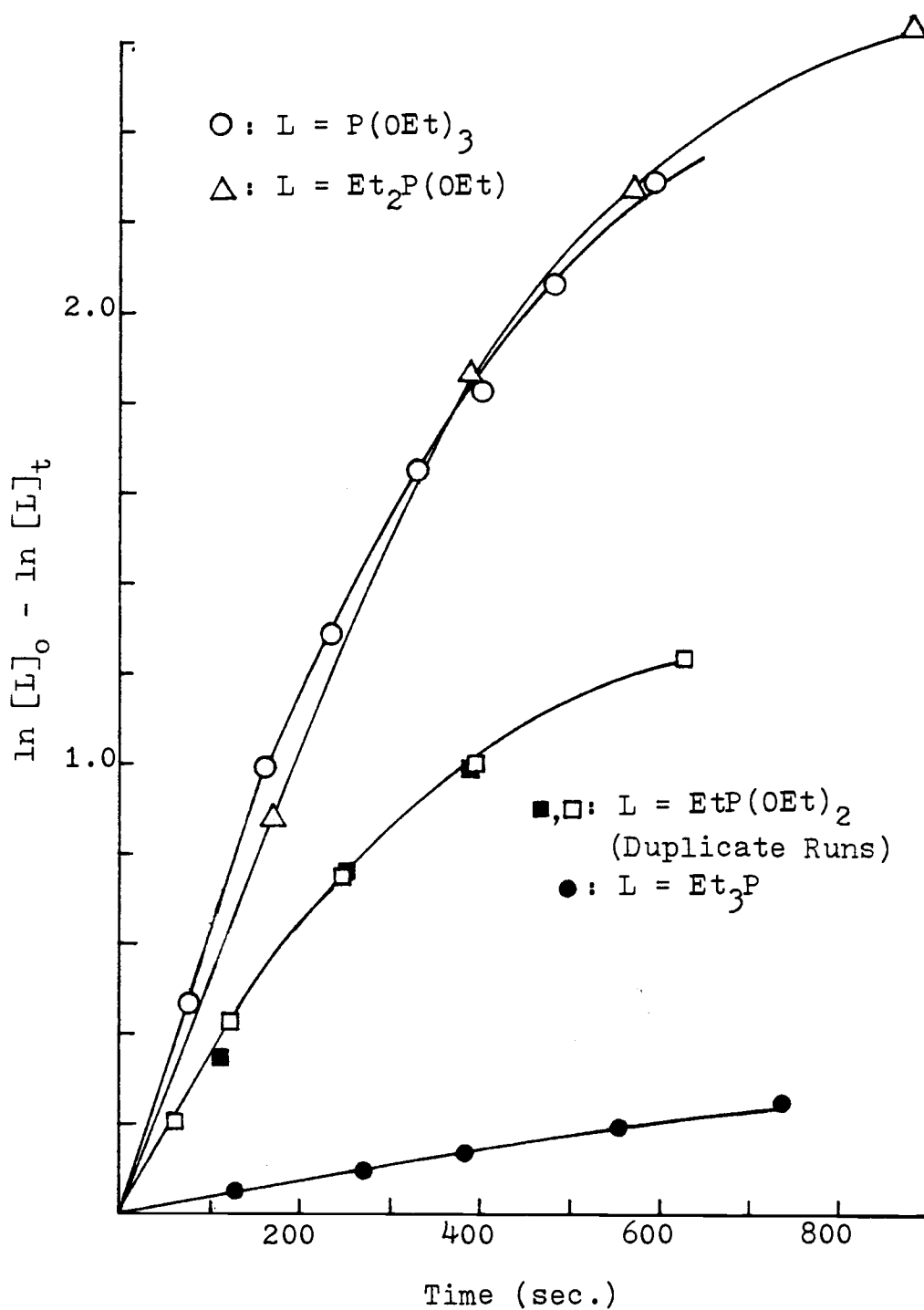


Figure 15. Pseudo-First Order Kinetic Plot for Autoxidation at $L:CoCl_2$ Mole Ratio 2.00

Table IX. Pseudo-First Order Rate Constants for Autoxidation at Mole Ratio $L:CoCl_2=2.00$ in Benzene at 25° ; 1.00 atm. O_2 . (100 % of Co in Form $CoCl_2L_2$)

<u>L</u>	<u>$k'(\text{sec}^{-1})$</u>
Et_3P	3.5×10^{-4}
Et_2POEt	5.1×10^{-3}
$EtP(OEt)_2$	3.3×10^{-3}
$P(OEt)_3$	6.2×10^{-3}

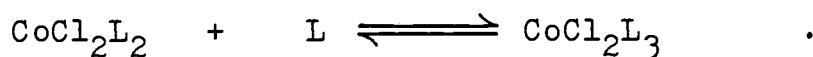
Table X. Initial Distribution of Oxidizable Species and Pseudo-First Order Rate Constants for Autoxidation at Mole Ratio $L:CoCl_2=3.00$ in Benzene at 25° ; 1.00 atm. O_2 .

<u>L</u>	<u>$[CoCl_2L_3]_0 \text{ M}$</u>	<u>$[CoCl_2L_2]_0 \text{ M}$</u>	<u>$[L]_0 \text{ M}$</u>	<u>$k'(\text{sec}^{-1})_M$</u>
Et_2POEt	0.1013 (83.4 % of Co)	0.0201 (15.6 % of Co)	0.0201	9.8×10^{-3}
$EtP(OEt)_2$	0.0483 (90.4 % of Co)	0.00515 (9.6 % of Co)	0.00515	1.2×10^{-2}
$P(OEt)_3$	0.0562 (70.2 % of Co)	0.0238 (29.8 % of Co)	0.0238	5.3×10^{-3}

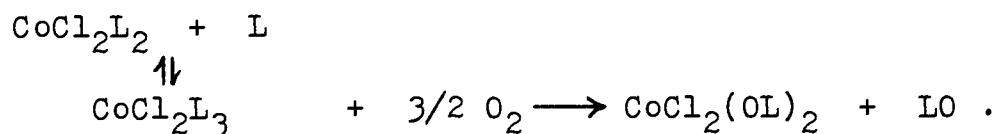
volume of oxygen gas consumed as a function of time.

C. Autoxidation Using a Ligand : Cobalt(II) Chloride Mole Ratio of 3.00

Unlike the case at mole ratio 2, where the substrate is all in the form CoCl_2L_2 , at mole ratio 3 there is present an equilibrium distribution of oxidizable species,



The equilibrium constants for these reactions were presented in Chapter IV. This raises immediate questions about what the autoxidation products and stoichiometry are. The results obtained in this portion of the research answer these questions as follows. For each of the ligands $\text{L} = \text{Et}_n\text{P}(\text{OEt})_{3-n}$, $n = 0 - 2$, the autoxidation reactions proceed with no change in the value of n , and the quantitative reaction stoichiometry in each case is



The g.c. analytical data for samples withdrawn from autoxidation reaction mixtures at various times showed that, for each n , only $\text{Et}_n\text{P}(\text{OEt})_{3-n}$ and $\text{Et}_n\text{P}(\text{O})(\text{OEt})_{3-n}$ were present and that the sum of their concentrations remained constant. Analytical data were obtained up to 78 % conversion for $n = 0$, 96 % conversion for $n = 1$, and 95 % conversion for $n = 2$.

Again, pseudo-first order kinetics were assumed and plots of $\ln([L]_o/[L]_t)$ versus time were prepared; these are shown in Figure 16. Such plots show good linearity for the initial stages of the reaction and up to ca. 70 %, 90 %, and 80 % of completion for $n = 0, 1$, and 2 , respectively. The slopes give the values of the pseudo-first order rate constants reported in Table X, where the calculated initial equilibrium concentrations of species are also reported.

The assumption that the true rate law involves first order dependence on the oxygen concentration,

$$\text{Rate} = k_{\text{pseudo}}[\text{CoCl}_2\text{L}_3] = k[\text{CoCl}_2\text{L}_3]\text{P}_{\text{O}_2}$$

was tested by carrying out an autoxidation reaction at a $\text{P}(\text{OEt})_3 : \text{CoCl}_2$ mole ratio of 3.00 in exactly the same way but using dry air ($\text{P}_{\text{O}_2} = 0.209 \text{ atm}$). Analytical data were obtained up to 68 % conversion. The $\ln([L]_o/[L]_t)$ versus time plot was linear up to 35 % of completion of reaction. It gave a pseudo-first order rate constant of $1.39 \times 10^{-3} \text{ sec}^{-1}$, in reasonable agreement with the value $1.11 \times 10^{-3} \text{ sec}^{-1}$ predicted as 0.209 times the value obtained at $\text{P}_{\text{O}_2} = 1.00 \text{ atm}$.

D. Catalysis of Autoxidation at High Triethyl Phosphite: Cobalt(II) Chloride Mole Ratios

Triethyl phosphite was chosen for this study because,

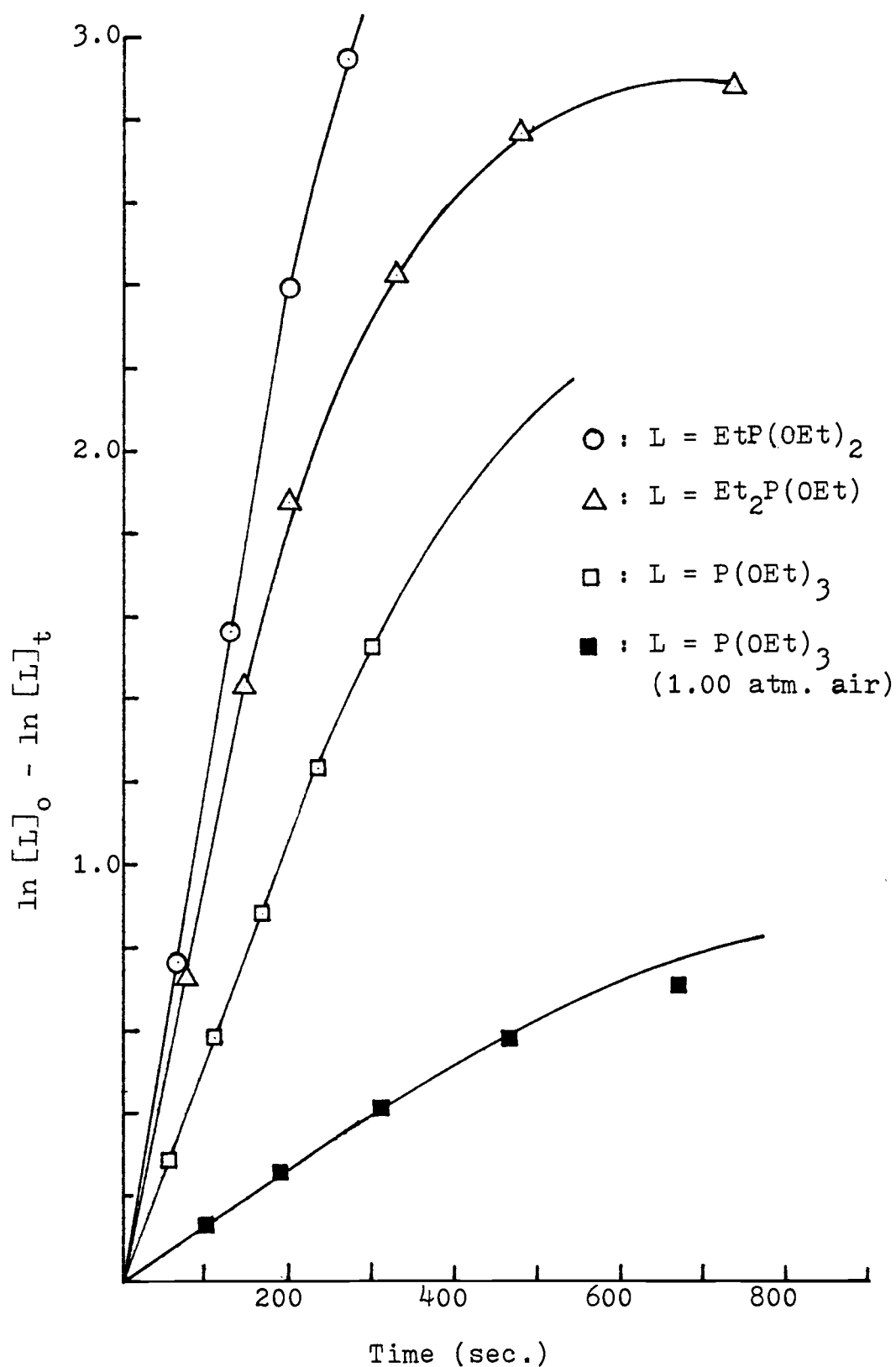


Figure 16. Pseudo-First Order Kinetic Plot for Autoxidation at L CoCl_2 Mole Ratio 3.00

of all the ligands in the group, it alone does not react with oxygen in the absence of initiation. A series of three experiments was designed in which the triethyl phosphite:cobalt(II) chloride mole ratio in benzene was very large and was varied, to see if small amounts of cobalt would catalyze the autoxidation of large amounts of phosphite.

Autoxidation was carried out at 25° and 1.00 atm oxygen pressure. Each solution was prepared to be 0.100 M in o-dichlorobenzene as the g.c. internal standard. The initial triethyl phosphite concentration was approximately 0.2 M in each case. The much smaller cobalt(II) chloride concentration was varied to give mole ratios of 53, 103, and 153. At these high mole ratios, 95 % of the cobalt would be in the form of CoCl_2L_3 , leaving approximately 50, 100, and 150 moles of uncomplexed phosphite per mole of cobalt.

The result of these experiments was that all the phosphite was oxidized in each case, giving dichlorobis-(triethyl phosphate)cobalt(II) plus extra triethyl phosphate as products. After the $t = 0$ point, where a small amount of triethyl phosphite would be retained in the non-volatile complex CoCl_2L_2 , all triethyl phosphite remaining would be found in the volatile fraction. More than enough triethyl

phosphate had been formed at all later times to give $\text{CoCl}_2(\text{OL})_2$ as the non-volatile residue.

Approximate initial rates were found graphically for $-\text{d}[\text{P}(\text{OEt})_3]/\text{dt}$ and for $+\text{d}[\text{P}(\text{O})(\text{OEt})_3]/\text{dt}$ as shown in Figures 17 and 18 by plotting g.c. analytical results for the volatile fractions of aliquots taken at zero time and at the first two reaction times sampled. The two kinds of plots are not in very good numerical agreement with each other, but do show good internal consistency in comparing the data for the three mole ratios used. The $-\text{d}[\text{P}(\text{OEt})_3]/\text{dt}$ approximate initial rates are in the ratio 0.35:0.67:1.00 and the $+\text{d}[\text{P}(\text{O})(\text{OEt})_3]/\text{dt}$ approximate initial rates are in the ratio 0.36:0.59:1.00 in the three experiments. The initial triethyl phosphite concentration (ca. 0.2 M) varied slightly, so the graphically evaluated initial rates should be normalized to give moles of reactant consumed, or product formed, per liter per second per mole of reactant initially present. The resulting normalized ratios are 0.37:0.69:1.00 and 0.36:0.61:1.00, respectively. The cobalt(II) chloride: triethyl phosphite mole ratios in these experiments, 1:53, 1:103, and 1:153, are in the sequence 0.35:0.67:1.00. That is, with the initial triethyl phosphite concentration constant, the initial rate is directly proportional to the cobalt(II) concentration.

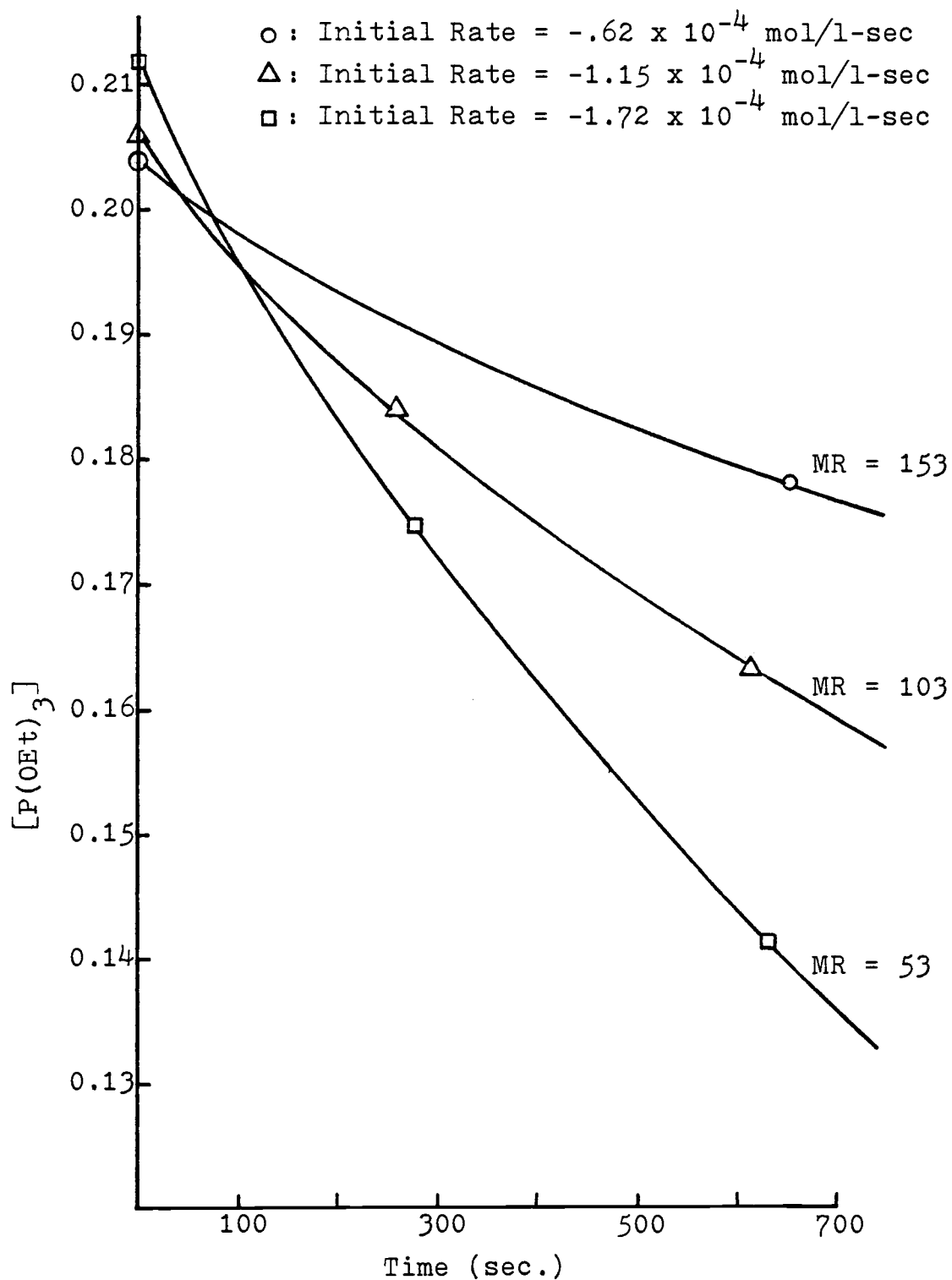


Figure 17. Autoxidation of Triethyl Phosphite at High L:CoCl₂ Mole Ratios.

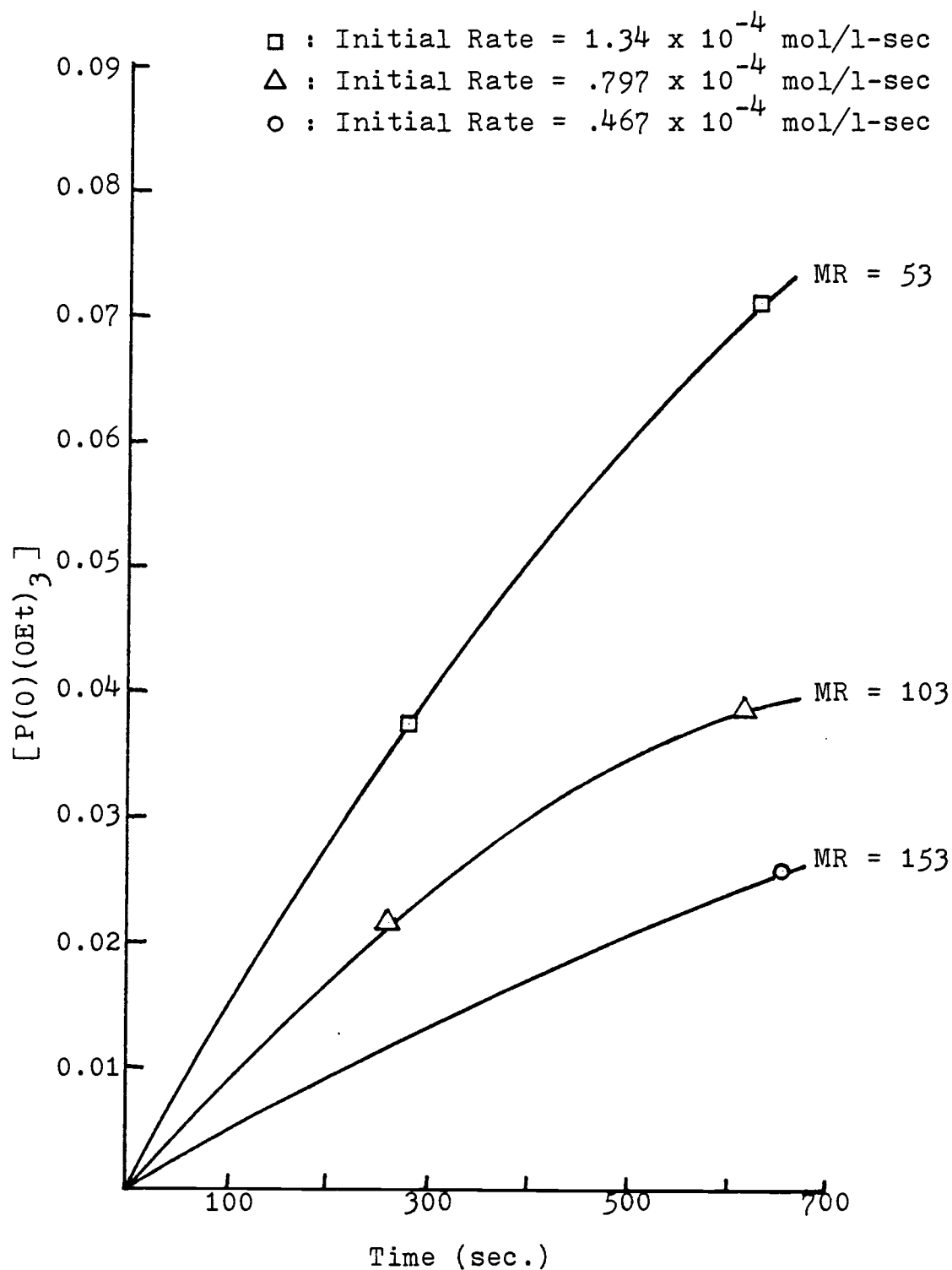


Figure 18. Formation of Triethyl Phosphate at High L:CoCl₂ Mole Ratios.

E. Discussion

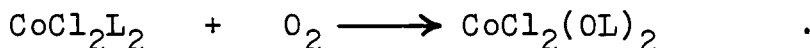
Schmidt (1971) showed that the autoxidation of dichlorobis(triethylphosphine)cobalt(II) differed from the autoxidation of free triethylphosphine in that it was non-radical in nature and gave a single product, triethylphosphine oxide (in its cobalt(II) chloride complex). He showed that the rate law for the initial stage of the reaction is

$$-d[\text{CoCl}_2\text{L}_2]/dt = k[\text{CoCl}_2\text{L}_2]\text{P}\text{O}_2$$

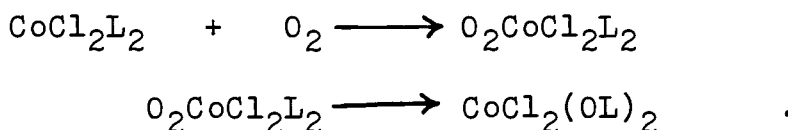
which at constant oxygen pressure takes the pseudo-first order form,

$$-d[\text{CoCl}_2\text{L}_2]/dt = k'[\text{CoCl}_2\text{L}_2] .$$

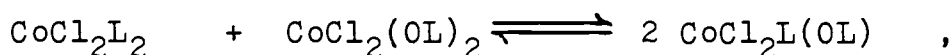
His work is confirmed by the present research and has been extended to encompass the entire series of CoCl_2L_2 complexes, $\text{L} = \text{Et}_n\text{P}(\text{OEt})_{3-n}$, $n = 0 - 3$. All of these complexes consume one mole of dioxygen per mole and give the corresponding phosphoryl complexes with no change in the value of n ,



All of these systems display pseudo-first order kinetics in the initial stage of the reaction. This is in accord with the postulated mechanism,

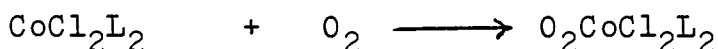


Indeed, first order plots of $\ln[L]_0/[L]$ versus time remain linear up to 50 % or 60 % of completion for the bis-phosphite, phosphonite, and phosphinite complexes, in contrast to the phosphine complex where deviation is observed after 35 % of completion. The deviation was attributed to the operation of the known (and independently studied) equilibrium reaction of the starting material with the reaction product,



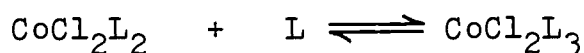
called the "redistribution" equilibrium. As L varies in the series $\text{L} = \text{Et}_n\text{P}(\text{OEt})_{3-n}$, $n = 0 - 3$, an effect on the redistribution equilibrium constant would be expected. By analogy to the work of Tolman (1970), it can be predicted that the equilibrium constant would be the largest in the case of $n = 3$, as the forward reaction relieves steric crowding in the CoCl_2L_2 complex and triethylphosphine has the largest cone angle of the four trivalent phosphorus ligands.

The rate constants shown in Table IX were obtained in the early stage of autoxidation where pseudo-first-order kinetics are followed. Here the triethylphosphine complex differs from the others in that its rate constant is an order of magnitude smaller. This also may be due to steric hindrance, now in the step



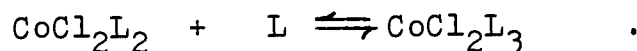
which is thought to be rate determining. The rate constants for the complexes of the other three ligands, $n = 0 - 2$, vary by less than a factor of two and irregularly with n . This may be due to a competition of two factors affecting formation of the dioxygen adduct, a steric one (where the phosphite complex is favored) and an inductive one (where the phosphinite complex would be favored since that ligand, the best sigma donor and poorest pi acceptor of the three, would give the highest electron density on cobalt).

As for the tris-complexes, the operation of a steric effect is obvious in that such a triethylphosphine complex does not even exist. The steric-inductive competition is also apparent in the stabilities of the three tris-complexes which do exist, CoCl_2L_3 , $\text{L} = \text{Et}_n\text{P}(\text{OEt})_{3-n}$, $n = 0 - 2$, where the equilibrium constants for

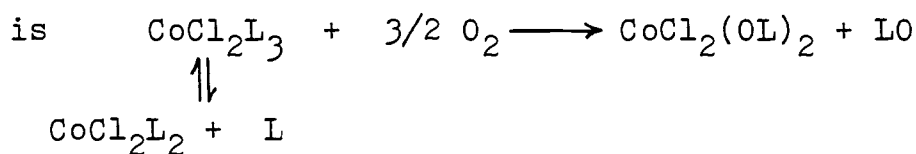


vary irregularly, decreasing in the order $n = 1, 2, 0$. Further operations of these effects may be expected in the interactions of the complexes with dioxygen.

At a $\text{L}:\text{CoCl}_2$ mole ratio of 3.00, an interplay between competitive kinetic rates and net stoichiometry might well be expected since three potentially oxidizable species are present in equilibrium,



Typical values of the initial equilibrium concentrations of each of these species are shown in Table X. In every case, small but significant concentrations of the free ligands L are present. Were the rate of autoxidation of free ligand, described in Chapter V, competitive with the rate of autoxidation of coordinated ligand, then mixed phosphoryl products would be observed in the cases $n = 1$ and $n = 2$. Joedicke's (1976) preliminary study indicated that such was the case for $n = 2$ but not for $n = 1$. It is now found that mixed phosphoryl products are not formed in any case. The quantitative net reaction stoichiometry is

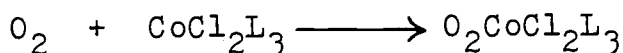


for all values of n , $n = 0 - 2$.

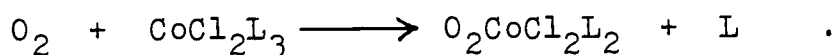
Free triethyl phosphite, $n = 0$, does not undergo autoxidation in benzene at 25° in the absence of initiation. Free diethyl ethylphosphonite and ethyl diethylphosphinite do, to give mixed products, but at rates which would depend on adventitious initiation by impurities or light. Even with purposeful AIBN initiation, the pseudo-first order rate constants for free ligand autoxidation at 50° (Figure 13) are much smaller than for CoCl_2L_3 autoxidation at 25° . Therefore, it is not surprising that the secondary products of autoxidation of the free ligands (which are only minor

solute components in the equilibrium mixtures in the first place) are not observed experimentally.

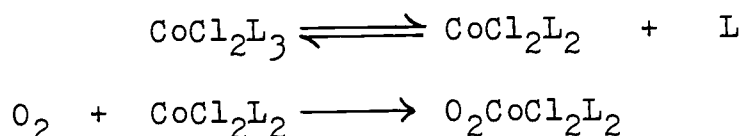
Given the net reaction stoichiometry, the next step is to consider its mechanistic implications. Assuming formation of a dioxygen adduct intermediate as a first step, the reaction might be simply



with an increase in the coordination number of cobalt from five to six. On the other hand, L might be displaced in the reaction,

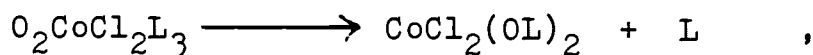


The possibility that only the bis-complexes can form dioxygen adducts,

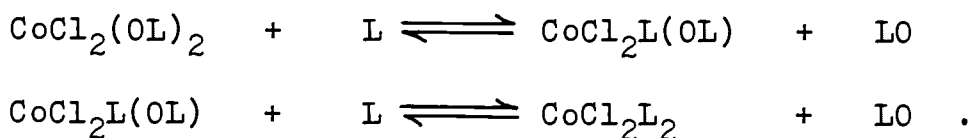


can be ruled out by a comparison of pseudo-first order rate constants at mole ratios 2 and 3 (Tables IX and X). At mole ratio 2, the bis-complexes constitute 100 % of the oxidizable substrate. At mole ratio 3, they constitute only a minor solute component, yet the apparent rate constants are comparable or significantly larger.

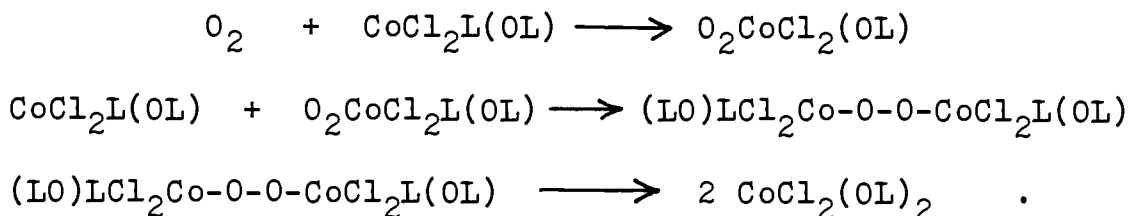
It is known (Schmidt 1971) that the phosphoryl ligands form only tetrahedral bis-complexes $\text{CoCl}_2(\text{OL})_2$ with cobalt(II) chloride. Therefore, in the next step,



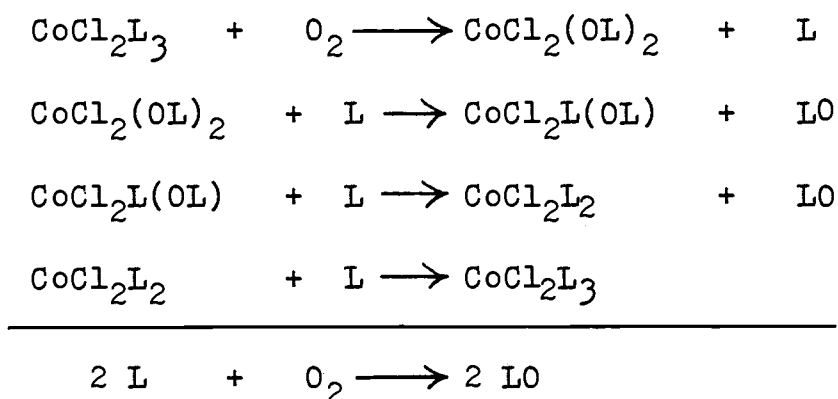
one mole of free L is liberated per mole of cobalt. (This had happened in step one if the dioxygen adduct is $\text{O}_2\text{CoCl}_2\text{L}_2$). Since all free ligand L is converted to phosphoryl product LO in the net reaction with no change in the value of n, meaning that L is oxidized while coordinated rather than while free, it follows that the liberated L must become reassociated,



The $\text{CoCl}_2\text{L}(\text{OL})$ mixed ligand complex is the same one which is known to be formed in the redistribution equilibrium, and for it Schmidt postulated additional steps in the autoxidation mechanism, which may be shown as



For a trace amount of cobalt(II) chloride to act successfully as a catalyst in the autoxidation of a large amount of trivalent organophosphorus substrate, the displacement of oxidized phosphoryl product from the coordination sphere of cobalt is essential.



A study was made using 150, 100, and 50 extra moles of triethyl phosphite per mole of dichlorotris(triethyl phosphite)cobalt(II), i.e., at $\text{CoCl}_2:\text{P}(\text{OEt})_3$ mole ratios of 1:153, 1:103, and 1:53 or 0.00654, 0.00971, and 0.00189. The latter numbers are themselves in the ratio 0.35:0.67:1.00.

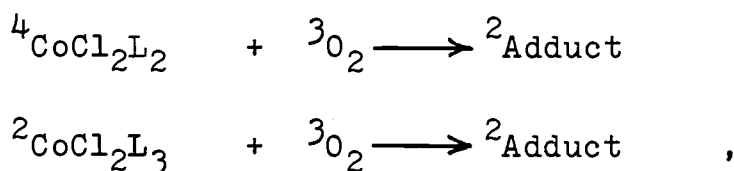
Triethyl phosphite was selected for study because it as a free ligand does not undergo autoxidation under the reaction conditions in the absence of initiator. (With AIBN initiation, its rate of autoxidation is zero order in phosphite and first order in AIBN). The result, that all the triethyl phosphite is rapidly oxidized to triethyl phosphate, proves that cobalt(II) chloride is involved in a highly effective catalytic cycle. Data from the three experiments, normalized to constant initial substrate concentration, show that the ratio of initial rates of triethyl phosphite consumption and of triethylphosphate formation are in excellent quantitative

correspondence with the ratio of cobalt chloride:substrate concentrations. Under these conditions, the reaction is kinetically first order in cobalt catalyst.

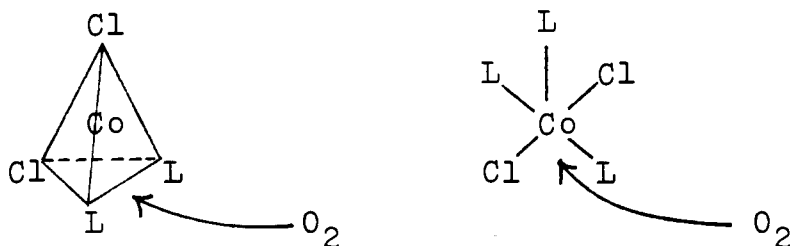
VIII. GENERAL DISCUSSION AND SUMMARY

Of the complexes of cobalt(II) chloride with the ligands $L = Et_nP(OEt)_{3-n}$, the bis(triethylphosphine) complex $CoCl_2(Et_3P)_2$ had been known since 1936, but it was not until the work in this laboratory of Studer (1972) that it was realized that the other three ligands, $n = 0 - 2$, form both bis-complexes $CoCl_2L_2$ and tris-complexes $CoCl_2L_3$. The former, like the long-known $CoCl_2(Et_3P)_2$, are blue or blue-green and are typical examples of a very common coordination state of d^7 cobalt(II), the four-coordinate high-spin state having three unpaired electrons,

At the time of the discovery of the tris-complexes, it was concluded qualitatively that they react much more rapidly with oxygen in the air than do the bis-complexes. Certainly the tris-complex autoxidation was much more obvious, as it involved a dramatic green to deep blue color change. Assuming that the mechanism involved initial formation of a cobalt(II) dioxygen adduct, the question arose as to whether the apparent more rapid autoxidation of the tris-complexes was due to the difference in the states of paramagnetic spin multiplicity,



or whether it was due to a geometric difference,

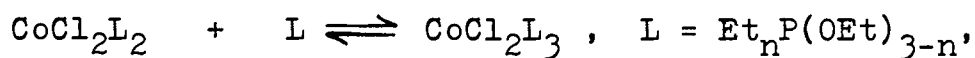


such as the (presumed) approximately square pyramidal five-coordinate complex having a vacant coordination position, thus facilitating attack by dioxygen.

The autoxidation reactions were of interest, not because the conversion of the trivalent organophosphorus compounds to their phosphoryl derivatives represents any synthetic problem, but because they offer an opportunity to study an example of the general phenomenon of transition metal ion catalysis of the autoxidation of organic compounds. In addition, the autoxidation of trivalent phosphorus compounds has long represented both a fundamental and an applied chemistry problem in the field of phosphorus chemistry. In this laboratory, Schmidt (1971) had made the startling discovery that the autoxidation of triethylphosphine, in its cobalt complex $\text{CoCl}_2(\text{Et}_3\text{P})_2$, differed completely in products and mechanistic type from the autoxidation of the free phosphine. Buckler had shown that autoxidation of tertiary phosphines involved an elaborate radical chain mechanism giving mixed phosphoryl products, in which phosphinites,

phosphonites, and phosphites appeared as intermediates. Schmidt showed that the coordinated phosphine was oxidized by a non-radical pathway to the phosphine oxide, quantitatively. Subsequently, other workers published reports of autoxidation of coordinated phosphines. In particular, Hanzlik and Williamson (1976) published a study of autoxidation of a cobalt complex containing only a single oxidizable phosphine ligand and postulated a markedly different type of mechanism than Schmidt's.

Meanwhile, Joedicke (1976) used the difference in paramagnetism of the bis- and tris-complexes to determine the equilibrium constants of the reactions



$$n = 0 - 2$$

by a refinement of the Evans nmr method for determining magnetic susceptibilities. Joedicke developed the method into a quantitative one for reasonably precise determination of equilibrium constants and free energy, enthalpy, and entropy changes over a range of temperatures. He also did some preliminary product studies on autoxidation of the free and coordinated ligands. Since the free organophosphorus ligands L are present in the above equilibrium mixtures, their autoxidation was of interest. There had been several autoxidation studies of trialkylphosphines, and some very limited work with trialkyl

phosphites, but nothing with phosphinites and phosphonites. Joedicke used t-butylbenzene as solvent in this work, but experience with it showed it to be a poor choice for reasons of limited solubility and limited solution stability in certain cases.

A major initial portion of the present research was to determine the bis \rightleftharpoons tris equilibrium constants and thermodynamic functions in benzene, the solvent chosen for detailed autoxidation studies, using the techniques and methods refined by Joedicke. The results are presented in Table V and discussed in Section IV D. For the ligand series $\text{Et}_n\text{P}(\text{OEt})_{3-n}$, an irregular variation of the equilibrium constants decreasing in the order $n = 1, 2, 0$ was found in benzene. The same irregular order had been observed in t-butylbenzene by Joedicke and attributed to a competition between opposing steric and inductive effects. The equilibrium constants are all somewhat smaller in benzene than in t-butylbenzene.

An unanticipated difficulty was encountered in the gas chromatographic analytical method needed for autoxidation product and kinetic studies. This was solved, as described in Section III D, by the use of two analyses for every sample, each of which does part of the job.

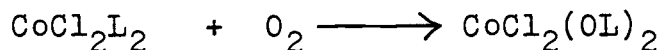
Detailed product distribution and rate studies were carried out on the AIBN-initiated autoxidation of the free ligands triethyl phosphite, diethyl ethylphosphonite,

and ethyl diethylphosphinite in benzene at 50°. The results are discussed in Section V C. Surprising behavior was found for triethyl phosphite, and a previous report in the literature was shown to be incorrect. The autoxidation of triethyl phosphite was found to be zero order in phosphite, first order in oxygen, and first order in AIBN initiator.

Product distribution studies in the autoxidation of diethyl ethylphosphonite and ethyl diethylphosphinite completely confirm the postulate by Buckler that these types of compounds are involved in the radical chain mechanism of trialkylphosphine autoxidation. The rate studies show these autoxidations are first order in phosphonite or phosphinite, and apparently independent of AIBN concentration (over a limited range). The dependence on oxygen pressure was not studied, but is assumed to be first order.

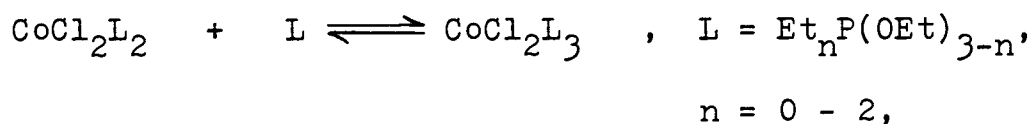
At a ligand:cobalt(II) chloride mole ratio of 2.00, all the solute present is in the form of the bis-complex CoCl_2L_2 . Products and rates of autoxidation of these complexes, $\text{L} = \text{Et}_n\text{P}(\text{OEt})_{3-n}$, were studied not only for the $n = 0 - 2$ ligands but also for the triethylphosphine ($n = 3$) case, to repeat the work of Schmidt under the present reaction conditions (25°, benzene solvent, one atmosphere of oxygen). The agreement with his work is gratifying since he used a completely different experimental method.

It is now found that the autoxidation of all the bis-complexes has the quantitative stoichiometry

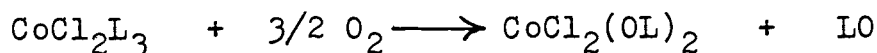


with no change in the value of n in any case. The kinetics (initial rates) at constant oxygen pressure are pseudo-first order in complex concentration. (First order dependence on oxygen pressure is expected in all cases and had been proved to be correct by Schmidt in the case where L is triethylphosphine). The rate constants are presented in Table IX and discussed in Section VII B and E. Their irregular decrease in the order $n = 0, 2, 1, 3$ is interpreted in terms of conflicting steric and inductive effects on the presumed rate-determining step, the formation of a cobalt dioxygen adduct intermediate.

At a ligand:cobalt(II) chloride mole ratio of 3.00, there is present an equilibrium mixture containing three potentially oxidizable substrates,



although CoCl_2L_3 is the major solute species in every case. Autoxidation product studies prove that the net reaction stoichiometry is



with no change in the value of n in any case. No detectable amounts are found of the mixed products, with changes

in the value of n , which would be expected if autoxidation of free ligand L ($n = 1, 2$) could compete with autoxidation of the complexes containing coordinated L . The kinetics (initial rates) at constant oxygen pressure are pseudo-first order in complex concentration (total cobalt concentration). First order dependence on oxygen pressure is expected in all cases and is experimentally proved to be correct in the case where L is triethyl phosphite. The rate constants are presented in Table X and discussed in Section V C and E.

In all the above discussion of the present experimental work, the "solvent" is taken to be just benzene. In fact, 5 vol % cyclohexane was present as the nmr reference standard in the complex equilibrium studies, and 0.1 - 0.2 M *o*-dichlorobenzene was present as the g.c. internal standard in all the autoxidation studies. It is assumed that these amounts of compounds related to benzene will not have a significant effect physically or chemically.

The best data for the solubility of oxygen in benzene are those of Horiuti (1931). For 1.00 atmosphere of oxygen pressure, the molarity of O_2 in the saturated benzene solution is 0.00911 M at 25° and 0.00936 M at 50° C. Using these values, apparent second order initial rate constants can be calculated for all the reactions which have been shown (free L , $n = 0$, $CoCl_2L_2$, $n = 3$, $CoCl_2L_3$, $n = 0$) or assumed (all the rest) to be first order in oxygen and

which have been shown to be first order in substrate. These second order rate constants are collected in Table XI.

Table XI. Apparent Initial Second Order Rate Constants, $M^{-1} \text{ sec}^{-1}$, In Benzene

$$-d[\text{Substrate}]/dt = k_2[\text{Substrate}][O_2]$$

Ligand	Substrate		
	^a L	^b $CoCl_2L_2$	^b $CoCl_2L_3$
$P(OEt)_3$	c	6.8×10^{-1}	5.8×10^{-1}
$EtP(OEt)_2$	8.00×10^{-2}	3.6×10^{-1}	1.3×10^0
Et_2POEt	2.53×10^{-2}	5.6×10^{-1}	1.1×10^0
Et_3P	d	3.8×10^{-2}	e

(a) $50^\circ C$, AIBN initiation

(b) $25^\circ C$

(c) Does not obey this rate law

(d) Not determined

(e) Does not exist

Perhaps the most surprising result is this: the pre-conception, that the low-spin five coordinate tris-complexes undergo much more rapid autoxidation than do the high-spin four coordinate bis-complexes, is incorrect.

The rate constants are probably equal within the experimental error for the triethyl phosphite complexes. With the other two ligands, the tris-complex rate constants are only two or three times larger.

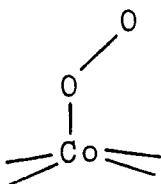
One aspect of catalysis deals with effects on rates, and while no quantitative complex versus free ligand comparisons can be made within the data of Table XI, one might easily call cobalt(II) chloride a catalyst. Another more significant aspect of catalysis deals with reaction mechanisms, and here cobalt(II) chloride clearly brings about the autoxidation of all the organophosphorus ligands by a totally different mechanism. In the three cases $n = 1, 2, 3$, a single phosphoryl product is formed, in contrast to the mixture resulting from autoxidation of the free ligands. In the case of triethyl phosphite, its autoxidation in the bis- and tris-complexes takes place readily in contrast to its totally unreactive behavior as the free ligand in the absence of initiator. Here can be seen a third aspect of catalysis-the ability of a small or trace amount of substance to bring about the reaction of a much larger amount of substrate. The experiments at very high triethyl phosphite : cobalt(II) chloride mole ratios presented in Section VII D show this type of catalytic behavior. Cobalt(II) chloride (and similar salts) in small amounts are eminently practical catalysts for the conversion of large amounts of tertiary phosphite

esters to the corresponding phosphates under mild conditions, such as room temperature and one atmosphere of air.

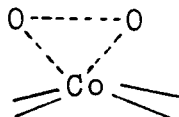
Finally, the previously hypothesized role of cobalt dioxygen adducts as autoxidation reaction intermediates is thoroughly proved by chemical evidence, although such an adduct was not isolated nor was the characterization by physical methods satisfactory. The chemical evidence, presented and discussed in Sections VI B and E, deals with the diethyl ethylphosphonite:cobalt(II) chloride mole ratio 3.00 system in *t*-butylbenzene. It gives incontrovertible proof of the formation at -46° of a 1:1 cobalt dioxygen adduct, whose formation is not reversed in vacuum at -23° , and which decomposes irreversibly to a phosphoryl product on being warmed to room temperature.

The kinetics of this decomposition, studied in the temperature range -9 to $+11^{\circ}$, are discussed in Section VI D and E. Extrapolation using the Arrhenius equation gives, for the unimolecular decomposition at 25° , a first order rate constant of $3.2 \times 10^{-2} \text{sec}^{-1}$. This may be compared to the pseudo-first order apparent initial rate constant $1.2 \times 10^{-2} \text{sec}^{-1}$ for autoxidation at a diethyl ethylphosphonite:cobalt(II) chloride mole ratio of 3.00 in benzene at 25° under one atmosphere of oxygen. Such a comparison supports the postulate that formation of the dioxygen adduct is the rate determining step at room temperature.

Ever since Schmidt's postulate that a dioxygen adduct was an intermediate (or transition state) in dichlorobis-(triethylphosphine)cobalt(II) autoxidation, there has been a conceptual problem as to the mode of decomposition of such an unsymmetrically bound species,



to give a symmetrical product, $\text{CoCl}_2(\text{OL})_2$. Emphasis was placed on compensation of the energy required to rupture the O-O bond by simultaneous formation of two P=O bonds. The ^{17}O epr evidence for rapid exchange of the unsymmetrically bound oxygens in other cobalt adducts suggests that a symmetrical transition state,



may be common to both the exchange and autoxidation processes.

BIBLIOGRAPHY

- Abel, E. W., Pratt, J. M., Whelam, R., and Wilkinson, P. J. (1974), J. Am. Chem. Soc. 96, 7119.
- Arbuzov, B. A., and Rizpolozhenskii, N. I. (1952), Izvest. Akad. Nauk. SSSR, Otdel Khim. Nauk. 854; Chem. Abstr. 47, 9903 (1953).
- Axtell, D. D., and Yoke, J. T. (1973), Inorg. Chem. 12, 1265.
- Basolo, F., Hoffman, B. M., and Ibers, J. A. (1975), Acc. Chem. Res. 8, 384.
- Basolo, F. (1977), Personal Communication.
- Beeby, M. H., and Mann, F. G. (1951), J. Chem. Soc. 411.
- Bentrude, W. G., Hansen, E. R., Khan, W. A., Min, T. B., and Rogers, P. E. (1973), J. Am. Chem. Soc. 95, 2286.
- Berlin, K. D., Austin, T. H., and Stone, K. L. (1964), J. Am. Chem. Soc. 86, 1787.
- Berlin, K. D., Austin, T. H., Nagabhushanam, M., Peterson, M., Calvert, J., Wilson, L. A., and Hopper, D. (1965), J. Gas Chromatog. 3(8), 256.
- Boschi, T., Nicolini, M., and Turco, A. (1966a), Coord. Chem. Rev. 1, 269.
- Boschi, T., Nicolini, M., and Turco, A. (1966b), Coord. Chem. Rev. 1, 133.
- Bressan, M., and Rigo, P. (1975), Inorg. Chem. 14, 38.
- Brown, L. D., and Raymond, K. N. (1975), Inorg. Chem. 14, 2595.
- Buckler, S. A. (1962), J. Am. Chem. Soc. 84, 3093.
- Burness, J. H., Dillard, J. G., and Taylor, L. T. (1975), J. Am. Chem. Soc. 97, 6080.
- Calligaris, M., Nardin, G., Randaccio, L., and Tauzher, G. (1973), Inorg. Nucl. Chem. Lett. 9, 419.

- Carter, M. J., Rillema, D. P., and Basolo, F. (1974), J. Am. Chem. Soc. 96, 392.
- Coe, D. G. (1958), Nature 181, 1519.
- Collman, J. P., Gagne, R. P., Kouba, J., and Ljusberg-Wahren, H. (1974), J. Am. Chem. Soc. 96, 6800.
- Cotton, F. A., and Wilkinson, G. (1972), Advanced Inorganic Chemistry, John Wiley & Sons, New York, N. Y. 3rd. Ed. p.784.
- Cox, J. R. Jr., and Westheimer, F. H. (1958), J. Am. Chem. Soc. 80, 5441.
- Crumbliss, A. L., and Basolo, F. (1970), J. Am. Chem. Soc. 92, 55.
- Davies, A. G., Griller, D., and Roberts, B. P. (1971), Angew. Chem. Internat. Edit. 10, 138.
- Davis, A., Roaldi, A., Michalovic, J. G., and Joseph, H. M. (1963), J. Gas Chromatog. 1(8), 23.
- Drago, R. S. (1979), Inorg. Chem. 18, 1408.
- Ellern, J. B., and Ragsdale, R. O. (1968), Inorg. Synth. 11, 82.
- Ellis, J., Pratt, J. M., and Green, M. (1973), J. Chem. Soc. Chem. Commun. 781
- Evans, D. F. (1959), J. Chem. Soc., 2003.
- Feinland, R., Saaa, J., Buckler, S. A. (1963), Anal. Chem. 35, 920.
- Field, L. R., Wilhelm, E., and Battino, R. (1974), J. Chem. Thermo. 6, 237.
- Floyd, M. B., and Boozer, C. E. (1963), J. Am. Chem. Soc. 85, 984.
- Gall, R. S., and Schaeffer, W. P. (1976), Inorg. Chem. 15, 2758.
- Geoffroy, G. L., Denton, D.A., and Eigenbrot, C.W. (1976), J. Am. Chem. Soc. 15, 2310.

- Getz, D., Melamud, E., Silver, B. L., and Dori, Z.
(1975), J. Am. Chem. Soc. 97, 3846.
- Gudzinowicz, B. J., and Campbell, R. H. (1961), Anal. Chem. 33, 1510.
- Halpern, J., Goodall, B. L., Khare, G. P., Lim, H. S., and Pluth, J. J. (1975), J. Am. Chem. Soc. 97, 2301.
- Handbook of Chemistry and Physics, 56th Ed. (1975),
C.R.C. Press, Cleveland, Ohio.
- Hanzlik, R. P., and Smith, D. F. (1974), J. Chem. Soc. Chem. Commun. 528.
- Hanzlik, R. P., and Williamson, D. (1976), J. Am. Chem. Soc. 98, 6570.
- Hatfield, W. E., and Yoke, J. T. (1962), Inorg. Chem. 1, 475.
- Henrici-Olivé, G., and Olivé, S. (1974), Angew. Chem. Internat. Edit. 13, 29.
- Hoffman, B. M., Diemente, D. L., and Basolo, F. (1970), J. Am. Chem. Soc. 92, 61.
- Hoffman, B. M., Szymanski, T., and Basolo, F. (1975), J. Am. Chem. Soc. 97, 673.
- Hooker Chemical Co., British Patent 937,560 (1963);
Chem. Abstr. 60, 15733 (1964).
- Horiuti, J. (1931), Sci. Papers Inst. Phys. Chem. Research (Tokyo) 17, 125.
- Howe, R. F., and Lunsford, J. H. (1975a), J. Am. Chem. Soc. 97, 5156.
- Howe, R. F., and Lunsford, J. H. (1975b), J. Phys. Chem. 79, 1836.
- Huie, B. T., Leyden, R. M., and Schaeffer, W. P. (1979), Inorg. Chem. 18, 125.
- Humphris, K. J., and Scott, G. (1973), Pure Appl. Chem. 36, 163.

- Huyser, E. S. (1970), Free-Radical Chain Reactions.
Wiley-Interscience, New York, N.Y.
- Jen, J. S., and Thomas, T. D. (1976), unpublished results.
- Jensen, K. A. (1936), Z. Anorg. Allg. Chem. 229, 282.
- Jensen, K. A., Nielsen, P. H., and Pedersen, C. T. (1963),
Acta. Chem. Scand. 17, 1115.
- Joedicke, I. B. (1976), Ph.D. Dissertation, Oregon State University.
- Joedicke, I. B., Studer, H. V., and Yoke, J. T. (1976),
Inorg. Chem. 15, 1352.
- Jones, C. E., and Coskran, K. J. (1971), Inorg. Chem. 10, 1536.
- Jones, R. D., Summerville, D. A., and Basolo, F. (1979),
Chem. Rev. 79, 139.
- Kharasch, M., Jensen, E. V., and Weinhouse, S. (1949),
J. Org. Chem. 14, 429.
- Khare, G. P., Lee-Ruff, E., and Lever, A. B. P. (1976),
Can. J. Chem. 54, 3424.
- Kinnear, A. M., and Perren, E. A. (1952), J. Chem. Soc., 3437.
- Kochi, J. K., and Krusic, P. J. (1969), J. Am. Chem. Soc. 91, 3944.
- Komkov, I. P., Karavanov, K. V., and Ivin, S. Z. (1958),
J. Gen. Chem. (USSR) 28, 1958.
- Krusic, P. J., Mahler, W., and Kochi, J. K. (1972),
J. Am. Chem. Soc. 94, 6033.
- Lewis, J., and Wilkins, R. G. (1960), Modern Coordination Chemistry, Interscience, New York, N.Y.
- McNair, H. M., and Bonelli, E. T. (1967), Basic Gas Chromatography, Varian Aerograph, Walnut Creek, Calif.
- Melamud, E., Silver, B. L., and Dori, Z. (1974), J. Am. Chem. Soc. 96, 4689.

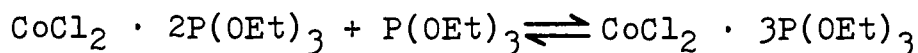
- Nakamoto, K. (1979), Private Communication.
- Nicolini, M., Pecile, C., and Turco, A. (1965), J. Am. Chem. Soc. 87, 2379.
- Ochiai, E. (1973), J. Inorg. Nucl. Chem. 35, 3375.
- Puxeddu, A., Marsich, N., and Casta, G. (1978), J. Chem. Soc. Chem. Commun. 339.
- Pierrard, J. C., Rimbault, J., and Hugel, R. P. (1977), J. Inorg. Nucl. Chem. 39, 1625.
- Plumb, J. B., and Griffin, C. E. (1963), J. Org. Chem. 28, 2908.
- Razumov, A. I., Mukhacheva, O. A., and Sim-Do-Khen. (1952), Izvest. Akad. Nauk. SSSR, Otdel Khim. Nauk. 854; Chem. Abstr. 47, 10466 (1953).
- Rigo, P., and Bressan, M. (1973), Inorg. Nucl. Chem. Lett. 9, 527.
- Rimbault, J., and Hugel, R. (1973), Inorg. Nucl. Chem. Lett. 9, 1.
- Rodley, G. A., and Robinson, W. T. (1972), Nature 235, 438.
- Schmidt, D. D. (1970), Ph.D. Dissertation, Oregon State University.
- Schmidt, D. D., and Yoke, J. T. (1970), Inorg. Chem. 9, 1176.
- Schmidt, D. D., and Yoke, J. T. (1971), J. Am. Chem. Soc. 93, 637.
- Seidell, A. (1940), Solubilities of Inorganic and Metal Organic Compounds, 3rd Ed. Van Nostrand, New York, N.Y.
- Smeykal, K., Baltz, H., and Fischer, H. (1963), J. Prakt. Chem. 22, 186.

- Stephen, H., and Stephen, T. (1963), Solubilities of Inorganic and Organic Compounds, Vol. I, Macmillan Co., New York, N.Y.
- Studer, H. V. (1972), M.S. Thesis, Oregon State University.
- Stynes, H. C., and Ibers, J. A. (1972), J. Am. Chem. Soc. 94, 1559.
- Sykes, A. G., and Weil, J. A. (1970), Prog. Inorg. Chem. 13, 1.
- Szymanski, T., Cape, T. W., Van Duyne, R. P., and Basolo, F. (1979), J. Chem. Soc. Chem. Commun. 117.
- Sznajder, J., Jablonski, A., and Wojciechowski, W. (1979), J. Inorg. Nucl. Chem. 41, 305.
- Takayanagi, T., Yamamoto, H., and Kwan, T. (1975), Bull. Chem. Soc. Japan 48, 2618.
- Tolman, C. A. (1970), J. Am. Chem. Soc. 92, 2956.
- Tolman, C. A., Seidel, W. C., and Gosser, L. W. (1974), J. Am. Chem. Soc. 96, 53.
- Urban, L. (1977), unpublished results.
- Valentine, J. S. (1973), Chem. Rev. 73, 235.
- Vaska, L. (1976), Acc. Chem. Res. 9, 175.
- Walker, F. A. (1970), J. Am. Chem. Soc. 92, 4235.
- Walling, C., and Rabinowitz, R. (1959), J. Am. Chem. Soc. 81, 1243.
- Wayland, B. B., and Abd-Elmageed, M. E. (1974), J. Am. Chem. Soc. 96, 4809.
- Wilhelm, E., and Battino, R. (1973), Chem. Rev. 73, 1.
- Wilkins, R. G. (1971), Adv. Chem. Series 100, 111.
- Willis, C. J. (1974), J. Chem. Soc. Chem. Commun. 117.

APPENDIX I

NMR Shift Data and Equilibrium
Constant Calculations

Table XII. Data for Equilibrium Constant Calculation
From NMR Shifts: Cobalt(II) Chloride-
Triethyl Phosphite System



(A)

(B)

$$(\text{MW})_A = 462.15$$

$$(\text{MW})_B = 628.31$$

$$(\text{DC})_A = -0.269 \times 10^{-3}$$

$$(\text{DC})_B = -0.374 \times 10^{-3}$$

$$\chi_o = -0.7068 \times 10^{-6}$$

(1) $T = 283.2^\circ\text{K}$

$$\Delta\nu_A = 12.78$$

$$\Delta\nu_B = 3.82$$

$$\chi_{M_A}^{\text{cor}} = 6.195 \times 10^3$$

$$\chi_{M_B}^{\text{cor}} = 1.870 \times 10^3$$

Soln	$(M \times 10^3)^a$	$(MR)^b$	$\Delta\nu_{\text{obs}}$	$d_o - d_s$
1	10.154	3.100	8.44	-0.0021
2	10.173	3.200	8.25	-0.0019
3	10.193	3.300	8.10	-0.0018
4	10.213	3.400	7.91	-0.0017

Soln	$(N_A)^c$	$(\text{MW})^d$	$(\text{DC} \times 10^3)^d$	$(\chi_{M_{\text{obs}}}^{\text{cor}} \times 10^3)^d$
1	0.5156	542.6	-0.320	4.051
2	0.4944	546.2	-0.322	3.940
3	0.4777	548.9	-0.324	3.855
4	0.4565	552.5	-0.326	3.752

Soln	$(\text{MW})^e$	$(\text{DC} \times 10^3)^e$	$(\chi_{M_{\text{obs}}}^{\text{cor}} \times 10^3)^e$	$(N_A)^f$
1	544.5	-0.321	2.460	0.5043
2	548.8	-0.324	3.940	0.4786
3	552.0	-0.326	3.855	0.4590
4	556.0	-0.328	3.751	0.4349

Table XII. (Continued)

Soln	$MR + N_A - 3$	$1-N_A/N_{AM}$
1	0.6043	96.80
2	0.6786	107.1
3	0.7591	115.6
4	0.8350	127.2

Linear least squares results : $MR + N_A - 3 = K' \frac{1-N_A}{N_{AM}}$

$K_{eq} = \frac{1}{K'} = 129.53 \pm 6.21$ This value rejected because
 Intercept = -0.1429 ± 0.0415] intercept does not include
 zero within 3σ .

Linear correlation coefficient $r = 0.9976$

(2) $T=288.2^\circ K$

$$\Delta v_A = 12.52$$

$$\Delta v_B = 3.78$$

$$x_{MA}^{cor} = 6.110 \times 10^{-3}$$

$$x_{MB}^{cor} = 1.836 \times 10^{-3}$$

Soln	$(M \times 10^3)^a$	$(MR)^b$	Δv_{obs}	$d_o - d_s$
1	10.094	3.100	8.54	-0.0019
2	10.113	3.200	8.29	-0.0017
3	10.135	3.300	8.09	-0.0017
4	10.154	3.400	7.91	-0.0016

Soln	$(N_A)^c$	$(MW)^d$	$(DC \times 10^3)^d$	$(x_{M_{obs}}^{cor} \times 10^3)^d$
1	0.5446	537.8	-0.317	4.110
2	0.5160	542.6	-0.320	3.969
3	0.4931	546.4	-0.322	3.866
4	0.4760	549.2	-0.324	3.781

Table XII. (Continued)

Soln	(MW) ^e	(DCx10 ³) ^e	($\chi_{\text{M obs}}^{\text{cor}}$ x10 ³) ^e	(N _A) ^f
1	539.9	-0.318	4.109	0.5318
2	545.4	-0.322	3.970	0.4993
3	549.4	-0.324	3.866	0.4750
4	552.7	-0.326	3.780	0.4548

Soln	MR + N _A - 3	1-N _A /N _A M
1	0.6318	87.22
2	0.6993	99.16
3	0.7751	109.1
4	0.8549	118.1

Linear least squares results : $\text{MR} + \text{N}_A - 3 = K' \frac{1-\text{N}_A}{\text{N}_A \text{M}}$

$$K' = (7.216 \pm 0.523) \times 10^{-3} \quad K_{\text{eq}} = 138.59 \pm 10.04$$

$$\text{Intercept} = -0.00578 \pm 0.0544$$

$$\text{Linear correlation coefficient } r = 0.9947$$

(3) T=293.2°K

	$\Delta v_A = 12.27$	$\Delta v_B = 3.73$		
	$\chi_{\text{M}_A}^{\text{cor}} = 6.028 \times 10^{-3}$	$\chi_{\text{M}_B}^{\text{cor}} = 1.804 \times 10^{-3}$		
Soln	(Mx10 ³) ^a	(MR) ^b	Δv_{obs}	d _o -d _s
1	10.036	3.100	8.55	-0.0018
2	10.053	3.200	8.30	-0.0015
3	10.076	3.300	8.10	-0.0016
4	10.096	3.400	8.03	-0.0016

Table XII. (Continued)

Soln	$(N_A)^c$	$(MW)^d$	$(DC \times 10^3)^d$	$(\chi_{M_{obs}}^{cor} \times 10^3)^d$
1	0.5644	534.5	-0.315	4.132
2	0.5351	539.4	-0.318	3.984
3	0.5117	543.3	-0.320	3.886
4	0.5035	544.6	-0.321	3.846

Soln	$(MW)^e$	$(DC \times 10^3)^e$	$(\chi_{M_{obs}}^{cor} \times 10^3)^e$	$(N_A)^f$
1	536.7	-0.316	4.132	0.5511
2	542.6	-0.320	3.984	0.5161
3	546.4	-0.322	3.886	0.4929
4	548.0	-0.323	3.846	0.4834

Soln	$MR + N_A - 3$	$1 - N_A/N_A^M$
1	0.6511	81.16
2	0.7161	93.27
3	0.7930	102.1
4	0.8835	105.9

Linear least squares results: $MR + N_A - 3 = K' \frac{1 - N_A}{N_A^M}$

$$K' = (8.726 \pm 1.871) \times 10^{-3} ; K_{eq} = \frac{1}{K'} = 114.6 \pm 24.6$$

$$\text{Intercept} = -0.0734 \pm 0.1798$$

$$\text{Linear correlation coefficient } r = 0.9569$$

Table XII. (Continued)

(4) $T=298.2^{\circ}\text{K}$

$$\begin{array}{ll} \Delta v_A = 12.02 & \Delta v_B = 3.67 \\ x_{M_A}^{\text{cor}} = 5.948 \times 10^{-3} & x_{M_B}^{\text{cor}} = 1.773 \times 10^{-3} \end{array}$$

Soln	$(M \times 10^3)^a$	$(MR)^b$	Δv_{obs}	$d_o - d_s$
1	9.9770	3.100	8.61	-0.0016
2	9.9970	3.200	8.37	-0.0016
3	10.017	3.300	8.16	-0.0015
4	10.037	3.400	8.10	-0.0016

Soln	$(N_A)^c$	$(MW)^d$	$(DC \times 10^3)^d$	$(x_{M_{\text{obs}}}^{\text{cor}} \times 10^3)^d$
1	0.5916	530.0	-0.312	4.170
2	0.5629	534.8	-0.315	4.048
3	0.5377	539.0	-0.318	3.933
4	0.5305	540.2	-0.318	3.902

Soln	$(MW)^e$	$(DC \times 10^3)^e$	$(x_{M_{\text{obs}}}^{\text{cor}} \times 10^3)^e$	$(N_A)^f$
1	532.9	-0.314	4.170	0.5741
2	537.8	-0.317	4.048	0.5449
3	542.3	-0.320	3.933	0.5174
4	543.6	-0.320	3.902	0.5099

Soln	$MR + N_A - 3$	$1 - N_A / N_{AM}$
1	0.6741	74.36
2	0.7449	83.54
3	0.8175	93.12
4	0.9100	95.94

Table XII. (Continued):

Linear least squares results: $MR + N_A - 3 = K' \frac{1-N_A}{N_A M}$

$$K' = (9.897 \pm 1.990) \times 10^{-3}; \quad K_{eq} = \frac{1}{K'} = 101.04 \pm 20.3$$

$$\text{Intercept} = -0.0718 \pm 0.1734$$

Linear correlation coefficient $r = 0.9618$

(5) $T = 303.2^\circ\text{K}$

$$\Delta\nu_A = 11.76$$

$$\Delta\nu_B = 3.59$$

$$x_{M_A}^{\text{cor}} = 5.870 \times 10^{-3} \quad x_{M_B}^{\text{cor}} = 1.743 \times 10^{-3}$$

Soln	$(M \times 10^3)^a$	$(MR)^b$	$\Delta\nu_{\text{obs}}$	$d_o - d_s$
1	9.9185	3.100	8.71	-0.0015
2	9.9383	3.200	8.47	-0.0015
3	9.9595	3.300	8.27	-0.0015
4	9.9795	3.400	8.20	-0.0016

Soln	$(N_A)^c$	$(MW)^d$	$(DC \times 10^3)^d$	$(x_{M_{\text{obs}}}^{\text{cor}} \times 10^3)^d$
1	0.6267	524.2	-0.308	4.237
2	0.5973	529.1	-0.311	4.113
3	0.5728	533.1	-0.314	4.008
4	0.5643	534.5	-0.315	3.975

Soln	$(MW)^e$	$(DC \times 10^3)^e$	$(x_{M_{\text{obs}}}^{\text{cor}} \times 10^3)^e$	$(N_A)^f$
1	527.9	-0.311	4.238	0.6046
2	532.9	-0.314	4.113	0.5743
3	537.1	-0.316	4.007	0.5486
4	538.5	-0.317	3.974	0.5406

Table XII. (Continued):

Soln	$MR + N_A - 3$	$1 - N_A / N_{AM}$
1	0.7046	65.94
2	0.7743	74.59
3	0.8487	82.62
4	0.9407	85.15

Linear least squares results: $MR + N_A - 3 = K' [1 - N_A / N_{AM}]$

$$K' = (1.120 \pm 0.231) \times 10^{-2}; \quad K_{eq} = \frac{1}{K'} = 89.29 \pm 18.51$$

$$\text{Intercept} = -0.0461 \pm 0.1785$$

Linear correlation coefficient $r=0.9601$

(6) $T=308.2^\circ \text{K}$

$$\Delta \nu_A = 11.58$$

$$\Delta \nu_B = 3.53$$

$$x_{M_A}^{\text{cor}} = 5.794 \times 10^{-3} \quad x_{M_B}^{\text{cor}} = 1.714 \times 10^{-3}$$

Soln	$(M \times 10^3)^a$	$(MR)^b$	$\Delta \nu_{\text{obs}}$	$d_o - d_s$
1	9.8588	3.100	8.83	-0.0013
2	9.8785	3.200	8.62	-0.0013
3	9.9007	3.300	8.44	-0.0014
4	9.9206	3.400	8.35	-0.0015

Soln	$(N_A)^c$	$(MW)^d$	$(DC \times 10^3)^d$	$(x_{M_{\text{obs}}}^{\text{cor}} \times 10^3)^d$
1	0.6584	518.9	-0.305	4.307
2	0.6323	523.2	-0.308	4.197
3	0.6099	527.0	-0.310	4.108
4	0.5988	528.8	-0.311	4.063

Table XII. (Continued)

152

Soln	(MW) ^e	(DCx10 ³) ^e	($\chi_{M_{obs}}^{cor}$ x10 ³) ^d	(N _A) ^f
1	522.7	-0.307	4.307	0.6355
2	527.2	-0.310	4.196	0.6083
3	530.8	-0.312	4.107	0.5865
4	532.7	-0.314	4.063	0.5757

Soln	MR + N _A - 3	$1-N_A/N_{AM}$
1	0.7355	58.18
2	0.8083	65.18
3	0.8866	71.21
4	0.9758	74.29

Linear least squares results: $MR + N_A - 3 = K' [1 - N_A/N_{AM}]$

$$K' = (1.420 \pm 0.214) \times 10^{-2}; \quad K_{eq} = \frac{1}{K'} = 70.42 \pm 10.62$$

$$\text{Intercept} = -0.1030 \pm 0.1445$$

Linear correlation coefficient $r=0.9780$

$$(7) T=313.2^\circ K$$

$$\Delta v_A = 11.46$$

$$\Delta v_B = 3.48$$

$$\chi_{M_A}^{cor} = 5.720 \times 10^{-3} \quad \chi_{M_B}^{cor} = 1.686 \times 10^{-3}$$

Soln	(Mx10 ³) ^a	(MR) ^b	Δv_{obs}	$d_o - d_s$
1	9.8002	3.100	9.04	-0.0012
2	9.8198	3.200	8.83	-0.0012
3	9.8419	3.300	8.66	-0.0013
4	9.8617	3.400	8.51	-0.0014

Table XII. (Continued)

Soln	$(N_A)^c$	$(MW)^d$	$(DC \times 10^3)^d$	$(\chi_{M_{obs}}^{cor} \times 10^3)^d$
1	0.6967	512.5	-0.301	4.430
2	0.6704	516.9	-0.304	4.318
3	0.6491	520.5	-0.306	4.232
4	0.6303	523.6	-0.308	4.158

Soln	$(MW)^e$	$(DC \times 10^3)^e$	$(\chi_{M_{obs}}^{cor} \times 10^3)^e$	$(N_A)^f$
1	515.3	-0.303	4.430	0.6802
2	519.9	-0.305	4.317	0.6522
3	523.4	-0.308	4.232	0.6311
4	526.5	-0.310	4.158	0.6128

Soln	$MR + N_A - 3$	$1 - N_A/N_{AM}$
1	0.7802	47.97
2	0.8522	54.31
3	0.9312	59.39
4	1.0129	64.07

Linear least squares results: $MR + N_A - 3 = K' [1 - N_A/N_{AM}]$

$$K' = (1.446 \pm 0.102) \times 10^{-2}; \quad K_{eq} = \frac{1}{K'} = 69.18 \pm 4.89$$

$$\text{Intercept} = 0.07837 \pm 0.05802$$

Linear correlation coefficient $r=0.9950$

$$(8) T=318.2^\circ K$$

$$\Delta \nu_A = 11.4$$

$$\Delta \nu_B = 3.44$$

$$\chi_{M_A}^{cor} = 5.648 \times 10^{-3} \quad \chi_{M_B}^{cor} = 1.658 \times 10^{-3}$$

Table XII. (Continued)

Soln	$(M \times 10^3)^a$	$(MR)^b$	Δv_{obs}	$d_o - d_s$
1	9.7416	3.100	9.31	-0.0011
2	9.7612	3.200	9.14	-0.0011
3	9.7831	3.300	9.01	-0.0012
4	9.8039	3.400	8.88	-0.0014

Soln	$(N_A)^c$	$(MW)^d$	$(DC \times 10^3)^d$	$(x_{M_{obs}}^{cor} \times 10^3)^d$
1	0.7374	505.8	-0.297	4.582
2	0.7161	509.3	-0.299	4.490
3	0.6997	512.0	-0.301	4.423
4	0.6834	514.8	-0.302	4.364

Soln	$(MW)^e$	$(DC \times 10^3)^e$	$(x_{M_{obs}}^{cor} \times 10^3)^d$	$(N_A)^f$
1	506.5	-0.297	4.582	0.7328
2	510.3	-0.299	4.489	0.7095
3	513.2	-0.301	4.422	0.6927
4	515.6	-0.303	4.365	0.6784

Soln	$MR + N_A - 3$	$1 - N_A / N_{AM}$
1	0.8328	37.43
2	0.9095	41.95
3	0.9928	45.35
4	1.0785	48.35

Linear least squares results: $MR + N_A - 3 = K' [1 - N_A / N_{AM}]$

$$K' = (2.243 \pm 0.193) \times 10^{-2}; \quad K_{eq} = \frac{1}{K'} = 44.59 \pm 3.83$$

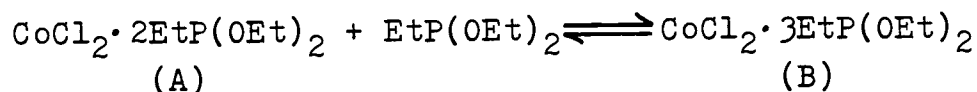
$$\text{Intercept} = -0.01699 \pm 0.08370$$

Linear correlation coefficient $r=0.9927$

Table XII. (Continued)

- (a) Corrected for temperature and flask volume.
- (b) Ligand : Cobalt(II) mole ratio.
- (c) Initial trial values calculated from shift difference ratio.
- (d) Trial values calculated using initial values of N_A .
- (e) Final values, reiteration complete.
- (f) Final value calculated from susceptibility ratio.

Table XIII. Data for Equilibrium Constant Calculation
From NMR Shifts: Cobalt(II) Chloride-
Diethyl Ethylphosphonite System



$$\chi_o = -0.7068 \times 10^{-6}$$

$$(\text{MW})_A = 430.13$$

$$(\text{MW})_B = 580.28$$

$$(\text{DC})_A = -0.260 \times 10^{-3}$$

$$(\text{DC})_B = -0.360 \times 10^{-3}$$

$$(1) T = 283.2^\circ \text{K}$$

$$\Delta \nu_A = 19.06$$

$$\Delta \nu_B = 3.38$$

$$\chi_{M_A}^{\text{cor}} = 8.964 \times 10^{-3}$$

$$\chi_{M_B}^{\text{cor}} = 1.639 \times 10^{-3}$$

Soln	$(M \times 10^3)^a$	$(MR)^b$	$\Delta \nu_{\text{obs}}$	$d_o - d_s$
1	10.127	2.800	7.05	-0.0024
2	10.127	2.950	5.85	-0.0024
3	10.148	3.100	4.82	-0.0024
4	10.168	3.200	4.67	-0.0024
5	10.188	3.300	4.31	-0.0024
6	10.107	3.400	3.89	-0.0024

Soln	$(N_A)^c$	$(MW)^d$	$(DC \times 10^3)^d$	$(\chi_{M_A}^{\text{cor}} \times 10^3)^d$
1	0.2431	545.1	-0.337	3.444
2	0.1575	556.6	-0.344	2.877
3	0.09184	566.5	-0.351	2.386
4	0.08227	567.9	-0.352	2.311
5	0.05931	571.4	-0.354	2.137
6	0.03253	575.4	-0.357	1.956

Table XIII. (Continued)

Soln	(MW) ^e	(DCx10 ³) ^e	(x _{M_A} ^{cor} x10 ³) ^e	(N _A) ^f
1	543.3	-0.335	3.443	0.2463
2	554.9	-0.343	2.877	0.1690
3	565.0	-0.350	2.386	0.1020
4	566.5	-0.351	2.311	0.09174
5	570.1	-0.353	2.137	0.06799
6	573.8	-0.356	1.956	0.04328

Soln	MR + N _A - 3	^{1-N_A} /N _A ^M
1	0.0463	302.2
2	0.1190	485.5
3	0.2020	867.6
4	0.2917	973.7
5	0.36799	1345
6	0.44328	2187

Linear least squares results: $MR + N_A - 3 = K' [^{1-N_A}/N_A^M]$

$$K_{eq} = \frac{1}{K'} = 4721.6 \pm 770.6$$

$$\text{Intercept} = 0.0271 \pm 0.041$$

Linear correlation coefficient $r=0.9506$

$$(2) T=288.2 \text{ } ^\circ\text{K}$$

$$\Delta v_A = 18.58$$

$$\Delta v_B = 3.32$$

$$x_{M_A}^{cor} = 8.806 \times 10^{-3}$$

$$x_{M_A}^{cor} = 1.613 \times 10^{-3}$$

Table XIII. (Continued)

Soln	$(M \times 10^3)^a$	$(MR)^b$	Δv_{obs}	$d_o - d_s$
1	10.070	2.800	7.09	-0.0024
2	10.070	2.950	5.90	-0.0024
3	10.090	3.100	4.88	-0.0024
4	10.110	3.200	4.69	-0.0024
5	10.131	3.300	4.34	-0.0024
6	10.049	3.400	4.03	-0.0023

Soln	$(N_A)^c$	$(MW)^d$	$(DC \times 10^3)^d$	$(x_{MA}^{\text{cor}} \times 10^3)^d$
1	0.2471	543.2	-0.335	3.481
2	0.1691	554.9	-0.343	2.916
3	0.1022	564.9	-0.350	2.428
4	0.08978	566.8	-0.351	2.333
5	0.06684	570.3	-0.353	2.162
6	0.04653	573.3	-0.355	2.027

Soln	$(MW)^e$	$(DC \times 10^3)^e$	$(x_{MA}^{\text{cor}} \times 10^3)^e$	$(N_A)^f$
1	541.3	-0.334	3.481	0.2597
2	553.1	-0.342	2.916	0.1811
3	563.3	-0.349	2.428	0.1133
4	565.2	-0.350	2.334	0.1002
5	568.8	-0.352	2.162	0.07632
6	571.6	-0.354	2.027	0.05756

Soln	$MR + N_A - 3$	$1 - N_A / N_{AM}$
1	0.0597	283.1
2	0.1311	449.0
3	0.2133	775.6
4	0.3002	888.2
5	0.37632	1195
6	0.45756	1629

Table XIII (Continued)

Linear least squares results: $MR + N_A - 3 = K' [1 - N_A/N_A^M]$

$$K_{eq} = \frac{1}{K'} = 3324.7 \pm 289.1$$

$$\text{Intercept} = -0.0053 \pm 0.026$$

Linear correlation coefficient $r=0.9852$

(3) $T=293.2^\circ\text{K}$

$$\Delta v_A = 18.16$$

$$\Delta v_B = 3.25$$

$$\chi_{M_A}^{\text{cor}} = 8.654 \times 10^{-3}$$

$$\chi_{M_B}^{\text{cor}} = 1.589 \times 10^{-3}$$

Soln	$(M \times 10^3)^a$	$(MR)^b$	Δv_{obs}	$d_o - d_s$
1	10.012	2.800	7.15	-0.0023
2	10.012	2.950	5.96	-0.0023
3	10.032	3.100	5.01	-0.0023
4	10.052	3.200	4.79	-0.0023
5	10.072	3.300	4.46	-0.0023
6	9.9916	3.400	4.19	-0.0023
Soln	$(N_A)^c$	$(MW)^d$	$(DC \times 10^3)^d$	$(\chi_{M_{\text{obs}}}^{\text{cor}} \times 10^3)^d$
1	0.2616	541.0	-0.334	3.524
2	0.1818	553.0	-0.342	2.955
3	0.1180	562.6	-0.348	2.496
4	0.1033	564.8	-0.350	2.388
5	0.08059	568.2	-0.352	2.225
6	0.06246	570.9	-0.354	2.115
Soln	$(MW)^e$	$(DC \times 10^3)^e$	$(\chi_{M_{\text{obs}}}^{\text{cor}} \times 10^3)^e$	$(N_A)^f$
1	539.2	-0.333	3.524	0.2739
2	551.3	-0.341	2.955	0.1933
3	561.0	-0.347	2.496	0.1284

Table X III. (Continued)

Soln	(MW) ^e	(DCx10 ³) ^e	($\chi_{M_{obs}}^{cor} \times 10^3$) ^e	(N _A) ^f
4	563.3	-0.349	2.388	0.1131
5	566.8	-0.351	2.225	0.09002
6	569.1	-0.353	2.116	0.07459

Soln	MR + N _A - 3	$1 - N_A / N_{AM}$
1	0.0739	264.8
2	0.1433	417.3
3	0.2284	676.7
4	0.3131	780.1
5	0.39002	1004
6	0.47459	1242

Linear least squares results: $MR + N_A - 3 = K' [1 - N_A / N_{AM}]$

$$K_{eq} = \frac{1}{K'} = 2407.0 \pm 112.9$$

$$\text{Intercept} = -0.0331 \pm 0.0156$$

Linear correlation coefficient $r=0.9956$

$$(4) T=298.2^\circ K$$

$$\Delta\nu_A = 17.71$$

$$\Delta\nu_B = 3.20$$

$$\chi_{M_A}^{cor} = 8.507 \times 10^{-3}$$

$$\chi_{M_B}^{cor} = 1.565 \times 10^{-3}$$

Soln	(Mx10 ³) ^a	(MR) ^b	$\Delta\nu_{obs}$	d _o - d _s
1	9.9543	2.800	7.18	-0.0022
2	9.9543	2.950	6.06	-0.0022
3	9.9743	3.100	5.13	-0.0022
4	9.9943	3.200	4.96	-0.0022
5	10.014	3.300	4.68	-0.0023
6	9.9345	3.400	4.33	-0.0023

Table XIII. (Continued)

Soln	$(N_A)^c$	$(MW)^d$	$(DC \times 10^3)^d$	$(\chi_{M_{obs}}^{cor} \times 10^3)^d$
1	0.2743	539.1	-0.333	3.552
2	0.1971	550.7	-0.340	3.014
3	0.1330	560.3	-0.347	2.563
4	0.1213	562.1	-0.348	2.477
5	0.1019	565.0	-0.350	2.344
6	0.07782	568.6	-0.352	2.195

Soln	$(MW)^e$	$(DC \times 10^3)^e$	$(\chi_{M_{obs}}^{cor} \times 10^3)^e$	$(N_A)^f$
1	537.4	-0.331	3.551	0.2861
2	548.9	-0.339	3.014	0.2087
3	558.7	-0.346	2.563	0.1438
4	560.6	-0.347	2.477	0.1314
5	563.4	-0.349	2.344	0.1122
6	566.6	-0.351	2.196	0.09090

Soln	$MR + N_A - 3$	$1 - N_A / N_A^M$
1	0.0861	250.7
2	0.1587	380.9
3	0.2435	596.9
4	0.3314	661.4
5	0.4122	790.2
6	0.49090	1007

Linear least squares results: $MR + N_A - 3 = K' [1 - N_A / N_A^M]$

$$K_{eq} = \frac{1}{K'} = 1800.4 \pm 130.3$$

$$\text{Intercept} = -0.0541 \pm 0.0267$$

Linear correlation coefficient $r=0.9897$

Table XIII. (Continued)

(5) $T=303.2^{\circ}\text{K}$

$$\Delta v_A = 17.32$$

$$\Delta v_B = 3.13$$

$$\chi_{M_A}^{\text{cor}} = 8.366 \times 10^{-3}$$

$$\chi_{M_B}^{\text{cor}} = 1.542 \times 10^{-3}$$

Soln	$(M \times 10^3)^a$	$(MR)^b$	Δv_{obs}	$d_o - d_s$
1	9.8971	2.800	7.25	-0.0022
2	9.8971	2.950	6.20	-0.0022
3	9.9169	3.100	5.32	-0.0022
4	9.9368	3.200	5.11	-0.0022
5	9.9557	3.300	4.85	-0.0022
6	9.8762	3.400	4.48	-0.0022

Soln	$(N_A)^c$	$(MW)^d$	$(DC \times 10^3)^d$	$(\chi_{M_{\text{obs}}}^{\text{cor}} \times 10^3)^d$
1	0.2903	536.7	-0.331	3.607
2	0.2163	547.8	-0.338	3.099
3	0.1543	557.1	-0.345	2.669
4	0.1395	559.3	-0.346	2.562
5	0.1206	562.2	-0.348	2.433
6	0.09450	566.1	-0.351	2.274

Soln	$(MW)^e$	$(DC \times 10^3)^e$	$(\chi_{M_{\text{obs}}}^{\text{cor}} \times 10^3)^e$	$(N_A)^f$
1	534.8	-0.330	3.607	0.3026
2	546.0	-0.337	3.099	0.2282
3	555.5	-0.343	2.668	0.1650
4	557.8	-0.345	2.562	0.1495
5	560.7	-0.347	2.433	0.1306
6	564.2	-0.349	2.273	0.1071

Table XIII. (Continued)

Soln	$MR + N_A - 3$	$1 - N_A/N_{AM}$
1	0.1026	232.9
2	0.1782	341.7
3	0.2650	510.3
4	0.3495	572.5
5	0.4306	668.7
6	0.5071	844.2

Linear least squares results: $MR + N_A - 3 = K' [1 - N_A/N_{AM}]$

$$K_{eq} = \frac{1}{K'} = 1455.1 \pm 96.4$$

$$\text{Intercept} = -0.0577 \pm 0.0258$$

Linear correlation coefficient $r=0.9913$

(6) $T=308.2^\circ K$

$$\Delta v_A = 16.94$$

$$\Delta v_B = 3.06$$

$$\chi_{M_A}^{cor} = 8.228 \times 10^{-3}$$

$$\chi_{M_B}^{cor} = 1.519 \times 10^{-3}$$

Soln	$(M \times 10^3)^a$	$(MR)^b$	Δv_{obs}	$d_o - d_s$
1	9.8387	2.800	7.41	-0.0021
2	9.8387	2.950	6.41	-0.0021
3	9.8584	3.100	5.59	-0.0021
4	9.8782	3.200	5.46	-0.0021
5	9.8981	3.300	5.17	-0.0022
6	9.8191	3.400	4.72	-0.0022

Soln	$(N_A)^c$	$(MW)^d$	$(DC \times 10^3)^d$	$(\chi_{M_{obs}}^{cor} \times 10^3)^d$
1	0.2903	536.7	-0.331	3.607
2	0.2163	547.8	-0.338	3.099
3	0.1543	557.1	-0.345	2.669

Table XIII. (Continued)

Soln	$(N_A)^c$	$(MW)^d$	$(DC \times 10^3)^d$	$(\chi_{M_{obs}}^{cor} \times 10^3)^d$
4	0.1395	559.3	-0.346	2.562
5	0.1206	562.2	-0.348	2.433
6	0.09450	566.1	-0.351	2.274

Soln	$(MW)^e$	$(DC \times 10^3)^e$	$(\chi_{M_{obs}}^{cor} \times 10^3)^e$	$(N_A)^f$
1	534.8	-0.330	3.607	0.3026
2	546.0	-0.337	3.099	0.2282
3	555.5	-0.343	2.668	0.1650
4	557.8	-0.345	2.562	0.1495
5	560.7	-0.347	2.433	0.1306
6	564.2	-0.349	2.273	0.1071

Soln	$MR + N_A - 3$	$1 - N_A/N_{AM}$
1	0.1026	232.9
2	0.1782	341.7
3	0.2650	510.3
4	0.3495	572.5
5	0.4306	668.7
6	0.5071	844.2

Linear least squares results: $MR + N_A - 3 = K' [1 - N_A/N_{AM}]$

$$K_{eq} = \frac{1}{K'} = 1455.1 \pm 96.4$$

$$\text{Intercept} = -0.0577 \pm 0.0258$$

Linear correlation coefficient $r=0.9913$

$$(7) T=313.2^\circ K$$

$$\Delta v_A = 16.75$$

$$\Delta v_B = 3.01$$

Table XIII. (Continued)

$\chi_{M_A}^{cor} = 8.096 \times 10^{-3}$ $\chi_{M_B}^{cor} = 1.497 \times 10^{-3}$				
Soln	$(M \times 10^3)^a$	$(MR)^b$	Δv_{obs}	$d_o - d_s$
1	9.7815	2.800	7.54	-0.0021
2	9.7815	2.950	6.60	-0.0021
3	9.8011	3.100	5.86	-0.0021
4	9.8207	3.200	5.82	-0.0021
5	9.8405	3.300	5.49	-0.0021
6	9.7619	3.400	5.05	-0.0022
Soln	$(N_A)^c$	$(MW)^d$	$(DC \times 10^3)^d$	$(\chi_{M_{obs}}^{cor} \times 10^3)^d$
1	0.3297	530.8	-0.327	3.785
2	0.2613	541.0	-0.334	3.326
3	0.2074	549.1	-0.339	2.957
4	0.2045	549.6	-0.340	2.933
5	0.1811	553.1	-0.342	2.766
6	0.1488	557.9	-0.345	2.580
Soln	$(MW)^e$	$(DC \times 10^3)^e$	$(\chi_{M_{obs}}^{cor} \times 10^3)^e$	$(N_A)^f$
1	528.2	-0.325	3.785	0.3467
2	538.7	-0.332	3.325	0.2770
3	547.1	-0.338	2.957	0.2212
4	547.6	-0.338	2.932	0.2175
5	551.4	-0.341	2.766	0.1923
6	555.6	-0.344	2.580	0.1641
Soln	$MR + N_A - 3$	$1 - N_A / N_{AM}$		
1	0.1467	192.6		
2	0.2270	266.8		
3	0.3212	359.2		

Table XIII. (Continued)

Soln	MR + N _A - 3	$1-N_A/N_{AM}$
4	0.4175	366.2
5	0.4923	426.8
6	0.5641	521.8

Linear least squares results: $MR + N_A - 3 = K' [1 - N_A/N_{AM}]$

$$K_{eq} = \frac{1}{K'} = 744.2 \pm 80.5$$

$$\text{Intercept} = -0.116 \pm 0.054$$

Linear correlation coefficient $r=0.9774$

$$(8) T=318.2^\circ K$$

$$\Delta v_A = 16.47$$

$$\Delta v_B = 2.96$$

$$\chi_{MA}^{cor} = 7.967 \times 10^{-3}$$

$$\chi_{MB}^{cor} = 1.476 \times 10^{-3}$$

Soln	$(M \times 10^3)^a$	$(MR)^b$	Δv_{obs}	$d_o - d_s$
1	9.7231	2.800	7.82	-0.0020
2	9.7231	2.950	6.83	-0.0020
3	9.7425	3.100	6.22	-0.0020
4	9.7621	3.200	6.11	-0.0020
5	9.7817	3.300	5.81	-0.0020
6	9.7037	3.400	5.36	-0.0020

Soln	$(N_A)^c$	$(MW)^d$	$(DC \times 10^3)^d$	$(\chi_{M_{obs}}^{cor} \times 10^3)^d$
1	0.3595	526.3	-0.324	3.937
2	0.2865	537.3	-0.331	3.450
3	0.2413	544.0	-0.336	3.144
4	0.2332	545.3	-0.337	3.085
5	0.2114	548.5	-0.339	2.932
6	0.1780	553.6	-0.342	2.734

Table XIII. (Continued)

Soln	(MW) ^e	(DCx10 ³) ^e	($\chi_{M_{obs}}^{cor} \times 10^3$) ^e	(N _A) ^f
1	524.6	-0.323	3.878	0.3701
2	534.6	-0.330	3.451	0.3043
3	541.7	-0.334	3.144	0.2570
4	543.1	-0.335	3.084	0.2477
5	546.6	-0.338	2.933	0.2245
6	551.2	-0.341	2.734	0.1938

Soln	MR + N _A - 3	$1 - N_A / N_{AM}$
1	0.1701	175.0
2	0.2543	235.1
3	0.3570	296.7
4	0.4477	311.1
5	0.5245	353.1
6	0.5938	428.7

Linear least squares results: $MR + N_A - 3 = K' [1 - N_A / N_{AM}]$

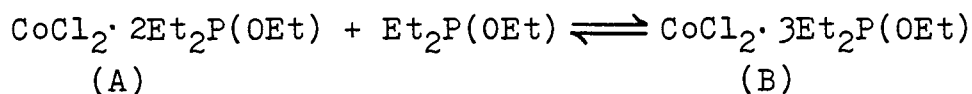
$$K_{eq} = \frac{1}{K'} = 580.5 \pm 59.4$$

Intercept = -0.122 ± 0.055

Linear correlation coefficient $r=0.9797$

- (a) Corrected for temperature and flask volume.
- (b) Ligand : Cobalt(II) mole ratio.
- (c) Initial trial values calculated from shift difference ratio.
- (d) Trial values calculated using initial values of N_A.
- (e) Final values, reiteration complete.
- (f) Final value calculated from susceptibility ratio.

Table XIV. Data for Equilibrium Constant Calculation
From NMR Shifts: Cobalt(II) Chloride-
Ethyl Diethylphosphinite System



$$(\text{MW})_A = 398.13$$

$$(\text{MW})_B = 532.28$$

$$(\text{DC})_A = -0.251 \times 10^{-3}$$

$$(\text{DC})_B = -0.346 \times 10^{-3}$$

$$\chi_o = -0.7068 \times 10^{-6}$$

$$(1) T = 283.2^\circ \text{K}$$

$$\Delta\nu_A = 19.16$$

$$\Delta\nu_B = 3.62$$

$$\chi_{M_A}^{\text{cor}} = 9.074 \times 10^{-3}$$

$$\chi_{M_B}^{\text{cor}} = 1.738 \times 10^{-3}$$

Soln	$(M \times 10^3)^a$	$(MR)^b$	$\Delta\nu_{\text{obs}}$	$d_o - d_s$
1	10.160	3.0000	7.70	-0.0052
2	10.154	3.1501	6.90	-0.0051
3	10.114	3.3003	6.37	-0.0051
4	10.165	3.4004	5.88	-0.0051

Soln	$(N_A)^c$	$(\text{MW})^d$	$(\text{DC} \times 10^3)^d$	$(\chi_{M_{\text{obs}}}^{\text{cor}} \times 10^3)^d$
1	0.2625	497.1	-0.321	3.961
2	0.2111	504.0	-0.326	3.570
3	0.1770	508.5	-0.329	3.337
4	0.1454	512.8	-0.332	3.087

Soln	$(\text{MW})^e$	$(\text{DC} \times 10^3)^e$	$(\chi_{M_{\text{obs}}}^{\text{cor}} \times 10^3)^e$	$(N_A)^f$
1	491.6	-0.317	3.961	0.3030
2	498.8	-0.322	3.569	0.2496
3	503.0	-0.325	3.336	0.2178
4	507.6	-0.329	3.087	0.1839

Table XIV.(Continued)

Soln	$MR + N_A - 3$	$1-N_A/N_{AM}$
1	0.3030	226.4
2	0.3997	296.1
3	0.5180	355.1
4	0.5843	436.6

Linear least squares results: $MR + N_A - 3 = K' [1-N_A/N_{AM}]$

$$K' = (1.381 \pm 0.163) \times 10^{-3} \quad K_{eq} = \frac{1}{K'} = 723.97 \pm 85.55$$

$$\text{Intercept} = -0.002544 \pm 0.055$$

Linear correlation coefficient $r=0.9863$

(2) $T=288.2^\circ K$

$$\Delta v_A = 18.8$$

$$\Delta v_B = 3.56$$

$$\chi_{M_A}^{cor} = 8.925 \times 10^{-3}$$

$$\chi_{M_B}^{cor} = 1.719 \times 10^{-3}$$

Soln	$(M \times 10^3)^a$	$(MR)^b$	Δv_{obs}	$d_o - d_s$
1	10.100	3.0000	8.28	-0.0050
2	10.096	3.1501	7.45	-0.0050
3	10.054	3.3003	7.10	-0.0049
4	10.106	3.4004	6.48	-0.0049

Soln	$(N_A)^c$	$(MW)^d$	$(DC \times 10^3)^d$	$(\chi_{M_{obs}}^{cor} \times 10^3)^d$
1	0.3097	490.7	-0.317	4.234
2	0.2552	498.0	-0.322	3.843
3	0.2323	501.1	-0.324	3.688
4	0.1916	506.6	-0.328	3.375

Table XIV. (Continued)

Soln	(MW) ^e	(DCx10 ³) ^e	($\chi_{M_{obs}}^{cor} \times 10^3$) ^e	(N _A) ^f
1	485.5	-0.313	4.234	0.3490
2	492.7	-0.318	3.843	0.2948
3	495.6	-0.320	3.688	0.2732
4	501.5	-0.324	3.375	0.2298

Soln	MR + N _A - 3	$1 - N_A/N_A^M$
1	0.3490	184.7
2	0.4449	236.9
3	0.5735	264.6
4	0.6302	331.6

Linear least squares results: $MR + N_A - 3 = K' [1 - N_A/N_A^M]$

$$K' = (1.985 \pm 0.418) \times 10^{-3} \quad K_{eq} = \frac{1}{K'} = 503.73 \pm 106.28$$

$$\text{Intercept} = -0.002544 \pm 0.055$$

Linear correlation coefficient $r=0.9863$

$$(3) T=293.2^\circ K$$

$$\Delta v_A = 18.42$$

$$\Delta v_B = 3.51$$

$$\chi_{M_A}^{cor} = 8.780 \times 10^{-3}$$

$$\chi_{M_B}^{cor} = 1.700 \times 10^{-3}$$

Soln	(Mx10 ³) ^a	(MR) ^b	Δv_{obs}	$d_o - d_s$
1	10.041	3.0000	8.87	-0.0048
2	10.036	3.1501	8.10	-0.0048
3	9.9951	3.3003	7.71	-0.0047
4	10.046	3.4004	7.13	-0.0047

Table XIV. (Continued)

Soln	$(N_A)^c$	$(MW)^d$	$(DC \times 10^3)^d$	$(\chi_{M_{obs}}^{cor} \times 10^3)^d$
1	0.3595	484.1	-0.312	4.526
2	0.3078	491.0	-0.317	4.162
3	0.2817	494.5	-0.319	3.984
4	0.2428	499.7	-0.323	3.690

Soln	$(MW)^e$	$(DC \times 10^3)^e$	$(\chi_{M_{obs}}^{cor} \times 10^3)^e$	$(N_A)^f$
1	478.7	-0.308	4.526	0.3992
2	485.6	-0.313	4.162	0.3477
3	489.0	-0.315	3.984	0.3226
4	494.6	-0.319	3.689	0.2809

Soln	$MR + N_A - 3$	$1 - N_A / N_{AM}$
1	0.3992	149.9
2	0.4978	186.9
3	0.6229	210.1
4	0.6813	254.8

Linear least squares results: $MR + N_A - 3 = K' [1 - N_A / N_{AM}]$

$$K' = (2.795 \pm 0.494) \times 10^{-3} \quad K_{eq} = \frac{1}{K'} = 357.82 \pm 63.31$$

Intercept = -0.00983 ± 0.1009

Linear correlation coefficient $r=0.9701$

(4) $T=298.2^\circ K$

$$\Delta v_A = 18.06$$

$$\Delta v_B = 3.45$$

$$\chi_{M_A}^{cor} = 8.641 \times 10^{-3}$$

$$\chi_{M_B}^{cor} = 1.681 \times 10^{-3}$$

Table XIV. (Continued)

Soln	$(M \times 10^3)^a$	$(MR)^b$	Δv_{obs}	$d_o - d_s$
1	9.9824	3.0000	9.56	-0.0046
2	9.9767	3.1501	8.95	-0.0045
3	9.9369	3.3003	8.54	-0.0045
4	9.9867	3.4004	7.92	-0.0045

Soln	$(N_A)^c$	$(MW)^d$	$(DC \times 10^3)^d$	$(\chi_{M_{obs}}^{cor} \times 10^3)^d$
1	0.4182	476.2	-0.306	4.868
2	0.3765	481.8	-0.310	4.571
3	0.3484	485.5	-0.313	4.391
4	0.3060	491.2	-0.317	4.075

Soln	$(MW)^e$	$(DC \times 10^3)^e$	$(\chi_{M_{obs}}^{cor} \times 10^3)^e$	$(N_A)^f$
1	470.9	-0.302	4.868	0.4579
2	476.6	-0.307	4.572	0.4154
3	480.0	-0.309	4.391	0.3894
4	486.1	-0.313	4.074	0.3438

Soln	$MR + N_A - 3$	$1 - N_A/N_A^M$
1	0.4579	118.6
2	0.5655	141.1
3	0.6897	157.8
4	0.7442	191.1

Linear least squares results: $MR + N_A - 3 = K' [1 - N_A/N_A^M]$

$$K' = (4.030 \pm 0.842) \times 10^{-3} \quad K_{eq} = \frac{1}{K'} = 248.11 \pm 51.86$$

Intercept = 0.001092 ± 0.1301

Linear correlation coefficient $r=0.9590$

Table XIV. (Continued)

(5) $T=303.2^{\circ}\text{K}$

$$\Delta\nu_A=17.71$$

$$\Delta\nu_B=3.39$$

$$\chi_{M_A}^{\text{cor}} = 8.505 \times 10^{-3}$$

$$\chi_{M_B}^{\text{cor}} = 1.663 \times 10^{-3}$$

Soln	$(M \times 10^3)^a$	$(MR)^b$	$\Delta\nu_{\text{obs}}$	$d_o - d_s$
1	9.9229	3.0000	10.22	-0.0044
2	9.9172	3.1501	9.40	-0.0043
3	9.8777	3.3003	9.19	-0.0043
4	9.9283	3.4004	8.57	-0.0043

Soln	$(N_A)^c$	$(MW)^d$	$(DC \times 10^3)^d$	$(\chi_{M_{\text{obs}}}^{\text{cor}} \times 10^3)^d$
1	0.4770	468.3	-0.301	5.201
2	0.4260	475.1	-0.306	4.845
3	0.4050	477.9	-0.308	4.716
4	0.3617	483.8	-0.312	4.397

Soln	$(MW)^e$	$(DC \times 10^3)^e$	$(\chi_{M_{\text{obs}}}^{\text{cor}} \times 10^3)^e$	$(N_A)^f$
1	462.9	-0.297	5.201	0.5171
2	469.9	-0.302	4.845	0.4651
3	472.4	-0.304	4.716	0.4462
4	478.7	-0.308	4.397	0.3996

Soln	$MR + N_A - 3$	$1 - N_A / N_{AM}$
1	0.5171	94.11
2	0.6152	116.0
3	0.7465	125.7
4	0.8000	151.3

Linear least squares results: $MR + N_A - 3 = K' [1 - N_A / N_{AM}]$

$$K' = (5.152 \pm 1.141) \times 10^{-3} \quad K_{\text{eq}} = \frac{1}{K'} = 194.11 \pm 43.00$$

Table XIV. (Continued)

Linear correlation coefficient $r=0.9543$ (6) $T=308.2^{\circ}\text{K}$

$$\Delta v_A = 17.33$$

$$\Delta v_B = 3.33$$

$$\chi_{M_A}^{\text{cor}} = 8.374 \times 10^{-3}$$

$$\chi_{M_B}^{\text{cor}} = 1.645 \times 10^{-3}$$

Soln	$(M \times 10^3)^a$	$(MR)^b$	Δv_{obs}	$d_o - d_s$
1	9.8634	3.0000	10.82	-0.0042
2	9.8588	3.1501	10.21	-0.0042
3	9.8184	3.3003	9.88	-0.0041
4	9.8678	3.4004	9.40	-0.0041

Soln	$(N_A)^c$	$(MW)^d$	$(DC \times 10^3)^d$	$(\chi_{M_{\text{obs}}}^{\text{cor}} \times 10^3)^d$
1	0.5350	460.5	-0.295	5.509
2	0.4914	466.4	-0.299	5.215
3	0.4679	469.5	-0.302	5.065
4	0.4336	474.1	-0.305	4.812

Soln	$(MW)^e$	$(DC \times 10^3)^e$	$(\chi_{M_{\text{obs}}}^{\text{cor}} \times 10^3)^e$	$(N_A)^f$
1	455.3	-0.291	5.508	0.5741
2	461.1	-0.296	5.216	0.5307
3	464.1	-0.298	5.065	0.5082
4	469.1	-0.301	4.811	0.4705

Soln	$MR + N_A - 3$	$1 - N_A / N_{AM}$
1	0.5741	75.21
2	0.6808	89.70
3	0.8085	98.56
4	0.8709	114.0

Table XIV. (Continued)

Linear least squares results $MR + N_A - 3 = K' [^{1-N_A}/N_A^M]$

$$K' = (7.972 \pm 1.227) \times 10^{-3} \quad K_{eq} = \frac{1}{K'} = 125.43 \pm 19.3$$

Intercept $= -0.01880 \pm 0.1171$

Linear correlation coefficient $r=0.9771$

(7) $T=313.2^\circ K$

$$\Delta v_A = 17.00$$

$$\Delta v_B = 3.28$$

$$\chi_{M_A}^{cor} = 8.247 \times 10^{-3}$$

$$\chi_{M_B}^{cor} = 1.628 \times 10^{-3}$$

Soln	$(M \times 10^3)^a$	$(MR)^b$	Δv_{obs}	$d_o - d_s$
1	9.8038	3.0000	11.30	-0.0040
2	9.7993	3.1501	10.71	-0.0040
3	9.7602	3.3003	10.55	-0.0040
4	9.8130	3.4004	10.04	-0.0040
Soln	$(N_A)^c$	$(MW)^d$	$(DC \times 10^3)^d$	$(\chi_{M_{obs}}^{cor} \times 10^3)^d$
1	0.5845	453.9	-0.290	5.760
2	0.5415	459.6	-0.295	5.477
3	0.5299	461.2	-0.296	5.414
4	0.4927	466.2	-0.299	5.144
Soln	$(MW)^e$	$(DC \times 10^3)^e$	$(\chi_{M_{obs}}^{cor} \times 10^3)^e$	$(N_A)^f$
1	448.5	-0.287	5.761	0.6244
2	454.3	-0.291	5.477	0.5815
3	455.5	-0.292	5.414	0.5720
4	461.0	-0.295	5.143	0.5310

Table XIV. (Continued)

Soln	$MR + N_A - 3$	$1 - N_A/N_A^M$
1	0.6244	61.36
2	0.7316	73.44
3	0.8723	77.66
4	0.9314	90.03

Linear least squares results: $MR + N_A - 3 = K [1 - N_A/N_A^M]$

$$K' = (1.107 \pm 0.280) \times 10^{-2} \quad K_{eq} = \frac{1}{K'} = 90.33 \pm 2.29$$

Intercept $= -0.0450 \pm 0.213$

Linear correlation coefficient $r=0.9415$

(8) $T=318.2^\circ \text{K}$

$$\Delta v_A = 16.73$$

$$\Delta v_B = 3.24$$

$$\chi_{M_A}^{\text{cor}} = 8.123 \times 10^{-3}$$

$$\chi_{M_B}^{\text{cor}} = 1.611 \times 10^{-3}$$

Soln	$(M \times 10^3)^a$	$(MR)^b$	Δv_{obs}	$d_o - d_s$
1	9.7454	3.0000	11.67	-0.0039
2	9.7398	3.1501	11.28	-0.0038
3	9.7010	3.3003	11.04	-0.0038
4	9.7507	3.4004	10.52	-0.0038

Soln	$(N_A)^c$	$(MW)^d$	$(DC \times 10^3)^d$	$(\chi_{M_{\text{obs}}}^{\text{cor}} \times 10^3)^d$
1	0.6249	448.4	-0.287	5.971
2	0.5960	451.2	-0.289	5.775
3	0.5782	454.7	-0.291	5.673
4	0.5397	459.9	-0.295	5.396

Table XIV. (Continued)

Soln	(MW) ^e	(DCx10 ³) ^e	($\chi_{M_{obs}}^{cor}$ x10 ³) ^e	(N _A) ^f
1	442.5	-0.282	5.970	0.6694
2	446.5	-0.285	5.775	0.6394
3	448.6	-0.287	5.673	0.6238
4	454.3	-0.291	5.396	0.5812

Soln	MR + N _A - 3	$1 - N_A / N_{AM}$
1	0.6694	50.68
2	0.7895	57.90
3	0.9241	62.17
4	0.9816	73.79

Linear least squares results: $MR + N_A - 3 = K [1 - N_A / N_{AM}]$

$$K' = (1.362 \pm 0.344) \times 10^{-2} \quad K_{eq} = \frac{1}{K'} = 73.44 \pm 18.59$$

Intercept = 0.00874 ± 0.2127

Linear correlation coefficient $r = 0.9415$

-
- (a) Corrected for temperature and flask volume.
- (b) Ligand : Cobalt(II) mole ratio.
- (c) Initial trial values calculated from shift difference ratio.
- (d) Trial values calculated using initial values of N_A.
- (e) Final values, reiteration complete.
- (f) Final value calculated from susceptibility difference ratio.

Table XV. Calculation of Thermodynamic Parameters
From Equilibrium Constants: Cobalt(II)
Chloride-Triethyl Phosphite System

$$\text{CoCl}_2 \cdot 2\text{P}(\text{OEt})_3 + \text{P}(\text{OEt})_3 \rightleftharpoons \text{CoCl}_2 \cdot 3\text{P}(\text{OEt})_3$$

K_{eq}	$\ln K_{\text{eq}}$	$T^\circ \text{K}$	$\frac{1}{T} \times 10^3$	Calc.	
				K_{eq}^{a}	ΔG^{b}
129.53 ^c	4.8639 ^c	283.2	3.531	172.9	-2.90
138.59	4.9315	288.2	3.470	142.8	-2.84
114.60	4.7414	293.2	3.411	118.8	-2.78
101.04	4.6155	298.2	3.353	99.4	-2.72
89.29	4.4919	303.2	3.298	83.7	-2.67
70.42	4.2545	308.2	3.245	70.8	-2.61
69.18	4.237	313.2	3.193	60.3	-2.55
44.59	3.798	318.2	3.143	51.6	-2.49

$$\ln K_{\text{eq}} = - \frac{\Delta H^\circ}{R} \left(\frac{1}{T} \right) + \frac{\Delta S^\circ}{R}$$

$$\text{Slope} = \frac{-\Delta H^\circ}{R} = 3114.83 \pm 336.86$$

$$\Delta H^\circ = -6190 \pm 669 \text{ cal/mole} = -6.19 \pm 0.67 \text{ Kcal/mole}$$

$$\text{Intercept} = \frac{\Delta S^\circ}{R} = -5.8462 + 1.1129$$

$$\Delta S^\circ = -11.6 + 2.2 \text{ cal/mole}$$

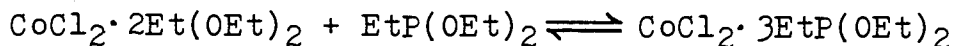
Linear correlation coefficient $r=0.9720$

(a) Calculated from $\ln K_{\text{eq}} = 3114.83 \left(\frac{1}{T} \right) - 5.8462$

(b) Calculated from $\Delta G^\circ = \Delta H^\circ - T\Delta S^\circ$, Kcal/mole

(c) This value rejected (see page 146)

Table XVI. Calculation of Thermodynamic Parameters
From Equilibrium Constants: Cobalt(II)
Chloride-Diethyl Ethylphosphonite System



K_{eq}	$\ln K_{\text{eq}}$	$T^\circ \text{K}$	$\frac{1}{T} \times 10^3$	Calc.	
				K_{eq}^a	$\Delta G^{\circ b}$
4721.6	8.4599	283.2	3.531	4693	-4.76
3324.7	8.1091	288.2	3.470	3386	-4.65
2407.0	7.7861	293.2	3.411	2471	-4.55
1800.4	7.4958	298.2	3.353	1822	-4.45
1455.1	7.2828	303.2	3.298	1357	-4.34
1066.3	6.9720	308.2	3.245	1020	-4.24
744.2	6.6123	313.2	3.193	774.3	-4.14
580.5	6.3639	318.2	3.143	592.7	-4.04

$$\ln K_{\text{eq}} = - \frac{\Delta H^\circ}{R} \left(\frac{1}{T} \right) + \frac{\Delta S^\circ}{R}$$

$$\text{Slope} = \frac{-\Delta H^\circ}{R} = 5327.45 \pm 115.02$$

$$\Delta H^\circ = -10.6 \pm 0.2 \text{ Kcal/mole}$$

$$\text{Intercept} = \frac{\Delta S^\circ}{R} = -10.3578 + 0.3833$$

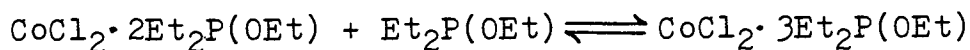
$$\Delta S^\circ = -20.6 + 0.8 \text{ e.u.}$$

Linear correlation coefficient $r=0.9986$

$$(a) \text{ Calculated from } \ln K_{\text{eq}} = -5327.45 \left(\frac{1}{T} \right) - 10.3578$$

$$(b) \text{ Calculated from } \Delta G^\circ = \Delta H^\circ - T\Delta S^\circ, \text{ Kcal/mole}$$

Table XVII. Calculation of Thermodynamic Parameters
From Equilibrium Constants: Cobalt(II)
Chloride-Ethyl Diethylphosphinite System



K_{eq}	$\ln K_{\text{eq}}$	$T^\circ \text{ K}$	$\frac{1}{T} \times 10^3$	Calc.	
				K_{eq}^a	$\Delta G^{\circ b}$
723.97	6.5848	283.2	3.531	728.9	-3.71
503.73	6.2220	288.2	3.470	504.2	-3.56
357.82	5.8800	293.2	3.411	353.2	-3.42
248.11	5.5139	298.2	3.353	250.4	-3.27
194.11	5.2684	303.2	3.298	179.5	-3.13
125.43	4.8318	308.2	3.245	130.1	-2.98
90.33	4.5035	313.2	3.193	95.28	-2.84
73.44	4.2965	318.2	3.143	70.46	-2.69

$$\ln K_{\text{eq}} = - \frac{\Delta H^\circ}{R} \left(\frac{1}{T} \right) + \frac{\Delta S^\circ}{R}$$

$$\text{Slope} = - \frac{\Delta H^\circ}{R} = 6015.6 \pm 127.0$$

$$\Delta H^\circ = -11954 \pm 252 = -12.0 \text{ Kcal/mole}$$

$$\text{Intercept} = \frac{\Delta S^\circ}{R} = -14.65 + 0.42$$

$$\Delta S^\circ = -29.11 + 0.84 = -29.1 \text{ e.u.}$$

Linear correlation coefficient $r=0.9987$

$$(a) \text{ Calculated from } \ln K_{\text{eq}} = -14.65 \left(\frac{1}{T} \right) - 29.11$$

$$(b) \text{ Calculated from } \Delta G^\circ = \Delta H^\circ - T\Delta S^\circ, \text{ Kcal/mole}$$

APPENDIX II

Spectrophotometric Data on Dioxygen
Adduct Decomposition

Table XVIII. Calculation of First Order Rate Constant for
Thermal Decomposition of $\text{O}_2\text{CoCl}_2(\text{EtP}(\text{OEt})_2)_3$
From Spectrophotometric Data at -9°C ,
 $\lambda = 550 \text{ nm}$ (t-Butylbenzene)

Time (min)	Abs	Time (min)	Abs	Time (min)	Abs
0	0.340	29.0	0.458	67.0	0.660
1.0	0.350	30.0	0.463	69.5	0.670
2.0	0.350	31.0	0.470	72.0	0.680
3.0	0.357	32.0	0.473	74.5	0.690
4.0	0.3500	33.0	0.481	77.0	0.700
5.0	0.341	34.0	0.490	79.0	0.706
6.0	0.352	35.0	0.498	81.0	0.709
7.0	0.361	36.0	0.505	83.0	0.718
8.0	0.368	37.0	0.510	85.0	0.723
9.0	0.371	38.0	0.517	88.0	0.727
10.0	0.373	39.0	0.520	90.0	0.730
11.0	0.375	40.0	0.526	94.0	0.730
12.0	0.377	41.0	0.531	98.0	0.734
13.0	0.380	42.0	0.540	100.0	0.737
14.0	0.379	43.0	0.545	103.0	0.743
15.0	0.373	44.0	0.549	105.0	0.747
16.0	0.372	45.0	0.553	109.0	0.750
17.0	0.376	46.0	0.559	112.0	0.752
18.0	0.381	47.0	0.564	115.0	0.757
19.0	0.392	48.0	0.574	118.0	0.760
20.0	0.405	50.0	0.580	120.0	0.762
21.0	0.415	51.0	0.588	123.0	0.765
22.0	0.419	52.0	0.590	127.0	0.768
23.0	0.421	54.0	0.600	129.0	0.772
24.0	0.428	56.0	0.610	132.0	0.775
25.0	0.434	57.5	0.620	134.0	0.774
26.0	0.440	60.0	0.632	138.0	0.774
27.0	0.446	61.0	0.635	140.0	0.776
28.0	0.453	62.0	0.640	144.0	0.777
29.0	0.458	64.5	0.650	146.0	0.779

Table XVIII. (Continued)

<u>Time(min.)</u>	<u>Abs</u>	<u>Time(min)</u>	<u>Abs</u>	<u>Time(min)</u>	<u>Abs</u>
148.0	0.781	178.0	0.803	193.0	0.812
150.0	0.784	180.0	0.806	194.0	0.815
152.0	0.785	181.0	0.807	195.0	0.813
155.0	0.786	183.0	0.807	197.0	0.814
159.0	0.788	185.0	0.808	198.0	0.815
163.0	0.793	188.0	0.811	200.0	0.816
165.0	0.797	189.0	0.811	201.0	0.815
168.0	0.799	190.0	0.812	205.0	0.814
170.0	0.800	191.0	0.813	210.0	0.815
173.0	0.801	192.0	0.813	220.0	0.814
175.0	0.800				

$$\text{Abs}(t=\infty)=0.815$$

$$\ln ((A_{\infty} - A_1) / (A_{\infty} - A_t)) = k (t - t_1)^a$$

Linear least squares results:

$$\text{Slope} = k^b = 2.152 \times 10^{-2} \text{ min}^{-1} \quad \text{or} \quad k = 3.587 \times 10^{-4} \text{ sec}^{-1}.$$

$$\text{Intercept} = 0.04114$$

Linear correlation coefficient $r = 0.9997$

- (a) Curve of Abs. vs. t was plotted and points were selected from the middle range of the curve for the calculation.
 $t_1 = 20.0 \text{ min}$, $A_1 = 0.398$ (the first data point selected).

- (b) Obtained from fifteen sets of selected data.

Table XIX. Calculation of First order Rate Constant for
Thermal Decomposition of $\text{O}_2\text{CoCl}_2(\text{EtP}(\text{OEt})_2)_3$
From Spectrophotometric Data at -2°C ,
 $\lambda = 550 \text{ nm}$ (*t*-Butylbenzene)

<u>t (min)</u>	<u>Abs</u>	<u>t (min)</u>	<u>Abs</u>	<u>t (min)</u>	<u>Abs</u>
0	0.226	14.0	0.358	28.5	0.432
0.5	0.234	14.5	0.361	29.0	0.436
1.0	0.242	15.0	0.364	29.5	0.438
1.5	0.250	15.5	0.366	30.0	0.440
2.0	0.257	16.0	0.368	30.5	0.441
2.5	0.263	16.5	0.371	31.0	0.443
3.0	0.268	17.0	0.374	31.5	0.445
3.5	0.273	17.5	0.377	32.0	0.447
4.0	0.279	18.0	0.381	32.5	0.448
4.5	0.284	18.5	0.384	33.0	0.448
5.0	0.290	19.0	0.386	33.5	0.450
5.5	0.296	19.5	0.389	34.0	0.451
6.0	0.301	20.0	0.392	34.5	0.453
6.5	0.306	20.5	0.392	35.0	0.454
7.0	0.312	21.0	0.396	36.0	0.456
7.5	0.316	21.5	0.398	37.0	0.460
8.0	0.321	22.0	0.401	38.0	0.463
8.5	0.325	23.0	0.406	39.0	0.466
9.0	0.329	23.5	0.409	40.0	0.468
9.5	0.332	24.0	0.412	41.0	0.469
10.0	0.336	24.5	0.414	42.0	0.472
10.5	0.338	25.0	0.415	43.0	0.470
11.0	0.342	25.5	0.418	44.0	0.473
11.5	0.344	26.0	0.420	45.0	0.474
12.0	0.348	26.5	0.423	46.0	0.474
12.5	0.351	27.0	0.425	47.0	0.475
13.0	0.354	27.5	0.428	48.0	0.478
13.5	0.355	28.0	0.431	49.0	0.476

Table XIX. (Continued)

<u>t (min)</u>	<u>Abs</u>	<u>t (min)</u>	<u>Abs</u>	<u>t (min)</u>	<u>Abs</u>
50.0	0.475	65.0	0.478	90.0	0.480
52.0	0.477	70.0	0.478	92.0	0.480
54.0	0.479	75.0	0.477	95.0	0.478
55.0	0.476	78.0	0.480	97.0	0.482
56.0	0.478	80.0	0.488	98.0	0.482
57.0	0.480	82.0	0.479	99.0	0.479
58.0	0.477	85.0	0.479		
59.0	0.479	87.0	0.477		
60.0	0.481	89.0	0.477		

$$\text{Abs}(t=\infty)=0.480$$

$$\ln((A_{\infty} - A_1) / (A_{\infty} - A_t)) = k (t - t_1)^a$$

Linear least squares results:

$$\text{Slope} = k^b = 5.448 \times 10^{-2} \text{ min}^{-1}, \text{ or } k = 9.080 \times 10^{-4} \text{ sec}^{-1}$$

$$\text{Intercept} = -0.01991$$

Linear correlation coefficient $r = 0.9991$

(a) Curve of Abs. vs. t was plotted and points were selected from the curve for the calculation.

(t_1, A_1) is the first data point selected.

(b) Obtained from eight sets of selected data.

Table XX. Calculation of First Order Rate Constant for
Thermal Decomposition of $\text{O}_2\text{CoCl}_2(\text{EtP}(\text{OEt})_2)_3$
From Spectrophotometric Data at 3°C
 $\lambda = 550 \text{ nm}$ (t-Butylbenzene)

t (min)	Abs	t (min)	Abs	t (min)	Abs
0	0.309	15.0	0.743	30.0	0.905
0.5	0.303	15.5	0.760	30.5	0.905
1.0	0.306	16.0	0.771	31.0	0.906
1.5	0.310	16.5	0.776	31.5	0.908
2.0	0.316	17.0	0.782	32.0	0.911
2.5	0.328	17.5	0.787	32.5	0.917
3.0	0.342	18.0	0.794	33.0	0.915
3.5	0.356	18.5	0.803	33.5	0.917
4.0	0.373	19.0	0.811	34.0	0.916
4.5	0.382	19.5	0.826	34.5	0.919
5.0	0.404	20.0	0.830	35.0	0.919
5.5	0.425	20.5	0.831	35.5	0.921
6.0	0.449	21.0	0.835	36.0	0.922
6.5	0.473	21.5	0.842	36.5	0.919
7.0	0.498	22.0	0.849	37.0	0.920
7.5	0.519	22.5	0.857	37.5	0.921
8.0	0.537	23.0	0.860	38.0	0.920
8.5	0.557	23.5	0.860	38.5	0.922
9.0	0.576	24.0	0.867	39.0	0.923
9.5	0.596	24.5	0.872	39.5	0.921
10.0	0.612	25.0	0.869	40.0	0.920
10.5	0.632	25.5	0.877	40.5	0.921
11.0	0.651	26.0	0.882	41.0	0.920
11.5	0.667	26.5	0.885	41.5	0.921
12.0	0.680	27.0	0.887	42.0	0.920
12.5	0.696	27.5	0.890	42.5	0.922
13.0	0.710	28.0	0.892	43.0	0.918
13.5	0.715	28.5	0.892	43.5	0.922
14.0	0.720	29.0	0.902	44.0	0.919
14.5	0.734	29.5	0.905	44.5	0.921

Table XX. (Continued)

<u>t (min)</u>	<u>Abs</u>	<u>t (min)</u>	<u>Abs</u>	<u>t (min)</u>	<u>Abs</u>
45.0	0.919	48.5	0.919	51.5	0.921
45.5	0.921	49.0	0.921	52.0	0.923
46.0	0.920	49.5	0.921	54.0	0.921
46.5	0.918	50.0	0.921	56.0	0.920
47.0	0.918	50.5	0.921	60.0	0.921
47.5	0.920	51.0	0.919	65.0	0.921
48.0	0.920				

$$\text{Abs}(t=\infty) = 0.921$$

$$\ln((A_{\infty} - A_1)/(A_{\infty} - A_t)) = k(t - t_1)^a$$

Linear least squares results:

$$\text{Slope} = k^b = 0.1179 \text{ min}^{-1}, \text{ or } k = 1.965 \times 10^{-3} \text{ sec}^{-1}$$

$$\text{Intercept} = -0.04260$$

Linear correlation coefficient $r = 0.9997$

(a) Curve of Abs. vs. t was plotted and points were selected from the curve for the calculation.

(t_1, A_1) is the first data point selected.

(b) Obtained from ten sets of selected data.

Table XXI. Calculation of First Order Rate Constant for
 Thermal Decomposition of $\text{O}_2\text{CoCl}_2(\text{EtP}(\text{OEt})_2)_3$
 From Spectrophotometric Data at 7°C
 $\lambda = 550 \text{ nm}$ (t-Butylbenzene)

<u>t (sec)</u>	<u>Abs</u>	<u>t (sec)</u>	<u>Abs</u>	<u>t (sec)</u>	<u>Abs</u>
0	0.196	690	0.423	1380	0.495
30	0.200	720	0.429	1410	0.496
60	0.203	750	0.438	1440	0.498
90	0.205	780	0.445	1470	0.496
120	0.207	810	0.451	1500	0.495
150	0.207	840	0.453	1530	0.497
180	0.209	870	0.457	1560	0.499
210	0.212	900	0.463	1590	0.498
240	0.220	930	0.467	1620	0.496
270	0.228	960	0.470	1650	0.498
300	0.238	990	0.473	1680	0.498
330	0.258	1020	0.475	1710	0.498
360	0.279	1050	0.478	1740	0.496
390	0.297	1080	0.480	1770	0.498
420	0.313	1110	0.482	1800	0.497
450	0.330	1140	0.486	1860	0.498
480	0.343	1170	0.488	1920	0.497
510	0.357	1200	0.489	1980	0.498
540	0.368	1230	0.491	2100	0.498
570	0.387	1260	0.492	2200	0.498
600	0.393	1290	0.495	2320	0.497
630	0.401	1320	0.495	2460	0.498
660	0.412	1350	0.497	2700	0.498

$$\text{Abs}(t=\infty) = 0.498$$

Table XXI. (Continued)

$$\ln((A_{\infty} - A_1)/(A_{\infty} - A_t)) = k (t - t_1)^a$$

Linear least squares results:

$$\text{Slope} = k^b = 3.420 \times 10^{-3} \text{ sec}^{-1}$$

$$\text{Intercept} = -0.05949$$

Linear correlation coefficient $r = 0.9993$

(a) Curve of Abs. vs. t was plotted and points were selected from the curve for the calculation.

(t_1, A_1) is the first data point selected.

(b) Obtained from ten sets of selected data.

Table XXII. Calculation of First Order Rate Constant for
Thermal Decomposition of $\text{O}_2\text{CoCl}_2(\text{EtP}(\text{OEt})_2)_3$
From Spectrophotometric Data at 11°C
 $\lambda = 550 \text{ nm}$ (t-Butylbenzene)

t(sec)	Abs	t(sec)	Abs	t(sec)	Abs
0	0.480	490	0.914	1090	0.947
20	0.490	520	0.921	1120	0.945
50	0.510	550	0.926	1150	0.947
80	0.540	580	0.929	1180	0.948
100	0.570	610	0.932	1210	0.948
140	0.630	640	0.935	1240	0.948
170	0.670	670	0.938	1270	0.947
185	0.700	700	0.941	1300	0.948
205	0.720	730	0.941	1330	0.946
220	0.740	760	0.941	1360	0.945
235	0.760	790	0.942	1390	0.947
250	0.780	820	0.943	1420	0.946
270	0.800	850	0.942	1450	0.945
290	0.820	880	0.942	1480	0.948
310	0.830	910	0.943	1540	0.948
330	0.845	940	0.942	1600	0.948
390	0.865	970	0.946	1720	0.947
415	0.880	1000	0.945	1780	0.948
440	0.890	1030	0.944		
460	0.900	1060	0.945		

$$\text{Abs}(t=\infty) = 0.948$$

$$\ln((A_\infty - A_1)/(A_\infty - A_t)) = k(t - t_1)^a$$

Table XXII. (Continued)

Linear least squares results:

Slope = $k = 5.696 \times 10^{-3} \text{ sec}^{-1}$

Intercept = 0.02871

Linear correlation coefficient $r = 0.9998$

(a) Curve of Abs. vs. t was plotted and points were selected from the curve for the calculation.

(t_1, A_1) is the first data point selected.

(b) Obtained from ten sets of selected data.